OCEAN DRILLING PROGRAM

LEG 178 PRELIMINARY REPORT

ANTARCTIC GLACIAL HISTORY AND SEA-LEVEL CHANGE

Dr. Peter Barker
Co-Chief Scientist, Leg 178
British Antarctic Survey
High Cross, Madingley Road
Cambridge CB3 0ET
United Kingdom

Dr. Angelo Camerlenghi
Co-Chief Scientist, Leg 178
Osservatorio Geofisico Sperimentale
P.O. Box 2011
Triste Opicina 34016
Italy

Dr. Gary D. Acton
Staff Scientist, Leg 178
Ocean Drilling Program
Texas A&M University Research Park
1000 Discovery Drive
College Station, Texas 77845-9547
U.S.A.

Jack Baldauf
Deputy Director of
Science Operations
ODP/TAMU

Gary Acton
Leg Project Manager
Science Services
ODP/TAMU

June 1998

Preliminary Report No. 78

First Printing 1998

Distribution

Electronic copies of this publication may be obtained from the ODP Publications Home Page on the World Wide Web at http://www-odp.tamu.edu/publications.

D I S C L A I M E R

This publication was prepared by the Ocean Drilling Program, Texas A&M University, as an account of work performed under the international Ocean Drilling Program, which is managed by Joint Oceanographic Institutions, Inc., under contract with the National Science Foundation. Funding for the program is provided by the following agencies:

Australia/Canada/Chinese Taipei/Korea Consortium for the Ocean Drilling
Deutsche Forschungsgemeinschaft (Germany)
Institut Français de Recherche pour l'Exploitation de la Mer (France)
Ocean Research Institute of the University of Tokyo (Japan)
National Science Foundation (United States)
Natural Environment Research Council (United Kingdom)
European Science Foundation Consortium for the Ocean Drilling Program (Belgium, Denmark, Finland, Iceland, Italy, The Netherlands, Norway, Portugal, Spain, Sweden, Switzerland, and Turkey)
People's Republic of China

The following scientists were aboard the *JOIDES Resolution* for Leg 178 of the Ocean Drilling Program:

Peter F. Barker, Co-Chief Scientist (British Antarctic Survey, High Cross, Madingley Road, Cambridge CB3 0ET, United Kingdom, Internet: p.barker@bas.ac.uk)

Angelo Camerlenghi, Co-Chief Scientist (Osservatorio Geofisico Sperimentale, P.O. Box 2011, Trieste Opicina 34016, Italy, Internet: acamerlenghi@ogs.trieste.it)

Gary D. Acton, Staff Scientist (Ocean Drilling Program, Texas A&M University, 1000 Discovery Drive, College Station, Texas 77845, USA, Internet: gary_acton@odp.tamu.edu)

Stefanie A. Brachfeld, Paleomagnetist (Department of Geology and Geophysics, University of Minnesota, Minneapolis, 108 Pillsbury Hall, 310 Pillsbury Drive, Minneapolis, Minnesota 55455, USA, Internet: brac0009@gold.tc.umn.edu)

Ellen A. Cowan, Sedimentologist (Department of Geology, Appalachian State University, Boone, North Carolina 28608, USA, Internet: cowanea@appstate.edu)

James Daniels, Sedimentologist (School of Earth Sciences, University of Melbourne, Parkville 3052 Australia, Internet: j.daniels@pgrad.unimelb.edu.au)

Carlota Escutia, Sedimentologist/Seismic Stratigrapher (United States Geological Survey, MS 999, 345 Middlefield Road, Menlo Park, California 94025, USA, Internet: carlota@octopus.wr.usgs.gov)

Andrew J. Evans, Physical Properties Specialist (School of Geography, University of Leeds, Woodhouse Lane, Leeds, West Yorkshire LS2 9JT, United Kingdom, Internet: geoaje@leeds.ac.uk)

Nicholas Eyles, Sedimentologist (Environmental Earth Sciences, University of Toronto at Scarborough, 1265 Military Trail, Scarborough, Ontario M1C 1A4, Canada, Internet: eyles@scar.utoronto.ca)

Yohan J.B. Guyodo, Paleomagnetist (Department of Geology, University of Florida, 1112 Turlington Hall, Gainesville, Florida 32611-7340, USA, Internet: guyodo@ufl.edu)

Marina Iorio, Stratigraphic Correlator (Istituto di Riceaca “Geomare Sud,” Consiglio Nazionale della Ricerche, Via Vespucci n 9, Napoli 80142, Italy, Internet: iorio@gms01.geomare.na.cnr.it)

Masao Iwai, Paleontologist-Diatom (Department of Geology, Kochi University, 2-5-1 Akebono-cho, Kochi 780, Japan, Internet: iwaim@cc.kochi-u.ac.jp)

Frank T. Kyte, Inorganic Geochemist (Institute of Geophysics and Planetary Physics, University of California, Los Angeles, Slichter Hall, Los Angeles, California 90095-1567, USA, Internet: Kyte@igpp.ucla.edu)

Christine Later, LEO Logging Trainee (Laboratories de Measures en Forage, ODP-NEB, B.P. 72, 13545 Aix-en Provence, Cede 4, France, Internet: later@lmf_aix.gulliver.fr)

Andrus Maldonado, Sedimentologist (Instituto Andaluz de Ciencias de la Tierra, CSIC, Universidad de Granada, Facultad de Ciencias, Fuentenueve s/n, 18002 Granada, Spain, Internet: amaldona@goliat.ugr.es)

Tobias Moerz, JOIDES Logging Scientist (GEOMAR, Christian-Albrechts-Universität zu Kiel, Wischhofstrasse 1-3, Gebäude 4, Kiel 24148, Germany, Internet: tmoerz@geomar.de)

Lisa E. Osterman, Paleontologist-Foraminifers (Smithsonian Institution, Washington, DC 20560, USA. Mailing address: United States Geological Survey, MS 955, Reston, Virginia 20192, USA, Internet: osterman@geochange.er.usgs.gov)

Carol J. Pudsey, Sedimentologist (British Antarctic Survey, High Cross, Madingley Road, Cambridge CB3 0ET, United Kingdom, Internet: c.pudsey@bas.ac.uk)

Jeffrey D. Schuffert, Inorganic Geochemist (Department of Geological Sciences, Brown University, 324 Brook Street, Providence, Rhode Island 02912-1846, USA, Internet: schuff@brown.edu)

Charlotte M. Sjunneskog, Organic Geochemist (Institute of Earth Sciences, Uppsala University, Villávagen 16, Uppsala 75236, Sweden, Internet: charlotte.sjunneskog@netgeog.uu.se)

Kate L. Vigar, Physical Properties Specialist (Department of Geology, University of Leicester, University Road, Leicester LE1 7RH, United Kingdom, Internet: klv1@leicester.ac.uk)

Amy L. Weinheimer, Paleontologist-Radiolarians (Scripps Institution of Oceanography, University of California, San Diego, Climate Research Division, 9500 Gilman Drive, La Jolla, California 92093-0220, USA, Internet: aweinheimer@ucsd.edu)

Trevor Williams, LEO Logging Scientist (Department of Geology, University of Leicester, Leicester LE1 7RH, United Kingdom, Internet: tw7@leicester.ac.uk)

Diane M. Winter, Paleontologist-Diatoms/Nannofossils (Department of Geology, Florida State University, Tallahassee, Florida 32312-3026, USA, Internet: dwinter@unlinfo.unl.edu)

Thomas C.W. Wolf-Welling, Sedimentologist (GEOMAR, Christian-Albrechts-Universität zu Kiel, Wischhofstrasse 1-3, Gebäude C4, Kiel 24148, Germany, Internet: twolf@geomar.de)

ABSTRACT

The Antarctic Ice Sheet is both a major component of the global climate system (involved in global deep- and bottom-water formation and sea-level change) and a source of ambiguity in the oxygen isotopic record that limits the value of this record to other studies of Cenozoic paleoclimate. The proposal on which this leg was based is one of five linked proposals intended to extract the Cenozoic glacial history of Antarctica from the sediments of its continental margin. On Ocean Drilling Program (ODP) Leg 178, nine sites (Figs. 1– 3) were drilled on the continental margin of the Antarctic Peninsula. These included a transect of the outer continental shelf and complementary sites on a hemipelagic drift on the continental rise, both extending back 6–10 m.y., as well as shallow holes at two sites on the inner continental shelf that provide an ultrahigh-resolution Holocene record.

INTRODUCTION

At present, the history of the Antarctic Ice Sheet is unknown. It has been inferred from low-latitude proxy data such as oxygen isotopic measurements on deep-ocean benthic foraminifers and the record of eustatic sea-level change adduced from sediments on low-latitude margins (Miller et al., 1987; Haq et al., 1987). However, these inferences are ambiguous and in disagreement (Sahagian and Watts, 1991; Barker, 1992), which leaves the history unresolved and limits the credibility and usefulness of both proxy data sets. For example, there is a dispute over whether the principal increases in Antarctic ice volume, which affect the benthic isotopic record, occurred at about 35 Ma, at 16–13 Ma, or only after 3 Ma. Similarly, changes in grounded ice volume provide the only generally accepted repeatable, rapid-acting cause for global, eustatic sea-level change, yet the timing and amplitudes of sea-level change adduced from low-latitude margin sediments are disputed. Changes also occur at times when there is no independent evidence for substantial volumes of grounded ice on Antarctica or elsewhere. Further, the isotopic and sea-level estimates of grounded ice volume disagree substantially at both long and short periods through most of the Cenozoic. Onshore Antarctic evidence of glacial history is sparse and presently controversial: the argument continues as to how stable the early Pliocene Antarctic Ice Sheet has been (Webb and Harwood, 1991; Denton et al., 1993).

Deep and intermediate Southern Ocean waters generally corrode the carbonate tests used in isotopic analysis. Therefore, despite the production of high-resolution data sets (e.g., Tiedemann et al., 1994; Shackleton et al., 1995), the problems of using distal proxy data will persist. Antarctic margin sediments hold a direct record of ice-sheet fluctuation that can determine ice-volume change and clear the way for a more useful interpretation of isotopic and sea-level data in the future.

The five linked Antarctic Offshore Acoustic Stratigraphy initiative (ANTOSTRAT) drilling proposals are aimed at estimating size variations of the Antarctic Ice Sheet through the Cenozoic. This will include warmer periods when the ice sheet was much smaller, reaching the margin in only a few places, with fluvial sediment transport and deposition elsewhere. The proposals sample both the East and West Antarctic margins and aim to distinguish an interior ice sheet, barely reaching the margin, from an ice sheet with a large coastal ice budget. For this, the proposals make use of numerical models to suggest the patterns of past glaciation and use modeling results to help select drilling locations. For example, Figure 4 (from Huybrechts, 1993) shows a glaciological model of ice sheets that cover only parts of the continent during warmer conditions. Some regions are clearly more sensitive to particular stages of ice-sheet volume change than others, and no single region will provide a complete history. The models allow data from different regions of the Antarctic margin to be combined in a complete history of ice-sheet development.

Glacial Sediment Transport

The collaborative interpretation of Antarctic margin seismic data through ANTOSTRAT (Cooper et al., 1994, 1995; Barker and Cooper, 1997) and the simplicity of the modern Antarctic glacial regime have led to rapid emergence and application of a unifying model of glacial-sediment transport and deposition (Alley et al., 1989; Larter and Barker, 1989; Bartek et al., 1991; Cooper et al., 1991; Kuvaas and Kristoffersen, 1991). Briefly, almost all ice transport to the ice-sheet margins takes place within broad, rapidly moving ice streams. Rapid flow is enabled by low basal friction, whose main source is an overpressured and undercompacted, unsorted, shearing basal till. The shear ensures that ice transport is accompanied by till transport, and virtually all of the transported till is melted out/dropped/deposited close to the grounding line, where the ice sheet becomes an ice shelf before calving into icebergs. The ice stream erodes and transports inshore of the grounding line and deposits offshore, in a high-latitude analog of the low-latitude subaerial erosion/shoreline/marine deposition system. Further, the grounding line advances and retreats under the influence of upstream ice provision and basal sediment supply (and sea-level change), all climate-related. The very large prograded sediment wedges beneath the Antarctic margin were developed during glacial maxima, when the ice sheet was grounded to the continental shelf edge (Fig. 5).

The glacial sedimentary regime has other characteristics. Progradation is usually focused into broad “trough-mouth fans” opposite the main ice streams, and the shelf is overdeepened (generally to between 300 and 600 m, but in places much deeper) and inward sloping. Continental slopes are often steep, and in places turbidity-current transport of the unstable component of slope deposition (with downcurrent deposition of suspended fines) has produced large hemipelagic sediment drifts on the continental rise (e.g., Kuvaas and Leitchenkov, 1992; Tomlinson et al., 1992; McGinnis and Hayes, 1995; Rebesco et al., 1996, 1997; Fig. 6). Sediment supply to the slope and rise is highly cyclic, with large quantities of unsorted diamict deposited during glacial maxima and very little deposited during interglacial periods.

Three depositional environments are recognized: shelf topsets and slope foresets of the prograded wedge and proximal hemipelagic drifts on the continental rise. Of these, the shelf record is potentially the least continuous. There, sediment is preserved mainly by slow subsidence, from cooling and from flexural response to the topset and foreset load, and the sediment is prone to re-erosion during the next glacial advance (e.g., Larter and Barker, 1989; Vanneste and Larter, 1995). Topsets tend to mark only the major changes in glacial history, so the more continuous foreset record is complementary. Before Leg 178, the drifts proximal to the rise were sparsely sampled (see Camerlenghi et al., 1997b) but potentially contained an excellent record, closely related to that of the upper-slope foresets from which they are derived. Existing seismic data and drill sites from around Antarctica had demonstrated the coarse- (but not yet the fine-) scale climate record in continental rise sediments and the likely climate sensitivity of margin-wedge geometry (Barker, 1995a). They had also revealed the partial nature of the shelf topset record (Hayes, Frakes, et al., 1975; Barron, Larsen, et al., 1989). During Leg 178, the glacial shelf prograded wedge was sampled at Site 1097, and the linked transect Sites 1100, 1102, and 1103 as well as the rise drifts were sampled at Sites 1095, 1096, and 1101.

The continental shelf is an area of high biogenic productivity during interglacials. Although long-term sediment preservation on the shelf is limited because grounded ice sheets erode during subsequent glacials, biogenic interbeds will be preserved within sequence groups composed mainly of thick glacial diamict topsets and foresets. In addition, glacially eroded deeps can preserve expanded Holocene sections that may be continuous and essentially biogenic, if the ice-sheet grounding line is remote enough that ice-rafted debris is minor or absent and the section is sufficiently protected from bottom currents. Such sections can provide a record of decadal and millennial variability that can be compared with records from low latitudes and the ice sheet itself. This environment is available on the inner shelf of the Antarctic Peninsula (Domack and McClennen, 1996; Leventer et al., 1996) and was sampled during Leg 178 in Palmer Deep at Sites 1098 and 1099.

The Antarctic Peninsula

Each ANTOSTRAT proposal is focused on the particular contributions its region might make toward understanding Antarctic glacial history. A single region does not offer the best opportunities for drilling in all respects. The particular value of drilling on the Antarctic Peninsula is the simplicity of its environment, together with the existing level of baseline understanding.

Tectonics and Subsidence

All Antarctic margins are extensional (or effectively so) in a thermal and flexural sense, but most are old. Age governs thermal subsidence and rigidity, which controls response to erosion and deposition and to cyclic ice loading. The Antarctic Peninsula behaves as a young passive margin, having subducted a ridge crest (50 Ma in the southwest to only 6–3 Ma in the northeast [Barker, 1982; Larter and Barker, 1991a]). The margin undergoes steady thermal subsidence, which means better preservation of topset beds of the prograded wedge than at an older, colder margin and a more local isostatic response to sediment load.

Tectonics and Age Constraint

Ridge subduction occurred well before the onset of glaciation in the southwest but not in the northeast. In the northeast, this provides a useful constraint on the maximum age of glacial sediments (which overlie young ocean floor of known age) but also threatens interference between tectonic and glacial events. For the older glacial history, it is prudent to avoid the northeast area of the margin.

Geological Simplicity

Sub-ice geology (resistance to erosion) is a significant variable, to the extent that a till base facilitates ice streaming. The peninsula interior is 2000 m high and is composed largely of Andean-type plutonic and volcanic rocks. Before ridge subduction, the Pacific margin was a well-developed forearc terrain on which the glacial regime has superposed an extensive prograded wedge (Larter and Barker, 1989, 1991b; Anderson et al., 1990; Larter and Cunningham, 1993; Bart and Anderson, 1995; Larter et al., 1997). The topography and geology of the peninsula vary little along strike, which simplifies the models of erosional and depositional response to climate change. Short cores on the outer shelf show diamicton beneath a thin cover of Holocene hemipelagic mud (Pope and Anderson, 1992; Pudsey et al., 1994).

Climate

Snow accumulation varies with temperature and is greatest around the continental edge, particularly along the Antarctic Peninsula, which is warmer than East Antarctica (Drewry and Morris, 1992). Snow accumulation governs the required rates of ice transport, hence basal sediment transport. Greater accumulation means an expanded sediment record. Warmer ice means (probably) faster ice flow, which also contributes to a rapid response to climate and an expanded sediment record.

Ice Catchment

The extent of the ice drainage basin affects the speed of response to climate change and adds the complexity of a distal to a proximal signal (which allows the possibility of seeing the effects of a small, purely inland ice sheet at the coast during less-glaciated periods). The Antarctic Peninsula is a narrow strip of interior upland, dissected by fjords and bordered by a broad continental shelf. It therefore has a low-reservoir, high-throughput glacial regime with only a proximal source and so is both simple and highly responsive to climate change.

Onshore evidence of Eocene and Oligocene glaciation on the South Shetland Islands (northern Antarctic Peninsula) has been published (see Birkenmajer, 1992), but this conflicts with other evidence of regional climate. The Antarctic Peninsula can probably provide a high-resolution record of glaciation back to perhaps 10 Ma. To go back further could involve entanglement with the tectonics of ridge-crest collision, making this a problem instead of an asset. However, because of the Antarctic Peninsula’s more northerly position, its glacial history is shorter than East Antarctica’s. The record before 10 Ma may be largely nonglacial, or it may reveal a stage of valley glaciation lacking regular ice-sheet extension to the continental shelf edge.

Scientific Objectives

The principal drilling objectives of Leg 178 are (1) to extract and compare high-resolution records of the past 10 m.y. of continental glaciation contained in topset beds (paleoshelf) of the glacial prograded wedge at the Antarctic Peninsula Pacific margin, in foreset beds (paleoslope) of the same sequence groups, and in a hemipelagic sediment drift on the continental rise; (2) to compile an optimal high-resolution history of grounded ice-volume fluctuation and compare it with low-latitude records of sea-level change and isotopic estimates of ice-volume change over the past 10 m.y.; (3) to assess the main controls on sediment transport and deposition during glacial intervals and use the insights gained to optimize investigation of the longer, more complicated East Antarctic record of glaciation and glacio-eustatic sea-level change; and (4) to extract an ultrahigh-resolution Holocene record from a protected basin on the inner continental shelf for comparison with similar records from the ice sheets and lower-latitude sites to investigate decadal- and millennial-scale climatic variation.

Continental Rise Drift Sites (1095, 1096, and 1101)

Site 1095

Site 1095 is the more distal of two sites on a hemipelagic sediment drift on the continental rise off the northwestern Pacific margin of the Antarctic Peninsula. Site 1095 lies in 3840 m of water on the northwestern, lower flank of the drift (Fig. 2) and was drilled to obtain the deeper part of the stratigraphic section, where the overlying sediments are thinner than at the drift crest (Site 1096). The location was chosen on the upper part of a gentle slope bordering to the southwest a deep-sea channel system that separates adjacent drifts (Fig. 7). Drilling at Site 1095 was intended to examine the earlier stages of drift development and glacial evolution and (together with Site 1096) to answer specific questions related to the state of glaciation of the continent:

1. Is the present depositional system a plausible analog for the older depositional environment reflected within the cored section?
2. Was deposition cyclic within the lower part of the drift section? What are the cycle frequencies and what does any such cyclicity represent?
3. Is there a relationship between drift development and continental glacial history? Can the onset of the present stage of continental glaciation (involving regular ice-sheet excursions to the shelf edge) be recognized in the drift sediments?
4. Can the terrigenous fraction be used to examine the uplift history of the Antarctic Peninsula?

These are ambitious objectives, and not all can be addressed immediately.

About 7 days were spent recovering (effectively) a double advanced hydraulic piston corer (APC) record to about 85 meters below seafloor (mbsf), with one hole deepened by APC and extended core barrel (XCB) to 561 mbsf and logged. Drilling in the deep hole was ended after clogged jets had dramatically reduced recovery when ship heave became excessive. One APC hole was lost to iceberg approach, and part of the logging was impeded by ship heave. Recovery was complete in the double APC section and was 89% down to 484 mbsf in the deep hole. The multiple records from the upper section have been spliced, using primarily magnetic susceptibility, and a common depth provided.

The sedimentary section extends from the Holocene to the early late Miocene at 480 m (Fig. 8). It comprises alternations of predominantly fine-grained terrigenous and hemipelagic deposits, containing only trace amounts of inorganic and organic carbon (<0.1 wt%). The uppermost 50 m consists of laminated and massive, often extensively bioturbated, diatom-bearing silty clays. Diatoms, radiolarians, and benthic and planktonic foraminifers all indicate a Quaternary age, and sedimentation rates are low (2.5 cm/k.y.) (Fig. 9). These deposits show a marked cyclic pattern of alternating gray, terrigenous, and brown biogenic-rich silty clays, the stratigraphic expression of successive glacial and interglacial cycles. Weak bottom (contour) currents influenced depositional patterns, with the bulk of fine-grained sediment probably introduced by dilute muddy turbidity currents. The base of the unit is marked by an increased frequency of parallel-laminated silty clay turbidites and beds of silty clay containing abundant ice-rafted debris.

The thickest lithostratigraphic unit at Site 1095 extends from 50 down to 435 mbsf and consists mainly of green laminated silts and muds of Pliocene and late Miocene age. Sedimentation rates are higher (5 to 7 cm/k.y.). Some intervals appear barren, based on limited shipboard sampling, but biostratigraphic control is usually good. Reworking of late Miocene diatoms is common. Cycles in which structureless, intensely bioturbated sections up to 1 m thick (with marked color changes and enhanced concentrations of ice-rafted debris), alternating with sections of abundant thin, graded silt laminae (distal turbidites), are interpreted as glacial cycles that controlled sediment supply. Longer period variations in construction of the continental shelf may be reflected in coarsening- and fining-upward trends. At the top of this unit lies a possible debris flow (seen in only one of two core sections) and, from paleomagnetic and seismic reflection evidence, a possible brief hiatus. Below 285 mbsf, in the late Miocene, is seen the neritic diatom *Paralia sulcata,* suggesting the existence of a shallow continental shelf.

Sediments below 435 mbsf at Site 1095 consist of nonbioturbated parallel-laminated siltstone-claystones with sporadic occurrences of late Miocene diatoms. This facies (thin-bedded turbidites) does not show the second-order cyclic pattern observed in overlying sediments, which may be significant for understanding glacial history. Core recovery is very poor below 480 mbsf and the lowermost sediments appear barren, so the age of the deepest sediment cored is uncertain. Core-based magnetostratigraphic control is excellent to this point, and geologic high-sensitivity magnetic tool (GHMT) log data show signs of being able to extend control to the base of the hole. Sedimentation rates are higher still, reaching 12 cm/k.y. (Fig. 9).

The characteristics of cores retrieved at Site 1095 are consistent with a distal deep-water setting accessible (until the Quaternary) to small-scale turbidity currents. The pronounced cyclicity of the depositional record is evident in visual core description and is recorded to date in color scanner, magnetic susceptibility, gamma-ray attenuation porosity evaluator (GRAPE), and downhole magnetic (GHMT) logging records, as well as (probably) in clay content. Preliminary shipboard analysis has shown this record to contain Milankovic orbital frequencies, which will allow comparison with the low-latitude record of orbitally induced climate change. The downhole variation of occurrence of biogenic components is in general inversely related to sedimentation rate, owing either to variation in surface primary production or to dilution by terrigenous components. The most abundant biogenic component is diatoms, which normally account for 10%–30% but occasionally reach 60% of the sediment.

Ice-rafted debris (IRD) is ubiquitous in Site 1095 cores, a significant part of the total flux of terrigenous sediment to the site. IRD is readily identified because of the fine-grained nature of the host sediment and occurs as scattered sand grains and granules, isolated pebbles (lonestones), and as lenses of granules and sand. In the absence of core X-radiographs, estimates of IRD abundance are qualitative. A more detailed study of IRD flux through time is potentially valuable but cannot ignore changes in rates of background sedimentation. This is clearly demonstrated by low IRD content in rapidly deposited turbidite sequences and enhanced content in bioturbated intervals that most probably record slower sedimentation.

Site 1095 sediments generally contain only trace amounts of inorganic (<0.5 wt%) and organic

(<0.1 wt%) carbon. Interstitial water chemistry shows evidence of organic matter decay and other diagenetic reactions, however, including carbonate and silica dissolution, cation exchange, and perhaps apatite and dolomite precipitation.

The deep hole was logged with the triple combination (TC) and GHMT tool strings, as well as a vertical seismic profile (VSP) with 12 stations. Hole and core correlation with seismic reflection profiles crossing Site 1095 is well constrained using VSP seismic traces and velocities, multisensor track (MST) and discrete sample velocities, and log and core densities. VSP data also correlate with strong reflectors on seismic profiles between 500 ms and oceanic basement at 1200 ms.

Site 1096

Site 1096 is the more proximal and the more elevated of two sites on a hemipelagic sediment drift on the continental rise off the northwestern Pacific margin of the Antarctic Peninsula (Fig. 2). Site 1096 lies in 3152 m of water close to the crest of the drift and was drilled to obtain the shallower part of the stratigraphic section, where it is most expanded (Fig. 10). With the more distal site (1095), Site 1096 was intended to answer specific questions about the state of glaciation of the continent. In particular:

1. Is the present depositional system on the drift, known from shallow piston cores, a plausible analog for the older depositional environment, as seismic profiles suggest?
2. Was deposition cyclic in the older part of the section? What are the cycle frequencies, and what does such cyclicity represent?
3. Is there a relationship between drift development and the glacial state of the continent, and can the glacial state be inferred from examination of the drift sections?

Not all of these questions can be answered immediately, but shipboard work provides the basic information needed.

In almost 9 days on site, we recovered a complete double APC section to 120 mbsf, extended the cored section to 607.7 mbsf by XCB drilling, and then logged the hole. Operations were not straightforward: clogged jets required a round trip, logging was achieved in two halves (upper and lower) because of a bridge, and the Formation MicroScanner (FMS)–sonic and well-seismic tools were not run because the hole had become too wide.

The sedimentary section extends from the Holocene to the early Pliocene (~ 4.7 Ma) at 607 m (Fig. 8). Sediments are predominantly fine-grained and terrigenous and are divided into three depositional units. Unit I (0 to 33 mbsf) consists of laminated and massive, often intensely bioturbated, diatom-bearing silty clays of Pleistocene age. These have a well-defined alternation of biogenic-rich and biogenic-poor horizons, which are the stratigraphic expression of glacial/interglacial cycles. Sedimentation rates averaged 7 cm/k.y. (Fig. 11). The top of Unit II is placed at the first appearance downcore of common parallel-laminated silt and mud turbidites. Unit II is a late-Pliocene to Pleistocene partly turbiditic succession some 140 m thick (33 to 173 mbsf) with a calcareous biogenic component, generally low. Sedimentation rates averaged 9 cm/k.y. Although the turbidite silts are thin and subordinate to muds, two coarsening-upward sequences may be discerned in the upper part of Unit II. A massive, well-sorted sand turbidite occurs at 112 mbsf. Unit III, Pliocene in age, extends from 173 mbsf to the bottom of the hole at 607.7 mbsf. It is composed of alternations, up to tens of meters thick, of (1) very thinly laminated and generally nonbioturbated clays derived from muddy turbidity currents and (2) intensely bioturbated homogenous silty clays with a higher biogenic component. Overall, Unit III has a sedimentation rate of 18 cm/k.y., although fluctuations in deposition rate may be recorded by intervals of intense bioturbation with more abundant ice-rafted debris. The biogenic component of Unit III is siliceous.

In Units II and III, the alternation of laminated turbidite facies and bioturbated hemipelagic facies records cyclic fluctuations in sediment supply and transport processes. Some of these fluctuations may be related to glacial/interglacial cycles along the Antarctic Peninsula margin similar to those identified within Unit I, but longer period cycles also exist. Likely proxies for glacial/interglacial variation include magnetic susceptibility, color reflectance, and clay-mineral composition.

Above 170 mbsf (Units I and II), the sediments contained calcareous nannofossils and foraminifers. The latter are rare to abundant only in this upper interval of Site 1096. *Neogloboquadrina pachyderma* sinistral dominates the planktonic foraminiferal assemblage. Benthic foraminifers are rare and consist mostly of shallow-water species presumed to be reworked from the continental shelf. Calcareous nannofossils provide the datums in this upper interval. Reworking is evident in the upper 170 m, with some samples containing an entire reworked assemblage. Radiolarians are present in several intervals, but the marker species for the two zones below Psi (Chi and Phi) were not found. In the upper 110 m, the diatom zonal boundary markers are not seen, and samples studied from 110 to 165 m are barren of diatoms. From 170 to 608 mbsf (Unit III) siliceous microfossils dominate, but the planktonic foraminifer *N. pachyderma* sinistral is seen to the base of the hole. The record of radiolarians is relatively complete for Unit III, and most of the marker species are present through the entire Upsilon Zone. The diatom record for the lower part of this site is also virtually complete, with zonal datums being available for nearly all the zones.

Magnetostratigraphic data from Site 1096 show promise. The Brunhes/Matuyama boundary is very well defined at 55 m. The Jaramillo and Olduvai Subchrons are not ideal for magnetostratigraphy because part of the interval shows a low remanent intensity resulting in a noisy inclination record. Below this, reversals are well defined, the oldest reversal observed being the onset of Chron C3n.2n (4.62 Ma) at 585 mbsf.

Physical properties and chemical data are interesting: below 170 mbsf grain density is reduced, and porosity increases steadily downhole within Unit III. Heat-flow measurements suggest that the base of the methane hydrate stability zone lies at about 290 m, but a gas hydrate bottom-simulating reflector (BSR) is not seen. The diffuse BSR at about 700 ms in the seismic section, not reached by coring, is assumed to be from silica diagenesis. A total of 172 bulk sediment and 35 interstitial water samples from Site 1096 have been analyzed. The sediment generally contains only minor amounts of inorganic (<0.1 wt%) and organic (<0.6 wt%) carbon, yet the interstitial water chemistry shows clear evidence of organic matter decay, with the sulfate reduction zone extending to 50 mbsf. Other diagenetic reactions occurring include carbonate precipitation, silica dissolution, cation exchange, and perhaps disseminated apatite precipitation. Methane concentrations were high and caused expansion in most cores, but methane/ethane ratios stayed above 200 to the base of the hole.

The deep hole was logged under unstable hole conditions, which both limited and complicated the operation. In total, the porosity-density–natural-gamma tool string was deployed through almost the entire hole (from 556 mbsf) and the GHMT (magnetic) tool between 510 and 356 mbsf. Natural-gamma activity was logged to the seafloor, and clay content can be estimated after correction for the gamma attenuation of the pipe.

Seismic unit boundaries defined at Site 1095 were traced across multichannel seismic (MCS) profiles to Site 1096. Only the upper three were penetrated at Site 1096 because of more rapid sedimentation.

Site 1101

Site 1101 is located in 3509 m water depth on the continental rise of the Pacific margin of the Antarctic Peninsula, centrally within a sediment drift approximately 500 km northeast of Sites 1095 and 1096 (Figs. 2, 12). Because the sediment drift (Drift 4) is much smaller than that drilled at Sites 1095 and 1096 (Drift 7), the site is no farther from the continental margin than Site 1096.

Site 1101 was chosen to answer questions raised by drilling at Sites 1095 and 1096:

1. Is the sedimentary record obtained at Sites 1095 and 1096 representative of the entire Pacific margin of the Antarctic Peninsula?
2. Does the regional correlation between seismic units observed in MCS profiles reflect actual lithological and stratigraphic correlation?
3. Can we test the hypothesis that sedimentary evidence of the late Pliocene Eltanin meteorite impact is to be found at Site 1096 as a coarse and well-sorted massive sand bed in a predominantly fine, muddy sedimentary sequence? Is a similarly anomalous sedimentary event to be found on a different drift?

The opportunity to drill Site 1101 came from the persistently unfavorable sea conditions encountered on the continental shelf (exceeding a 2-m limit on vessel heave during shallow-water drilling). In less than 2 days, a single hole was APC cored to 142.7 mbsf and extended by XCB drilling to 217.7 mbsf with 99.1% recovery. Having recovered the shallow section at Site 1101, and with improving sea conditions, the ship returned to shelf Hole 1100D.

Recovered sediments consist of 217.7 m of predominantly hemipelagic clayey silt that contains a nearly continuous distal glacial record of the past 3.1 to 3.4 m.y. (late Pliocene to present) (Fig. 21). Unit I (0–53.3 mbsf) and Unit II (53.3–142.7 mbsf) are composed of alternating biogenic-bearing massive clayey silts and laminated clayey silts that we interpret as sedimentary expression of interglacial and glacial periods, respectively. Sedimentation rates are fairly steady at about 7 cm/k.y. in the top 120 m, but a period of slow sedimentation may occur toward the base of Unit II (Fig. 13). Within Unit I, warm oxygen isotope stages are identified by diatom-bearing layers. Unit II has at least 19 discrete foraminifer-bearing layers in which carbonate concentration can be as high as 28 wt%, which alternate cyclically with barren laminated or massive intervals. Extremely well-developed cyclicity in magnetic susceptibility matches variation in color reflectance and the alternation of biogenic and terrigenous intervals in Units I and II. Unit III (142.7–217.7 mbsf) lacks the regular variation in carbonate content of the overlying units. Its upper part (above 198 mbsf) contains massive, barren clayey silt that could have originated in turbid plumes or sediment gravity flows from glaciers near the continental shelf edge as well as thin diamicts (deposited by ice rafting). The lower part of Unit III may represent a warmer interval with deposition of diatom-bearing massive and laminated facies. Sedimentation rates in Unit III are less well defined but may reach 10 cm/k.y.

Calcareous microfossils were found in the uppermost core as well as in carbonate-rich intervals between 50 and 134 mbsf (Unit II). Siliceous microfossils were found throughout the core and become more abundant in the lowest three cores. Several planktonic foraminiferal oozes were identified, mostly in Unit II. The only ooze in Unit I occurs in marine isotopic Stage 5. More than 90% of these assemblages are *N. pachyderma* sinistral with rare *N. pachyderma* dextral and *Globigerina bulloides*, plus benthic foraminifers. The carbonate-rich interval appears coeval at Sites 1101 and 1096. Calcareous nannofossils were recovered in the upper 120 m. The first and last occurrence of the large form of *Gephyrocapsa* spp. was observed, making the nannofossil record at Site 1101 more complete than at Site 1096. Diatoms were present throughout the hole, with alternating good preservation and barren intervals. The lowest six cores contain more diverse, abundant assemblages of diatoms than found above. Radiolarians were generally abundant and moderately preserved with only two barren intervals. The Psi through Upsilon Zones (Pleistocene–Pliocene) were recovered. Reworked late Pliocene assemblages (thick-shelled) occurred in the Pleistocene part of the section, which contained thin-shelled in situ specimens.

The Brunhes/Matuyama boundary occurs at ~55 mbsf, the same depth as at Site 1096. Site 1101 has the most complete, well-defined Matuyama epoch reversals of all of the drift sites. Coring disturbance in Core 178-1101A-16H appears to affect the record of the Reunion event. The termination of Chron C2A (2.58 Ma) was observed at approximately 170 mbsf, and the onset of

C2An.1n (3.04 Ma) was found at 210 mbsf.

The interstitial water chemistry profiles at Site 1101 closely resemble those of the upper 250 mbsf at Sites 1095 and 1096, reflecting the strong similarity in moderate sedimentation rates (5–10 cm/k.y.) and low organic carbon contents (<0.4 wt%) among the three rise sites. Sulfate decreases to zero and manganese reaches a minimum concentration at 130 mbsf, where measurable concentrations of methane and ethane first occur. Other indicators of organic-matter decay, such as alkalinity and ammonium, increase with depth and reach maximum values at the bottom of the hole. They probably continue to increase at greater depths, based on comparison with Sites 1095 and 1096. Dissolved silica concentrations remain high throughout the hole and reach the solubility limit of opal-A at 150 mbsf near the top of Unit III, suggesting that biogenic opal dissolves principally between 0 and 150 mbsf and that the interstitial water becomes saturated with respect to silica in Unit III. Dissolved calcium increases significantly downhole in the upper 50 mbsf, then decreases to a minimum at 130 mbsf near the base of the sulfate reduction zone. It increases again at the bottom of the hole. The low content of calcareous microfossils in Units I and III could therefore be traceable to dissolution of carbonates.

Porosity initially decreases downhole, as might be expected under normal consolidation conditions. However, porosity rises again below 140 mbsf. At Site 1101, we found a weak positive correlation between siliceous biogenic content and porosity, which was seen previously at Sites 1096, 1098, and 1099. This suggests that the presence of significant amounts of rigid, siliceous biogenic material in the sediment, associated with a relatively fast sedimentation rate, renders the lower part of the drift sedimentary column underconsolidated.

Continental Shelf Sites (1097, 1100, 1102, and 1103)

Site 1097

Site 1097 is located on the outer continental shelf of the Antarctic Peninsula in 552 m water depth, some 14 km from the continental shelf edge (Fig. 2). It lies in a topographic low between two of the lobate depocenters where the uppermost, fully glacial progradational sediment Sequence Groups S1 and S2, recognized in seismic data on the continental shelf, are best developed (Fig. 14). It was selected to examine the underlying Sequence S3 where that sequence would be more easily accessible, being less deeply buried. The nature of S3 was unknown, and the site was intended to examine Antarctic Peninsula paleoclimate before the fully glacial sediment sequence groups were deposited.

Drilling at Site 1097 was slow and difficult for three main reasons. First, the nature of the sediments (unsorted, including large clasts) confined us to rotary-core-barrel (RCB) drilling, not the best way of recovering the soft till matrix, and dictated a slow start. Second, icebergs interrupted drilling on two occasions; and third, limitations on ship heave in water depths less than 650 m also halted drilling twice. In rather more than 5 days, Site 1097A was drilled to a depth of 436.6 mbsf. The sediment shows glacial influence in all of the recovered intervals, including S3. Recovery varied from about 2.3% in the uppermost 80 m of Sequence Group S1 to 18% in Sequence Group S2 down to 150 m, and to 16% in S3.

Recovery was too poor for S1 to be described or dated. Material recovered from the underlying S2 is massive diamict, defined as poorly sorted sediment, with clasts supported by a muddy matrix. It appears to reflect subglacial deposition, in keeping with seismic reflection interpretations of the nature of S2. The age of S2 at this site is constrained, mainly by diatoms (*Fragilariopsis barronii* and upper part of *Thalassiosira inura* Zones) supported by a radiolarian assemblage (Upsilon Zone) with a broader age range, to younger than 4.6 Ma and older than about 3.8 Ma. The boundary between S2 and the underlying S3 (seen as conformable in presite seismic survey) lies within the upper *T. inura* and Upsilon Zones, at about 4.5 to 4.6 Ma.

S3 sediments are more variable but include similar massive diamicts, clast-rich with sizes ranging up to boulders (a 0.5-m granite boulder was drilled within S3), and containing reworked diatoms and foraminifers (as do S2 diamicts). Diamicts are interpreted as deformation tills formed by subglacial reworking and transport of marine muds because of a grounded ice sheet that periodically occupied the continental shelf (Fig. 15). Stratified diamicts in one core, with erosive bases that grade upward to clayey silt with dropstones, are interpreted as debris flows that occurred near the ice-sheet grounding line. Laminated and massive bioturbated muds contain variable amounts of iceberg-rafted debris and are considered glaciomarine. They show evidence of soft-sediment deformation that could be the result of iceberg turbation.

Biofacies variation throws light on the changing depositional environments sampled within S3. Three biofacies were distinguished—based on the degree of reworking of benthic foraminifers and other biogenic matter—that reflect subglacial deposition, ice-proximal deposition, and open shallow-marine shelf conditions (Fig. 15). On this basis, the topmost sediments of S3 are subglacial, as is S2. However, they are marine from 180 to 210 mbsf, subglacial from 220 to 290 mbsf, and vary between more marine and ice proximal beneath. This variation reflects periodic migration of the ice-grounding line across the continental shelf.

Preliminary biostratigraphic age determination of Sequence S3 was difficult because of reworked forms, but two possible diatom age constraints are (1) older than 4.85 Ma below 218 mbsf and (2) younger than 5.6 Ma below 289 mbsf. Radiolarians suggest an age older than 4.6 Ma below 294 mbsf. Regional similarities in benthic foraminifers suggest an early Pliocene age for much of S3 at this site. Paleomagnetic measurements show some stable high-inclination directions, others stable but low inclination (possible debris flows), and still others (diamicts) unstable. At this time, in the absence of clear biostratigraphic age constraints, a magnetostratigraphic interpretation is unjustified.

Downhole logs were not run because of hole instability, and many shipboard measurements on Site 1097 cores were of limited value because of poor recovery. The physical properties data are sparse, but porosity in Unit II as low as 30% may be attributed to subglacial shear consolidation. Also, natural gamma activity drops toward the base of the hole, matching a general decrease in clay content. Limited velocity and density measurements prevent an accurate correlation between hole and seismic profiles but serve to clearly distinguish the seismic sequences.

Drilling at the site was sufficient to confirm the nature of S1 and S2 and to establish the upper part of S3 as glacial (although perhaps less fully glacial than S1 and S2). The age and nature of the S3/S2 boundary were established.

Shelf Transect Sites (1100, 1102, and 1103)

A central objective of Leg 178 was to sample, date, and understand the glacially transported, unsorted sediments deposited in a generally progradational wedge on the outer continental shelf and continental slope. On the Antarctic Peninsula continental margin these sediments are focused into four lobes, in which both shelf topsets and progradational shelf foresets are maximal. The entire West Antarctic margin, however, to at least 105°W, shows the same seismic sequence groups. The main approach to this problem by Leg 178 was to drill a suite of sites along a transect through a well-developed progradational lobe off Anvers Island. Four sites were planned to describe the main changes in depositional geometry within the lobe (Fig. 16). An additional site (Site 1097) had already been drilled in an interlobe area to the southwest, where the deeper section, beneath the main glacial sequence groups, was more accessible.

We attempted three sites (1100, 1102, and 1103) along the shelf transect, with mixed success. One problem was the difficulty of recovering the sediment, which is unconsolidated in the upper section: it is ice-transported, so essentially unsorted, with hard clasts (some very large) within a soft, fine-grained matrix. Another, crucial problem was the 2-m limitation on vessel heave during shallow-water drilling, which severely slowed progress at all shelf sites but particularly at Sites 1100 and 1102. Site 1100 was chosen to sample and date the boundary between the two main glacial seismic sequence groups (S1 and S2), where S1 topsets overlie truncated S2 foresets at about 350 mbsf. The site lies at the edge of an area of hummocky, ice-scoured topography that has been interpreted as the top of a subglacial till, produced by the last ice-sheet advance. Four holes were drilled with very poor recovery in about 4 days. The deepest hole, 1100D, reached 110.5 mbsf but with only 4.8% recovery. By then, repeated pipe trips had so degraded the hole condition that the deep target (~400 mbsf) was judged impracticable.

The only core of Hole 1100C recovered 4.05 m of massive diamict, clast-rich in places and with a diatom-bearing silty clay matrix. In Hole 1100D, only the top three core catchers contained any trace of diatoms, with Section 178-1100D-3R-CC offering the most diverse assemblage. Traces of recrystallized and reworked radiolarians occurred in most core-catcher samples. Foraminifers were rare, and no age inferences can be drawn from the material examined because of the poor nature of preservation. In essence, faunas are open shelf, marine, but abraded. The sediments, poorly consolidated diamicts throughout, have been interpreted at the top of the section as tills and glaciomarine muds, reworked by iceberg grounding. They are useful analogs for deeper sediments at other shelf sites.

Site 1102, at the edge of the continental shelf in 442 m water depth, was selected to examine S1 foresets on the uppermost slope. Four holes were attempted in 1.5 days on site, but excessive heave limited penetration to 7 m at the first two. A camera survey of 50 m radius around the site bottom, undertaken while waiting on heave, showed massive rock boulders grading to a fine sediment cover, allowing Hole 1102C to be better located. Further heave curtailed 1102C at 6.5 m, but when this receded, very difficult conditions in Hole 1102D persuaded us that the rock carapace evident on the television images was thicker than anticipated and would prevent establishment of a stable hole. The rock field at the shelf edge may be the result of the sorting of tills by repeated iceberg scour, with bottom-current removal of suspended fines. Such a carapace may survive at paleoshelf breaks or may have been removed during a subsequent glacial advance.

Site 1103 was our final chance, at the inshore end of the shelf transect in 494 m water depth. Drilling might sample up to 250 m thickness of young S1 glacial topsets, with a deeper target, S3 glacial sediments, most likely slightly older than those reached in our other successful shelf hole at Site 1097. The long swell went away, and we were able to drill to 362.7 mbsf in about 3 days until drilling time expired. Recovery from the upper 247 m was only 2.3% but improved to 34% in the lower 115 m where the matrix became hard. We logged to 240 mbsf.

In the absence of a continuous sedimentary record, stratigraphic subdivision was not attempted. Three lithofacies, however, could be distinguished within the lower 115 m: (1) diamictites, (2) poorly sorted sandstones, and (3) muddy siltstones, interpreted as reflecting deposition on a glacially influenced slope (Fig. 17). Massive diamictites lack internal structure, but there are composite successions where thinner, massive diamictites are interbedded with thin zones of crudely stratified facies defined by deformed mudstone stringers. Because these stringers may demarcate bed contacts if muds are deposited on bed tops between gravity flow events, they were subsequently reworked. Textural grading in deformed mudstones might indicate they were emplaced as thin turbidites. Consequently, composite diamictite successions can be interpreted as the result of alternating debrite and turbidite deposition. The scale of downslope movement is uncertain, and therefore so is the environment of deposition. Protracted downslope motion results in the generation of mature, well-sorted, graded sandstones, but sandstones here are compositionally immature and poorly sorted. Diatoms are very rare and poorly preserved, and siltstone clasts are a source of reworked diatoms. A setting is indicated on a glacial continental shelf or slope, close to a source of poorly sorted debris. Biofacies are insufficient to constrain age, water depths, or position relative to the shelf break, but the open marine influence is less evident than at Site 1097.

Age-diagnostic biostratigraphic material is sparse in the poorly recovered upper part and is partly reworked in the lower part. Diatom valves were often fragmented beyond identification, yet these fragments could be abundant in the material recovered. From the top of the hole down to 210 m, several biostratigraphically important species (*Actinocyclus ingens, F. barronii, T. insigna, T. inura, T. oestrupii,* and *T. torokina*) were periodically present, allowing dates younger than their first appearances to be established. Below, identifiable diatoms were more sparse. Samples from ~290 m had some diatoms of low abundance and diversity (*Denticulopsis* spp., *Nitzschia januaria,* and *Rouxia californica*), possibly of late Miocene age. (Because of the preservation state of the assemblage, however, the sediment may not be of this age.) Radiolarians were sparse in core-catcher samples, precluding any biostratigraphic determination. Reworked Cretaceous radiolarians were present in four out of five of these. Sample 178-1103A- 24R-CC (228.0 mbsf) contained radiolarians from the Upsilon Zone, but marker species were not encountered in any other sample.

The foraminiferal fauna in core-catcher samples down to 218 mbsf contain rare, well-preserved, and white-colored *N. pachyderma* sinistral and older, reworked, darker colored benthics and planktonics, together with *Inoceramus* prisms and sponge spicules. Below 250 mbsf foraminifers are rarer with more evidence of reworking, but Samples 178-1103A-31R-CC and 33R-CC include a well-preserved assemblage of the shelf species *Cassidulinoides parkerianus.* The lowest three samples, 178-1103A-35R-CC to 38R-CC (338.77 to 355.34 mbsf), are barren. Several of the upper cores (178-1103A-13R, 14R, 15R, 17R, and 18R) contain partly dissolved calcareous nannofossils. No identifications were possible, but coccolith production is indicated.

At Site 1103 we measured the magnetization of cores spanning 250–350 mbsf. As with previous shelf sites, diamicts yielded unstable directions, and finer grained lithologies were stable. The low recovery and sparse occurrence of these lithologies make construction of a magnetostratigraphy difficult at this time. It may be possible to combine GHMT and split-core paleomagnetic data.

Hole 1103A was logged with the TC, GHMT, and FMS-sonic tool strings over an upper 150-m interval where there was no significant core recovery, but a blockage at 242 mbsf prevented penetration lower into the hole. The narrow hole diameter made for good-quality logs. Porosity varied between 30% and 50% (lower than at the rise sites), showing a change to higher porosity only at the base of the log below 225 mbsf, close to the lithified diamictite seen below 250 mbsf in the core. Resistivity and susceptibility display broad peaks and troughs, and individual clasts can be seen in FMS images, which are all of high quality. Distinct zones of spikes in the GHMT magnetic field log probably indicate clast-rich intervals. The magnetic induction of the sediment causes most of the remaining field anomaly, and it remains to be seen whether magnetic polarities can be determined for the clast-free intervals. Log sonic velocities, combined with Hamilton frame *P*-wave velocities from the lower hole, should allow the seismic record to be tied to drilling results. Poor core recovery from Site 1103 also means that there is no continuous MST record; physical properties data interpretation is therefore limited. Initial investigation suggests that the laminated beds below 250 mbsf are derived from the diamicts, or the same material source. Interestingly, this source differs from that at Site 1097, also on the shelf.

Palmer Deep Sites (1098 and 1099)

Sites 1098 and 1099 (Figs. 2, 18) lie in the inner-shelf basins of Palmer Deep, south of Anvers Island, where an expanded, mainly biogenic sediment record has accumulated since the retreat of the ice sheet. The prime site, 1098, was in the small, narrow Basin I, in 1012 m water depth. Site 1099 was in Basin III, a larger basin at 1425 m water depth. Seismic profiles had shown that sediments in Basin I were thinner than in Basin III (Fig. 19), but short piston cores showed that the sediment record in Basin I was less prone to deposition of locally derived turbidites. Drilling would provide an ultrahigh-resolution paleoclimatic record of the Holocene that would show short-term (200 yr) and longer-term (2500 yr) cyclic variation most probably related to global climate variation. It would then be compared with similar records from drilling in the Cariaco Basin, Santa Barbara Basin, and Saanich Inlet and with the record from ice cores.

Three APC holes extended to basement at 47 mbsf at Site 1098, and at Site 1099 a single section was recovered to 108 m (Fig. 20). At Site 1098 we recovered diatom oozes to diatom-bearing mud. Deposition was by pelagic settling of diatom blooms and by gravity flows from the steep margins of the basin. Three prominent silt or sand turbidites occur between 23 and 40 mbsf. The uppermost is nearly 4 m thick, graded from diatom-bearing sandy muds to ooze, and shows a magnetic-susceptibility high induced by the terrigenous component. Slumped and inclined diamict and thin-graded fine sand-silt beds were seen at the base of the holes, but most of the sequence at Site 1098 is horizontally bedded and finely laminated.

Laminae are diatom oozes of different species composition. Microfossil preservation is excellent, and this site will provide an unparalleled record of Antarctic Holocene paleoproductivity. Variation in magnetic susceptibility may show 200- and 2500-yr cyclicity in broad intervals of high susceptibility from 0 to 8 mbsf and 30 to 38 mbsf. Cores provide an extremely high-resolution record of variation in geomagnetic field direction. GRAPE densities show the turbidite sequences between 24 and 30 mbsf, superimposed on a general trend of increasing density with depth. The approach to basement is marked by a greater increase in density coincident with the lithologic change to terrigenous silt and sand at around 42 mbsf. Natural gamma levels may show some cyclicity on the order of 10 m while generally increasing downhole. Sampling for interstitial water at unusually high resolution (one per section) resulted in puzzling profiles of interstitial water chemistry at Site 1098. The sulfate reduction zone lies between 20 and 30 mbsf. Organic matter decay has surprisingly little effect on interstitial water chemistry above the sulfate reduction zone. Despite relatively high organic carbon content (1.0–1.2 wt%) and extremely rapid sedimentation, alkalinity, ammonium, and phosphate, direct by-products of organic matter decay, increase only slightly with depth in the upper 20 m. We speculate that the tightly encased *Chaetoceros* spores, the majority of diatoms in Palmer Deep, render organic material unavailable for bacterial consumption until dissolution breaches the external casing.

Site 1099 recovered a diatom ooze section like that of Site 1098 but greatly expanded by biogenic turbidites (Fig. 20). The lowest 20 m contained black, organic-rich, laminated diatom ooze. The major diatom species at Sites 1098 and 1099 reveal a downward trend of decreasing open-ocean influence and increasing sea-ice and basin restriction. Other microfossils show similar trends: radiolarians are common and well preserved in the upper 28 mbsf of Site 1098 with relatively diverse assemblages, but diversity and abundance gradually decrease to zero at the bottom of the hole. At Site 1099 the pattern of decreasing abundance and diversity downcore is similar, but it occurs over 108 m (the record was expanded because of increased terrigenous supply). Benthic foraminifers are well preserved and abundant in the upper 87 m of Hole 1099A. They appear similar to previously reported benthic foraminiferal fauna of the Bellingshausen Sea, fluctuating between open ocean (Circumpolar Deep Water [CDW]) and shelf-water conditions and tied to 200-yr productivity cycles. However, beneath 87 mbsf in Hole 1099B, the depth of the highest black interval, the microfossil assemblages suggest more restricted oceanographic conditions (decreased CDW influence and colder shelf waters). Samples at the bottom of the hole contain large amounts of pyrite and a few foraminifers.

The sulfate reduction zone at Site 1099 lies between the seafloor and 10 mbsf, shallower than at Site 1098, and is accompanied by a steady downward increase in alkalinity and ammonium. The unusual interstitial water chemistry profiles of Site 1098 are not found at Site 1099, but organic carbon contents are comparable. Overall, at Palmer Deep sites, organic carbon content was 1.0–1.5 wt%, and the effects of organic matter decay were an order of magnitude greater than at the continental rise sites (1095, 1096, and 1101).

MST data for the three holes at Site 1098 allow good correlation between holes to the full depth and match previous measurements on shallow cores in their upper part. The two broad intervals of high magnetic susceptibility at 0–8 and 30–38 mbsf are also marked in gamma-ray attenuation density. Deep-tow boomer records around Site 1098 show an upper stratified seismic unit and a lower, more transparent, unit. The base of the stratified unit corresponds at Site 1098 to the change from mainly bioturbated to mainly laminated sediments. At Site 1099, using a synthetic seismogram derived from MST data, eight distinct reflectors in the deep-tow boomer section correlate exactly with distinct turbidite horizons. A widespread, strong mid-basin reflector beneath them coincides with a sand and pebble layer at 33 mbsf.

Conclusions

Nine sites on the Pacific margin of the Antarctic Peninsula were drilled during Leg 178 in three depositional environments. Four (1097, 1100, 1102, and 1103) were on the glacial, overdeepened outer continental shelf to investigate sediments deposited by grounded ice over the past 10 m.y. Three (1095, 1096, and 1101) were on sediment drifts on the continental rise to examine the fine-grained component of glacial shelf sediments. These sediments, moved there by turbidity and bottom currents, contain a more complete, higher resolution, more easily recovered and dated glacial record. The two remaining sites (1098 and 1099) were drilled in Palmer Deep, an isolated basin of the inner shelf that contains an ultrahigh-resolution record of Holocene paleoenvironmental change.

The outer continental shelf sites and the rise sites are complementary: the more direct but less complete record on the shelf helps interpretation of the record on the rise. Together they provide insights useful in attempts to recover the much longer but possibly less-accessible record of East Antarctic glaciation. The inner-shelf basin record was assumed to represent regional paleoclimate and will be compared with records from similar environments drilled by ODP (Cariaco Basin, Santa Barbara Basin, and Saanich Inlet) and with ice-core records.

Sites 1095, 1096, and 1101 on the continental rise sediment drifts provided virtually continuous cores, back to about 10 Ma at Site 1095, 4.5 Ma at Site 1096, and 3.1 Ma at Site 1101 (Figs. 2, 3, 7, 10, 12). The depositional environments at the sites were different, ranging from a dominantly hemipelagic mode on the rise crest and center to a dominantly turbiditic mode at the distal site (Fig. 8). However, none of the sites was an end-member environment: the distal site received mainly fine-grained distal turbidites but with a substantial hemipelagic/pelagic component, and the rise-crest sites were not isolated from deposition of fine-grained graded beds within a dominantly hemipelagic environment. All sites revealed a cyclicity in sedimentation that, whatever the dominant depositional mode at the site, was considered to reflect the cyclic provision of glacial sediments to the uppermost continental slope. Concerning the value of drilling at this margin as a guide to drilling at other Antarctic margins, this mixed depositional environment was an advantage: few of the other drifts around Antarctica are as isolated from distal turbidite deposition as Drift 7 (Site 1096). It is therefore reassuring to know that a signal of cyclic glacial loading of the upper slope is provided also, within even a dominantly turbiditic environment such as Site 1095.

Sedimentation rates were highest on the drift crest (Site 1096 [Fig. 11]) and lowest on the distal flank (Site 1095 [Fig. 9]) as expected. At all three sites, the rates decreased through the Pliocene and into the Pleistocene (Fig. 21). The high rates make possible a detailed study of cyclicity in deposition. No such investigation has progressed far as yet, but it is reassuring to know that several parameters show a variability with a period similar to the Milankovic cyclicity seen in lower latitudes (notably 40 k.y. within the Pliocene). This includes lithologic alternations (turbidite abundance, bioturbation, possibly IRD, and color), magnetic susceptibility, and density (cores and logs). Clay mineralogy appears to have glacials and interglacials variability (Fig. 22) and could become a useful additional proxy. We even recovered nannofossils and foraminifers through part of the Pliocene–Pleistocene, an unexpected bonus. It would seem clear that the continental rise is sensitive to variations in the glacial state of the continent and that these reflect the orbital variation in insolation through much of the period examined. A downward change at Site 1095 that sees no cyclicity before about 9 Ma marks a change in the level or nature of glaciation on the shelf, if not its initiation.

The objectives of drilling on the continental shelf were to test the pre-existing depositional model, to date major changes in depositional geometry (so these could be compared with changes in continental rise deposition), and to improve understanding of shelf sedimentation ahead of similar proposed drilling elsewhere around Antarctica. We drilled three sites on a dip transect of a depositional lobe (1102, 1100, and 1103, in landward order [Fig. 16]), and 1097 was drilled in an interlobe area farther south (Fig. 14). Drilling was severely hindered by swell, and recovery was made difficult (as expected) by the unsorted nature of unconsolidated subglacial tills and related diamicts. In drilling we were largely limited to the basic RCB technique, and recovery was very poor until the fine-grained matrix of a diamict became hard enough to support the large clasts that were inevitably encountered. Recovery then improved (e.g., to an average 34% below 250 m at Site 1103).

The glacial nature of the youngest sequence group (S1) was amply confirmed, and much of it could be given a Pleistocene or latest Pliocene age, but recovery was poor everywhere (the outermost shelf was particularly unfriendly). The most information on S1 is likely to come from the broad suite of logs obtained at Site 1103 (Fig. 23). Sequence Group S2 was sampled only at Site 1097, where it is thin; its older part is early Pliocene in age (Fig. 24). Sequence S3, whose age and origin were in doubt before drilling, was sampled at Sites 1097 and 1103. This sequence is continuous and similar in seismic expression (Fig. 16) along the West Antarctic margin to at least 105°W, and it lacks the focus into depositional lobes of the overlying S2 and S1. It was clearly established as a mostly glacial sequence, although probably reflecting a greater range of environments than S2 and S1 (from subglacial to glacial marine) and likely a lesser level of glaciation. The conformity of its top with the base of S2, deduced from seismic profiles in the region of Site 1097, was essentially confirmed by the age range for the boundary (between 4.5 and 4.6 Ma) established by drilling. Seismic data suggest that the part of S3 sampled at Site 1103 is older than at Site 1097. The inferred depositional environment at Site 1097, near the paleoshelf edge, was perhaps more open marine than that at Site 1103, although the depositional environment was of lower energy. It is uncertain whether this reflects a time change in climate or in depositional environment. Dating of the lower part of S3 is uncertain as yet but should be improved by a range of shore-lab studies. It seems unlikely that the recovered sediments range back to 9 Ma, the time of a change in shelf environment inferred at Site 1095 on the rise.

Preliminary results of drilling in Palmer Deep accorded with expectations based on piston cores. Basin I, the narrowest basin with the thinner sediment fill, is less affected by turbiditic sedimentation than Basin III. The 45-m-thick sediment fill of Basin I (Site 1098) contains mainly laminated and massive muddy diatom ooze, with laminae probably reflecting changes in surface productivity (Fig. 20). In Basin III (Site 1099), the alternation of laminated and massive muddy diatom oozes is interrupted more frequently by turbidites with a terrigenous graded base. The highly reflective lower seismic unit (Fig. 19B) is an alternation of thin turbidites and laminated diatom ooze, with a strong impedance contrast with the upper semitransparent unit. At this stage, we cannot say how the sedimentary records of the two basins correlate. The downhole change of diatom and foraminifer assemblages indicating more restricted oceanographic conditions at the base of Basin I and in the lower part of Hole 1099B suggests that the two recovered sections underwent a similar evolution and may therefore be approximately coeval.

Shipboard analysis of Palmer Deep cores was limited, with sampling mainly postponed to the

Bremen Core Repository. It is worth noting, however, that the only high-resolution shipboard study (of pore-water composition) revealed anomalous and still-puzzling chemical gradients. Despite the inferred rapid but steady accumulation of sediment, pore waters in the upper 20 m at Site 1098 reveal a homogeneous composition that suggests almost complete mixing. The explanation of these gradients will come from postcruise studies of the relationships between pelagic settling of organic-rich material, turbiditic sedimentation, and bioturbation.

Several additional opportunities offered by Leg 178 drilling are being exploited by the shipboard party. The continuous, high-resolution, partly terrigenous record of the continental rise drift sites—and the high southern latitudes of this leg—provide excellent paleomagnetic data (e.g., Fig. 25). They also present opportunities for a wide range of studies, including field paleointensity, rock magnetism, detailed examination of particular reversals, and the nature of certain cryptochrons. The Palmer Deep sediments should also provide high-resolution paleointensity and secular variation data. The existence of a detailed high-latitude magnetostratigraphy and the location of the rise sites in a low-energy environment securely within the Antarctic water masses provide further opportunities to check and refine high-latitude biostratigraphy. These will be further enhanced if an orbital chronology can be established.

Pore-water geochemistry is of interest at several sites, notably Palmer Deep, where it seems capable of informing the wide range of high-resolution investigations currently planned. The logging effort, though curtailed by hole conditions in places, also shows promise. In general terms, we have a wide range of physical properties and log data from a cluster of generically related environments that will repay closer study. This leg has seen the first-ever FMS examination of subglacial tills (at Site 1103), and the comparison between high-quality core magnetostratigraphy and the GHMT record at Site 1095 is likely also to be productive. VSP and sonic logs will aid correlation between the hole and the seismic record and allow the results of drilling to feed back into the exceptionally large regional seismic reflection data set.

An additional opportunity, not considered within either proposal or discussed in the leg prospectus, was to detect at the continental rise sites the late Pliocene Eltanin asteroid impact. The renewed interest was generated by Gersonde et al. (1997). The Leg 178 sites lay 1300 km distant from the likely impact area. The rise drifts, being at their crest perhaps only three-quarters of the water depth of the direct path, seemed areas where a sedimentological event might be detectable, helping to guide us to geochemical and paleontological anomalies that would otherwise be difficult to find. At present, until stratigraphic control has improved, the impact is not clearly identified within the sediments. Each rise site, however, shows a single anomalous depositional or erosional event that may be associated with it.

REFERENCES

Alley, R.B., Blankenship, D.D., Rooney, S.T., and Bentley, C.R., 1989. Sedimentation beneath ice shelves: the view from Ice Stream B, *Mar. Geol*., 85:101–120.

Anderson, J.B., Pope, P.G., and Thomas, M.A., 1990. Evolution and hydrocarbon potential of the Antarctic Peninsula continental shelf. *In* B. St. John (Ed.), Antarctica as an exploration frontier-hydrocarbon potential, geology and hazards. *Am. Assoc. Petr. Geol. Studies in Geology*, 31:1–12.

Barker, P.F., 1982. The Cenozoic subduction history of the Pacific margin of the Antarctic Peninsula: ridge crest-trench interactions. *Geol. Soc. London J*., 139:787–801.

Barker, P.F., 1992. The sedimentary record of Antarctic climate change. *Philos. Trans. R. Soc. London B*., 338:259–267.

Barker, P.F., 1995a. The proximal marine sediment record of Antarctic climate since the late Miocene. *In* Cooper, A.K., Barker, P.F., and Brancolini G. (Eds.), *Geology and Seismic Stratigraphy of the Antarctic Margin*. Am. Geophys. Union Antarct. Res. Ser., 68:25–57.

Barker, P.F., 1995b. Tectonic framework of the east Scotia Sea. *In* Taylor, B. (Ed.), *Back-arc Basins: Tectonics and Magmatism:* New York (Plenum), 281–314.

Barker, P.F., and Cooper, A.K., 1997. *Geology and Seismic Stratigraphy of the Antarctic Margin*. Part 2. Antarctic Res. Ser., V. 71, 187pp, AGU Washington, D.C.

Barron, J., Larsen, B., et al., 1989. *Proc. ODP, Init. Repts.*, 119: College Station, TX (Ocean Drilling Program).

Bart, P.F., and Anderson, J.B., 1995. Seismic record of glacial events affecting the Pacific margin of the Northwestern Antarctic Peninsula. *In* Cooper, A.K., Barker, P.F., and Brancolini, G. (Eds.), *Geology and Seismic Stratigraphy of the Antarctic Margin.* Antarct. Res. Ser., 68, AGU Washington, D.C., 75–96.

Bartek, L.R., Vail, P.R., Anderson, J.B., Emmet P.A., and Wu, S., 1991. The effect of Cenozoic ice sheet fluctuations in Antarctica on the stratigraphic signature of the Nagano. *J. Geophys. Res.*, 96:6753–6778.

Birkenmajer, K., 1992. Evolution of the Bransfield basin and rift, West Antarctica. *In* Yoshida, Y., Kaminuma, K., and Shiraishi, K. (Eds.), *Recent Progress in Antarctic Earth Science.* Terra Sci. Publ., Tokyo, 405–410.

Camerlenghi, A., Cris, A., Pudsey, C.J., Accerboni, E., Laterza, R., and Rebesco, M., 1997a. Ten-month observation of the bottom current regime across a sediment drift of the Pacific margin of the Antarctic Peninsula. *Antarct. Sci*., 9:426–433.

Camerlenghi, A., Rebesco, M., and Pudsey, C.J., 1997b. High resolution terrigenous sedimentary record of a sediment drift on the Antarctic Peninsula Pacific margin. *In* Ricci, C.A. (Ed.), *The Antarctic Region: Geological Evolution and Processes*. Init. Results, SEDANO Program, 705–710.

Camerlenghi, A., Rebesco, M., DeSantis, L., Domack, E.W., and Kirby, M.E., in press. Seismic stratigraphy of Palmer Deep: a fault-bounded Late Quaternary sediment trap on the inner continental shelf, Antarctic Peninsula Pacific margin. *Mar. Geol.*

Cooper, A.K., Barker, P.F., Webb, P-N., and Brancolini, G., 1994. The Antarctic Continental Margin—the Cenozoic record of Glaciation, Paleoenvironments and Sea-level Change. *Terra Antarctica*, 1/2:236–480.

Cooper, A.K., Barrett, P.F., Hinz, K., Traube, V., Leitchenkov, G., and Stagg, H.M.J., 1991. Cenozoic prograding sequences of the Antarctic continental margin: a record of glacio-eustatic and tectonic events. *Mar. Geol.,* 102:175–213.

Cooper, A.K., Barker, P.F., and Brancolini, G., 1995. Geology and Seismic Stratigraphy of the Antarctic Margin. *Am. Geophys. Union Antarct. Res. Ser.*, 68. (Atlas, CD-ROM).

Denton, G.H., Sugden, D.E., Marchant, D.R., Hall, B.L., and Wilch, T.I., 1993. East Antarctic ice sheet sensitivity to Pliocene climate change from a Dry Valleys perspective. *Geografiska Annaler,* 75A:155–204.

Domack, E.W., and McClennen, C.E., 1996. Accumulation of glacial marine sediments in fjords of the Antarctic Peninsula and their use as late Holocene paleoenvironmental indicators. *Antarct. Res. Ser*., 70, AGU Washington, D.C., 135–154.

Drewry, D.J., and Morris, E.M., 1992. The response of large ice sheets to climate change. *Philos. Trans. R. Soc. London B.,* 338:235–242.

Gersonde, R., Kyte, F.T., Bleil, U., Flores, J.A., Gohl, K., Grahl, G., Hagen, R., Kuhn, G., Sierro, F.J., Abelmann, A., and Bostwick, J.A., 1997. Geological record and reconstruction of the late Pliocene impact of the Eltanin asteroid in the Southern Ocean. *Nature* 390:357–363.

Haq, B.U., Hardenbol, J., and Vail, P.R., 1987. Chronology of fluctuating sea levels since the Triassic. *Science*, 235:1156–1167.

Hayes, D.E., Frakes, L.A., et al., 1975. *Init. Repts., DSDP,* 28: Washington (U.S. Govt. Printing Office).

Huybrechts, P., 1993. Glaciological modelling of the Late Cenozoic East Antarctic ice sheet: stability or dynamism. *Geografiska Annaler*, 75A:221–238.

Kuvaas, B., and Leitchenkov, G., 1992. Glaciomarine turbidite and current-controlled deposits in Prydz Bay, Antarctica. *Mar. Geol.,* 108:365–381.

Kuvaas, B., and Kristoffersen, Y., 1991. The Crary Fan: a trough-mouth fan on the Weddell Sea continental margin, Antarctica, *Mar. Geol.,* 97:345–362.

Larter, R.D., and Barker, P.F., 1989. Seismic stratigraphy of the Antarctic Peninsula Pacific margin: a record of Pliocene-Pleistocene ice volume and paleoclimate. *Geology,* 17:731–734.

Larter, R.D., and Barker, P.F., 1991a. Effects of ridge-crest trench interaction on Antarctic-Phoenix spreading: Forces on a young subducting plate. *J.Geophys. Res.,* 96:19,583–19,607.

Larter, R.D., and Barker, P.F., 1991b. Nagano interaction of tectonic and glacial processes at the Pacific margin of the Antarctic Peninsula. *In* Macdonald, D.I.M., (Ed.), *Sedimentation, Tectonics and Eustasy,* Special Publication No. 12 of the International Association of Sedimentologists, Blackwell, Oxford, 165–186.

Larter, R.D., and Cunningham, A.P., 1993. The depositional pattern and distribution of glacial-interglacial sequences on the Antarctic Peninsula Pacific Margin. *Mar. Geol.,* 109:203–219.

Larter, R.D., Rebesco, M., Vanneste, L.E., Gamboa, P.A.P., and Barker, P.F., 1997. Cenozoic tectonic, sedimentary and glacial history of the continental shelf west of Graham Land, Antarctic Peninsula. *In* Barker, P.F., and Cooper, A.K. (Eds.), *Geology and Seismic Stratigraphy of the Antarctic Margin*, Part 2. Am. Geophys. Union Antarct. Res. Ser., 71:1–27.

Leventer, A., Domack, E.W., Ishman, E., Brachfeld, S., McClennen, C.E., and Manley, P., 1996. Productivity cycles of 200–300 years in the Antarctic Peninsula region: understanding linkages among the sun, atmosphere, oceans, sea ice, and biota. *Geol. Soc. Am. Bull.,* 108:1626–1644.

McGinnis, J.P., and Hayes, D.E., 1995. The roles of downslope and along-slope depositional processes: southern Antarctic Peninsula continental rise. *In* Cooper, A.K., Barker, P.F., and Brancolini, G. (Eds.), *Geology and Seismic Stratigraphy of the Antarctic Margin.* Antarct. Res. Ser., 68, AGU Washington, D.C. 141–156.

Miller, K.G., Fairbanks, R.G., and Mountain, G.S., 1987. Tertiary oxygen isotope synthesis, sea-level history and continental margin erosion. *Paleoceanography,* 2:1–19.

Pope, P.G., and Anderson, J.B., 1992. Late Quaternary glacial history of the northern Antarctic Peninsula's western continental shelf: evidence from the marine record. *Antarctic Research Series, American Geophysical Union*, 57:63–91.

Pudsey, C.J., Barker, P.F., and Larter, R.D., 1994. Ice sheet retreat from the Antarctic Peninsula shelf. *Continental Shelf Res.*, 14:1647–1675.

Rebesco, M., Larter, R.D., Barker, P.F., Camerlenghi, A., and Vanneste, L.E., 1997. The history of sedimentation on the continental rise west of the Antarctic Peninsula. *In* Barker, P. F., and Cooper, A.K. (Eds.), *Geology and Seismic Stratigraphy of the Antarctic Margin, II,* AGU Antarctic Research Series, 29–50.

Rebesco, M., Larter, R.D., Camerlenghi, A., and Barker, P.F., 1996. Giant sediment drifts on the continental rise of the Antarctic Peninsula. *Geo-Marine Letters*, 16:65–75.

Sahagian, D.L., and Watts, A.B., 1991. Introduction to the Special Section on measurement, causes and consequences of long-term sea level changes. *J. Geophys. Res.*, 96:6585–6589.

Shackleton, N.J., Hall, M.A., and Pate, D., 1995. Pliocene stable isotope stratigraphy of Site 846. *In* Pisaias, N.G., Mayer, L.A., Janecek, T.R., Palmer-Julson, A., and Van Andel, T.H. (Eds.), *Proc. ODP, Sci. Results*, 138: College Station, TX (Ocean Drilling Program), 337–355.

Tiedemann, R., Sarnthein, M., and Shackleton, N.J., 1994. Astronomic time scale for the Pliocene Atlantic ^{18}O and dust flux records of Ocean Drilling Program Site 659, *Paleoceanography,* 9:619–638.

Tomlinson, J.S., Pudsey, C.J., Livermore, R.A., Larter, R.D., and Barker, P.F., 1992. GLORIA survey of the Pacific margin of the Antarctic Peninsula: tectonic fabric and sedimentary processes. *In* Yoshida, Y., Kaminuma, K., and Shiraishi, K. (Eds.), *Recent Progress in Antarctic Earth Science.* Terra Sci. Publ., Tokyo, 423–429.

Vanneste, L.E., and Larter, R.D., 1995. Deep-tow boomer survey on the Antarctic Peninsula Pacific margin: an investigation of the morphology and acoustic characteristics of Late Quaternary sedimentary deposits on the outer continental shelf and upper slope. *In* Cooper, A.K., Barker, P.F., and Brancolini, G. (Eds.), *Geology and Seismic Stratigraphy of the Antarctic Margin.* Antarct. Res. Ser., 68, AGU Washington, D.C., 97–121.

Webb, P.-N., and Harwood, D.M., 1991. Late Cenozoic glacial history of the Ross Sea embayment, Antarctica. *Quat. Sci. Rev*., 10:215–223.

FIGURE CAPTIONS

Figure 1. General map of Leg 178 with ship track.

Figure 2. Bathymetric chart of the Antarctic Peninsula Pacific margin with Leg 178 sites marked (bathymetry in meters). SM = seamount.

Figure 3. Schematic figure of tectonic and glacial elements of the Antarctic Peninsula margin and sites drilled during Leg 178.

Figure 4. Graph and maps of ice-sheet size and location at mean sea-level temperatures 5, 9, 10, 15, 19, and 20 Kelvin (K) above present. The maps indicate where margin sedimentation might be sensitive to particular stages of ice-sheet growth. Antarctic Peninsula glaciation appears to have developed during the last 5–9 K of cooling (from Huybrechts,1993).

Figure 5. Sequence model of deposition on shelf and slope through a glacial cycle (adapted from Larter and Barker, 1989, 1991b). Unsorted till is deposited on the slope (foresets) during glacial maxima and on the shelf (topsets) during retreat. Pelagic or hemipelagic sediment is deposited on the slope and rise during interglacials. With re-advance, some or all shelf topsets may be eroded.

Figure 6. Schematic drawing of the processes active during glacial half-cycles, leading to the development of hemipelagic sediment drifts on the continental rise (adapted from Rebesco et al., 1997). The unstable component of unsorted upper-slope deposits forms first debris flows, then turbidity currents. The fine fraction is suspended and entrained in ambient bottom currents to be deposited downcurrent. Drifts are built above the level of the dendritic pattern of turbidity current channels because (in the case of the Antarctic Peninsula margin and perhaps elsewhere) subsequent turbidity currents erode the deposited sediment everywhere *except* upon the drifts and maintain the steeper drift slopes at the limit of stability.

Figure 7. Part of multichannel seismic (MCS) reflection profile I95-137 across Site 1095. S.P. = shotpoint.

Figure 8. Summary of lithostratigraphic, magnetostratigraphic, and biostratigraphic findings in Leg 178 sediment drift sites. The record of magnetic susceptibility and natural gamma-ray attenuation is shown for comparison.

Figure 9. Depth-age profile determined from geomagnetic reversals and diatom and radiolarian datums. Paleomagnetic data were drawn from analysis of split-core (X's) and geologic high-sensitivity magnetic tool (GHMT) logging data (diamonds). Separate curves for split-core (thin line) and GHMT magnetic data (heavy broken line) are interpolations that pass through all data points within each data set and match the slopes at those points. Diatom and radiolarian datum intervals are marked with an upright triangle at the base (B = base/first occurrence) and an inverted triangle at the top (T = top/last occurrence). TC = top of common occurrence/last common occurrence. *P. sulcata* abundance is shown with gray shaded bars. The hole is barren of microfossils below ~520 mbsf. Mean sedimentation rates (underlined) determined for the three intervals show an uphole decrease.

Figure 10. Part of MCS reflection profile I95-130A across Site 1096 (see location in Figure 1096-B-4). Note the bottom-simulating reflector at about 700 ms TWT below the seafloor, interpreted as the opal-A to opal-CT transition. S.P. = shotpoint.

Figure 11. Depth-age relationship for Site 1096 based on geomagnetic reversals (X) and diatom (solid symbols) and radiolarian (open symbols) datums. Paleomagnetic data were drawn from shipboard analysis of cores. Intervals of diatom and radiolarian datums are marked with an upright triangle at the base and an inverted triangle at the top. In labels indicating species identity, B = base/first occurrence and T = top/last occurrence. Sedimentation rates (underlined) for selected intervals are adjacent to the corresponding curve. Vertical solid arrows indicate dominant age-diagnostic fossil type (biosiliceous vs. calcareous) for respective intervals of this site. The dashed vertical line below B *Fragilariopsis interfrigidaria* datum interval indicates range of published ages for this datum.

Figure 12. A. Part of MCS reflection profile IT92-114 across Site 1101 (see location in Figure 1101-B-1B). **B.** Seismic stratigraphic record at location of proposed site APRIS-05A (proximal site on Drift 4). **C.** Seismic stratigraphic record at location of proposed site APRIS-06A (distal site on Drift 4). S.P. = shotpoint.

Figure 13. Depth-age profile determined from geomagnetic reversals and diatom and calcareous nannofossil datums. The curve fit to the paleomagnetic data is an interpolation that passes through all data points within the data set and matches the slope at those points. Diatom and calcareous nannofossil datum intervals are marked with solid (diatom) and open (nannofossil) triangles. B = base/first occurrence, T = top/last occurrence.

Figure 14. Location of Site 1097 on single-channel seismic reflection profile PD88-04 (Bart and Anderson, 1995) across the continental shelf seaward of Adelaide Island, Antarctic Peninsula.

Figure 15. Summary of facies recovered at Site 1097, associated biofacies, and environmental interpretation. Representative cores are identified at top.

Figure 16. Continental shelf transect. Location of Sites 1100, 1102, and 1103 on MCS reflection profile I95-152 across the continental shelf seaward of Adelaide Island, Antarctic Peninsula. S.P. = shotpoint.

Figure 17. Simplified lithostratigraphy at Site 1103 showing lithofacies.

Figure 18. Bathymetry and location of site-survey seismic reflection profiles on Palmer Deep. Tracks of the 3.5-kHz sub-bottom profiles obtained by the *JOIDES Resolution* are indicated by the thickest bold line.

Figure 19. Generator Injector (GI) air-gun seismic profile I97H-228G **(A)** across Palmer Deep Site 1098, Basin I, and **(B)** across Palmer Deep Site 1099, Basin III (modified from Camerlenghi et al., in press).

Figure 20. Lithostratigraphic columns for Sites 1098 and 1099.

Figure 21. Summary of biostratigraphic findings and correlation in Leg 178 continental rise sites.

Figure 22. Relative abundances of chlorite, illite, and mixed-layer clays in sediments from the continental shelf (Site 1097) and rise (Sites 1095, 1096, and 1101) analyzed on Leg 178.

Figure 23. Downhole logs of hole diameter, total natural gamma, bulk density, porosity, resistivity, sonic velocity (see text), and magnetic susceptibility from Hole 1103A, with core measurements of natural gamma, bulk density, porosity, sonic velocity, and magnetic susceptibility.

Figure 24. Biostratigraphic summary of shelf sites (Holes 1097A, 1100D, and 1103A), based on shipboard observation, with seismic correlation. Light gray horizons show materials of very rare diatom occurrence. Dark gray horizons show intervals barren of microfossils. Age assignment of S3 at Hole 1097A is based on benthic foraminifers, diatoms, and radiolarian biostratigraphy. The depths of seismic reflectors at Hole 1103A are refined with logging information.

Figure 25. Magnetostratigraphic summary for Leg 178 continental rise sites.

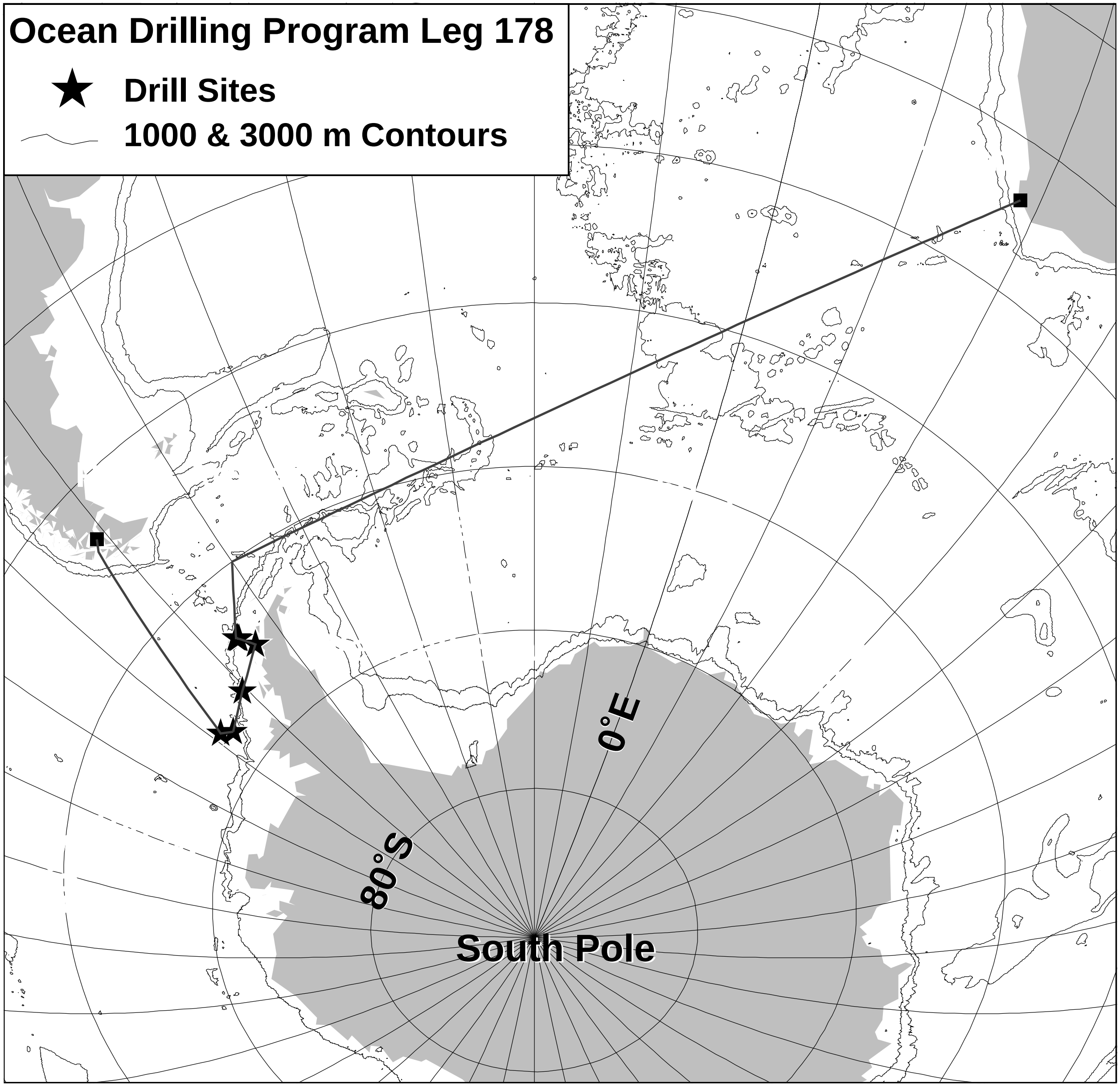
Ocean Drilling Program Leg 178
Drill Sites
1000 & 3000 m Contours
0°E
80°S
South Pole

Figure 1.

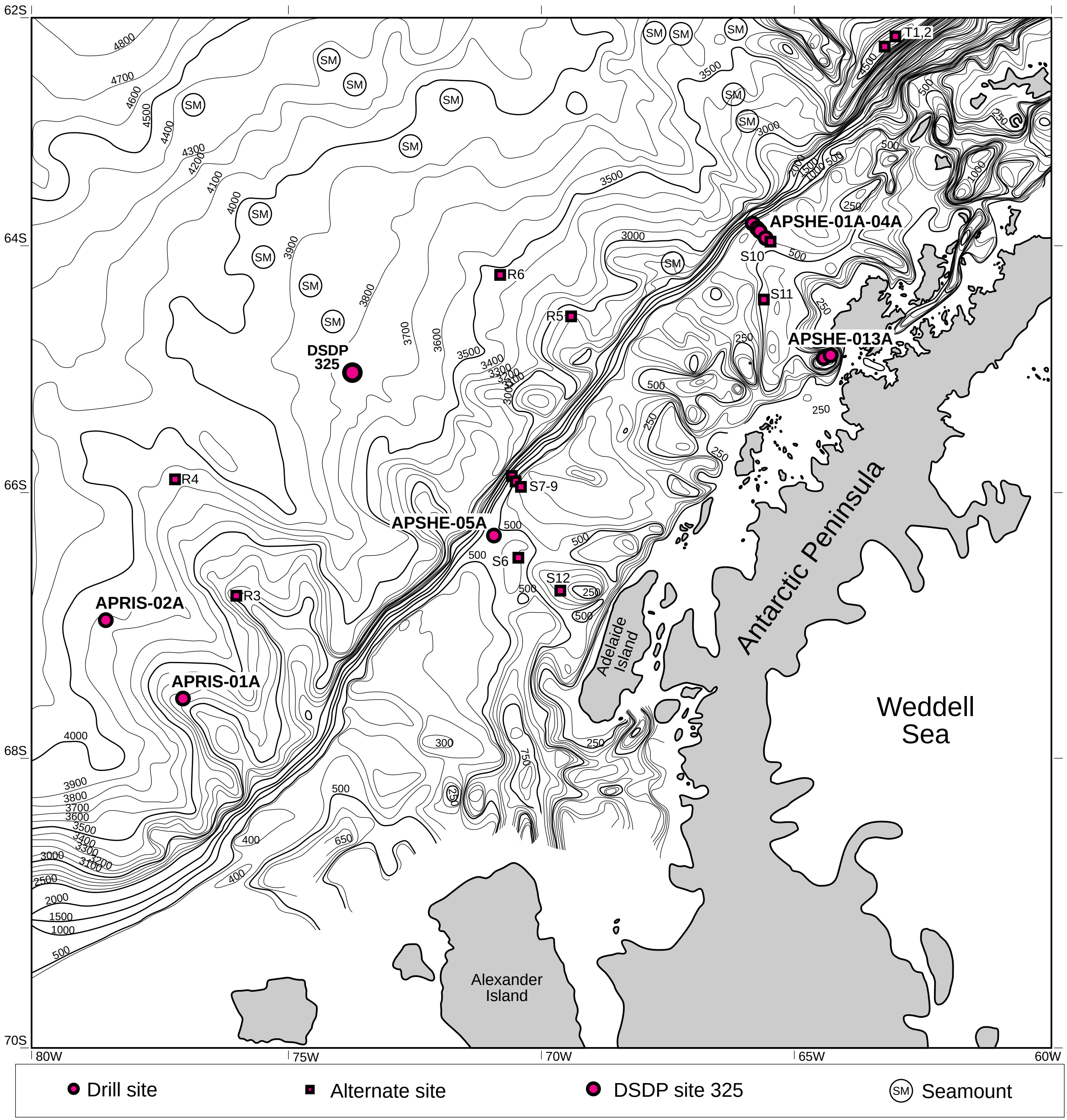
62S
64S
66S
68S
70S
80W
75W
70W
65W
60W
APSHE-01A-04A
APSHE-013A
APSHE-05A
APRIS-02A
APRIS-01A
DSDP
325
T1,2
S10
S11
R6
R5
R4
R3
S7-9
S6
S12
SM
Antarctic Peninsula
Adelaide Island
Alexander Island
Weddell Sea
Drill site
Alternate site
DSDP site 325
Seamount

Figure 2.

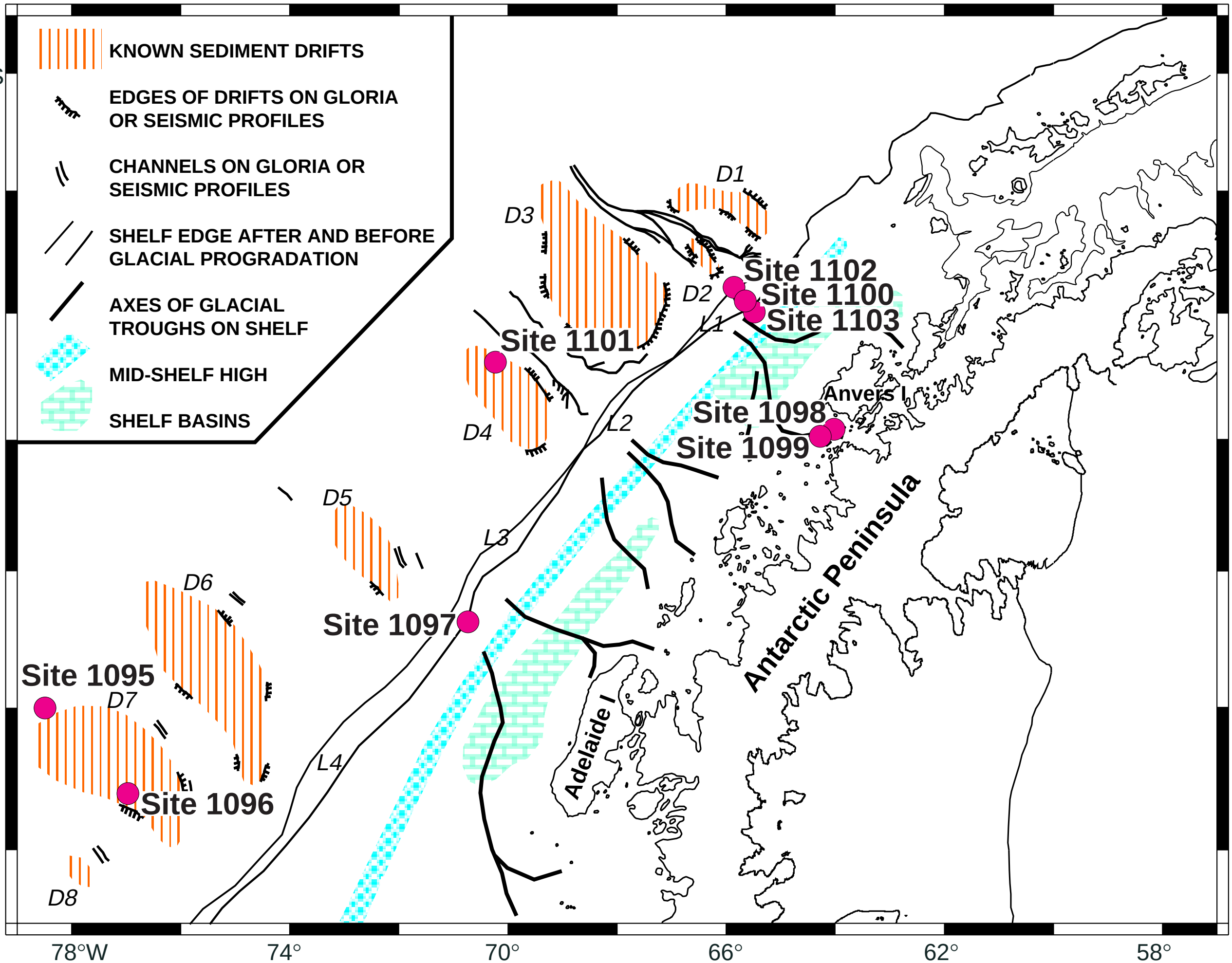

KNOWN SEDIMENT DRIFTS
EDGES OF DRIFTS ON GLORIA OR SEISMIC PROFILES
CHANNELS ON GLORIA OR SEISMIC PROFILES
SHELF EDGE AFTER AND BEFORE GLACIAL PROGRADATION
AXES OF GLACIAL TROUGHS ON SHELF
MID-SHELF HIGH
SHELF BASINS
62°S
64°
66°
68°
78°W
74°
70°
66°
62°
58°
D1
D2
D3
D4
D5
D6
D7
D8
L1
L2
L3
L4
Site 1095
Site 1096
Site 1097
Site 1098
Site 1099
Site 1100
Site 1101
Site 1102
Site 1103
Anvers I
Adelaide I
Antarctic Peninsula

Figure 3.

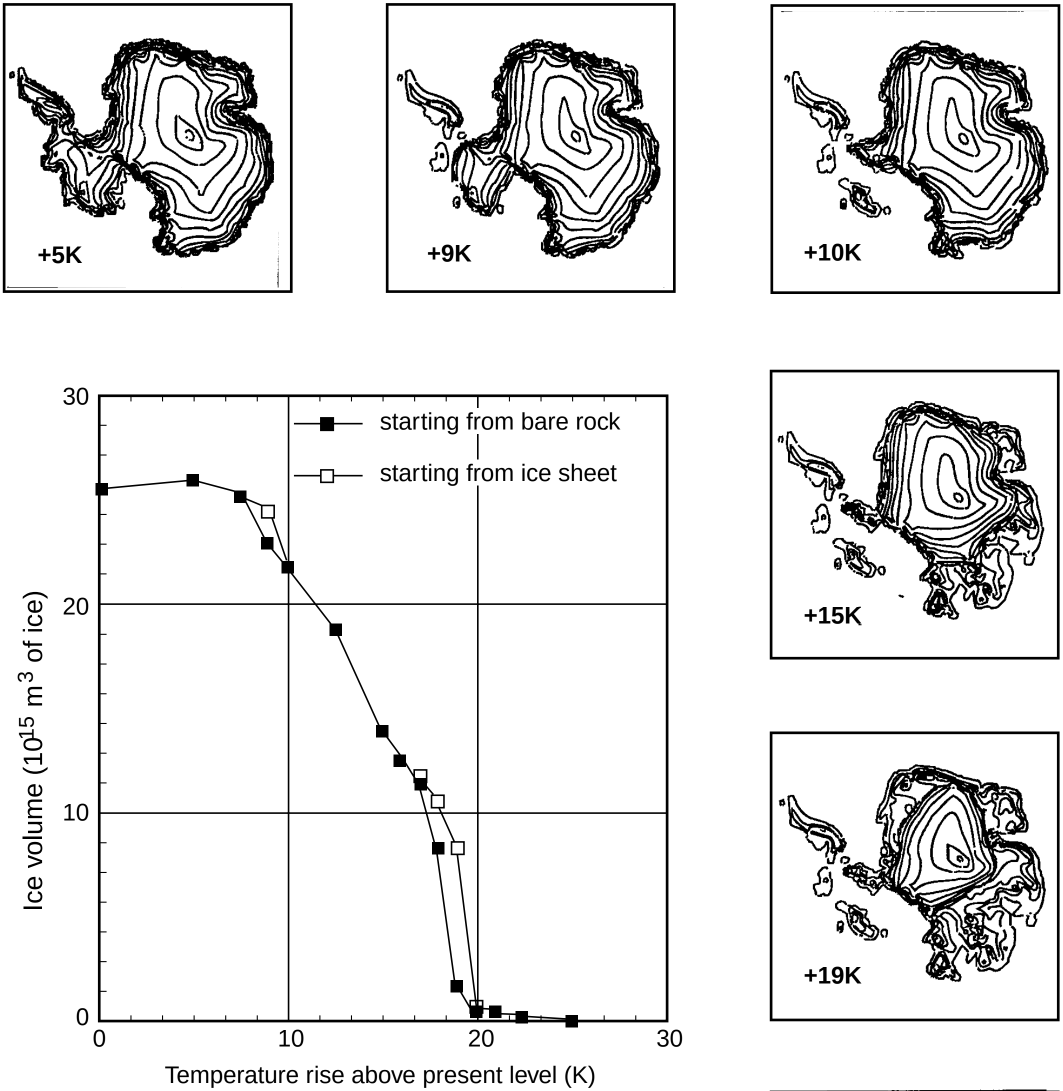
+5K
+9K
+10K
+15K
+19K
starting from bare rock
starting from ice sheet
Ice volume (10^{15} m^3 of ice)
Temperature rise above present level (K)
0
10
20
30
0
10
20
30

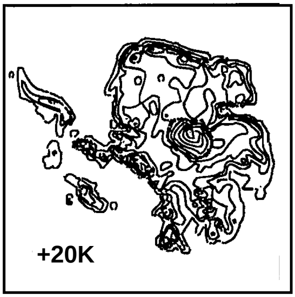
+20K

Figure 4.

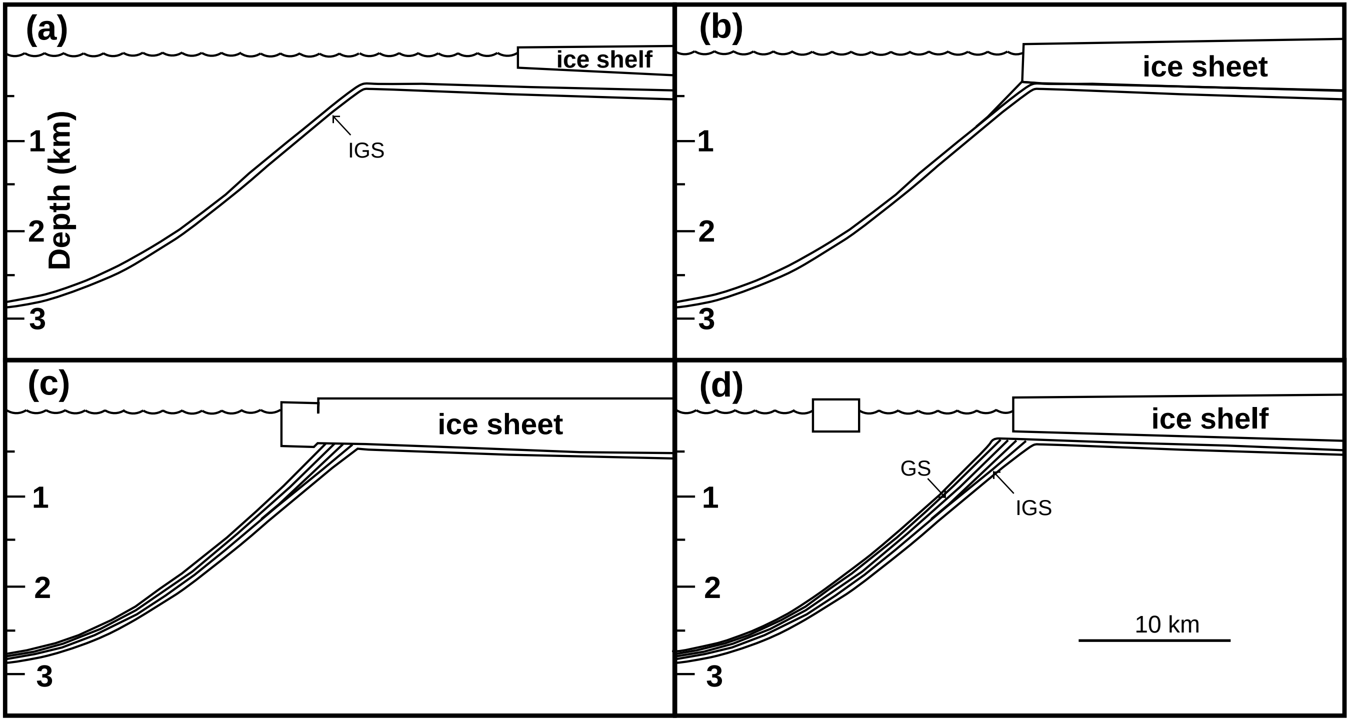

(a)
ice shelf
IGS
Depth (km)
1
2
3
(b)
ice sheet
1
2
3
(c)
ice sheet
1
2
3
(d)
ice shelf
GS
IGS
1
2
3
10 km

Figure 5.

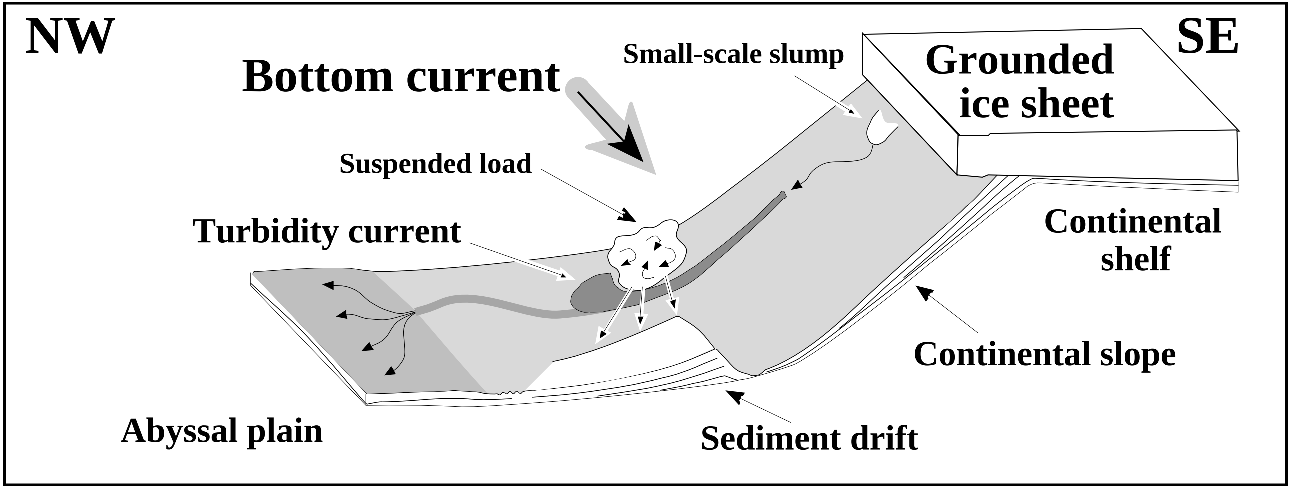
NW
SE
Bottom current
Small-scale slump
Grounded ice sheet
Suspended load
Turbidity current
Continental shelf
Continental slope
Abyssal plain
Sediment drift

Figure 6.

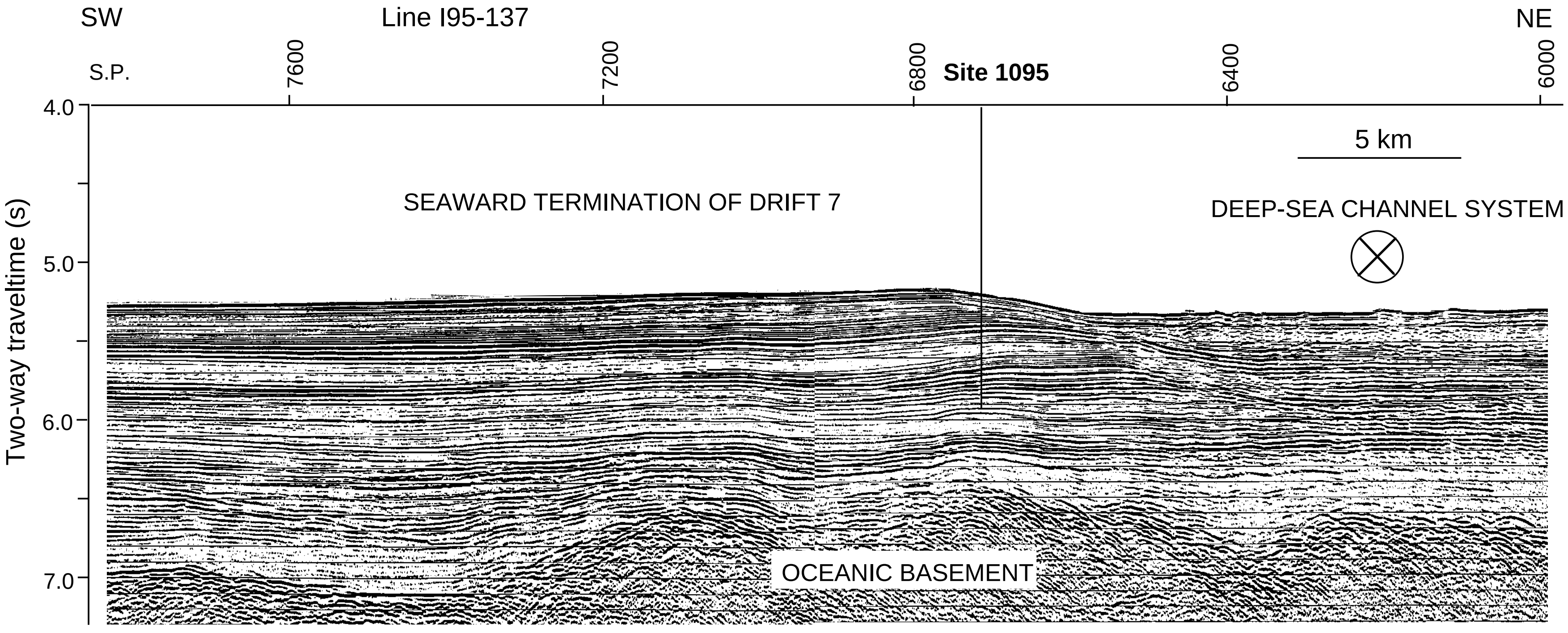

SW
Line I95-137
NE
S.P.
7600
7200
6800
Site 1095
6400
6000
4.0
5.0
6.0
7.0
Two-way traveltime (s)
5 km
SEAWARD TERMINATION OF DRIFT 7
DEEP-SEA CHANNEL SYSTEM
OCEANIC BASEMENT

Figure 7.

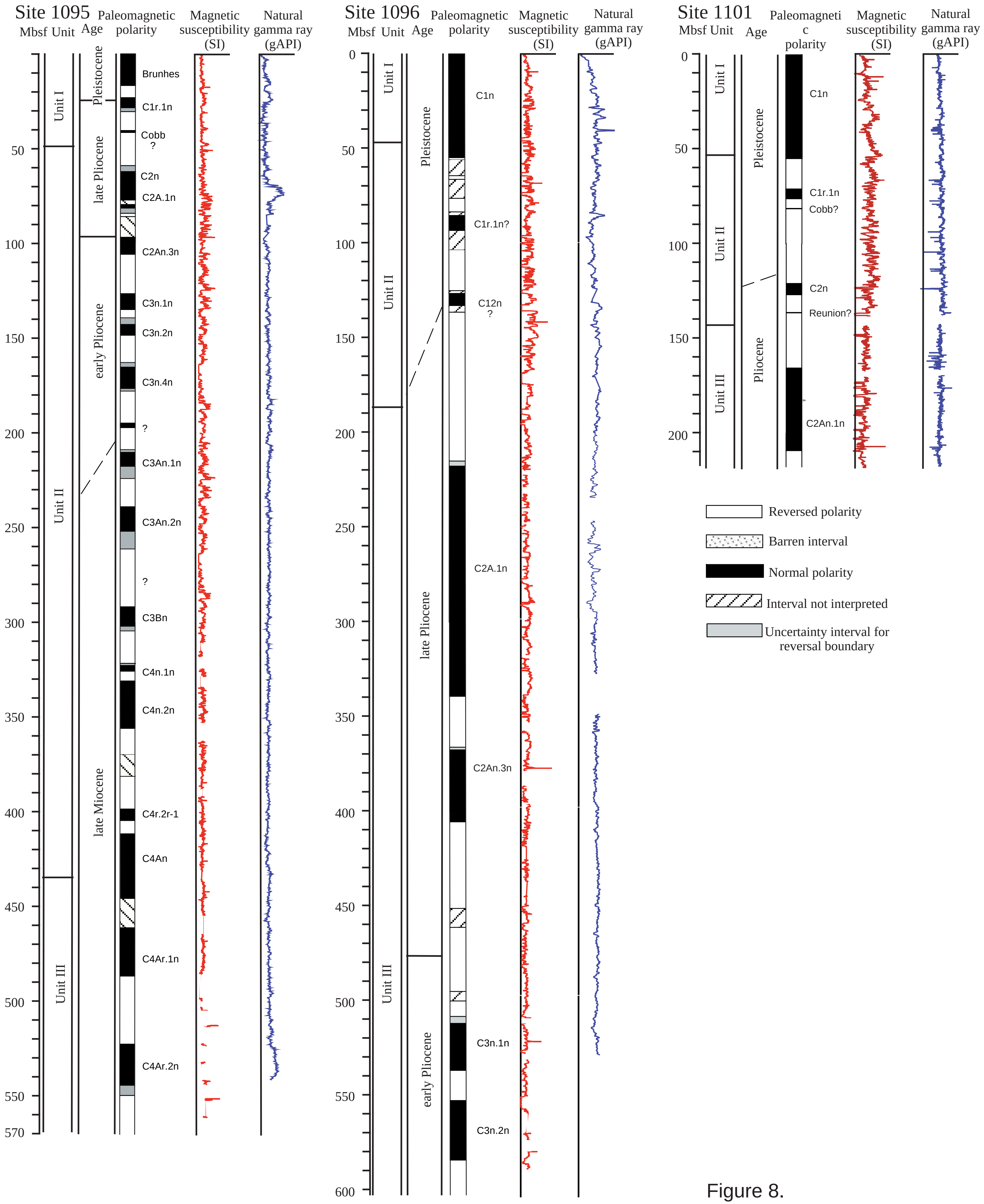
Site 1095
Mbsf Unit Age
Paleomagnetic polarity
Magnetic susceptibility (SI)
Natural gamma ray (gAPI)
Unit I
Unit II
Unit III
Pleistocene
late Pliocene
early Pliocene
late Miocene
Brunhes
C1r.1n
Cobb ?
C2n
C2A.1n
C2An.3n
C3n.1n
C3n.2n
C3n.4n
?
C3An.1n
C3An.2n
?
C3Bn
C4n.1n
C4n.2n
C4r.2r-1
C4An
C4Ar.1n
C4Ar.2n
50
100
150
200
250
300
350
400
450
500
550
570
Site 1096
Mbsf Unit Age
Paleomagnetic polarity
Magnetic susceptibility (SI)
Natural gamma ray (gAPI)
Unit I
Unit II
Unit III
Pleistocene
late Pliocene
early Pliocene
C1n
C1r.1n?
C12n ?
C2A.1n
C2An.3n
C3n.1n
C3n.2n
0
50
100
150
200
250
300
350
400
450
500
550
600
Site 1101
Mbsf Unit Age
Paleomagnetic polarity
Magnetic susceptibility (SI)
Natural gamma ray (gAPI)
Unit I
Unit II
Unit III
Pleistocene
Pliocene
C1n
C1r.1n
Cobb?
C2n
Reunion?
C2An.1n
0
50
100
150
200
Reversed polarity
Barren interval
Normal polarity
Interval not interpreted
Uncertainty interval for reversal boundary

Figure 8.

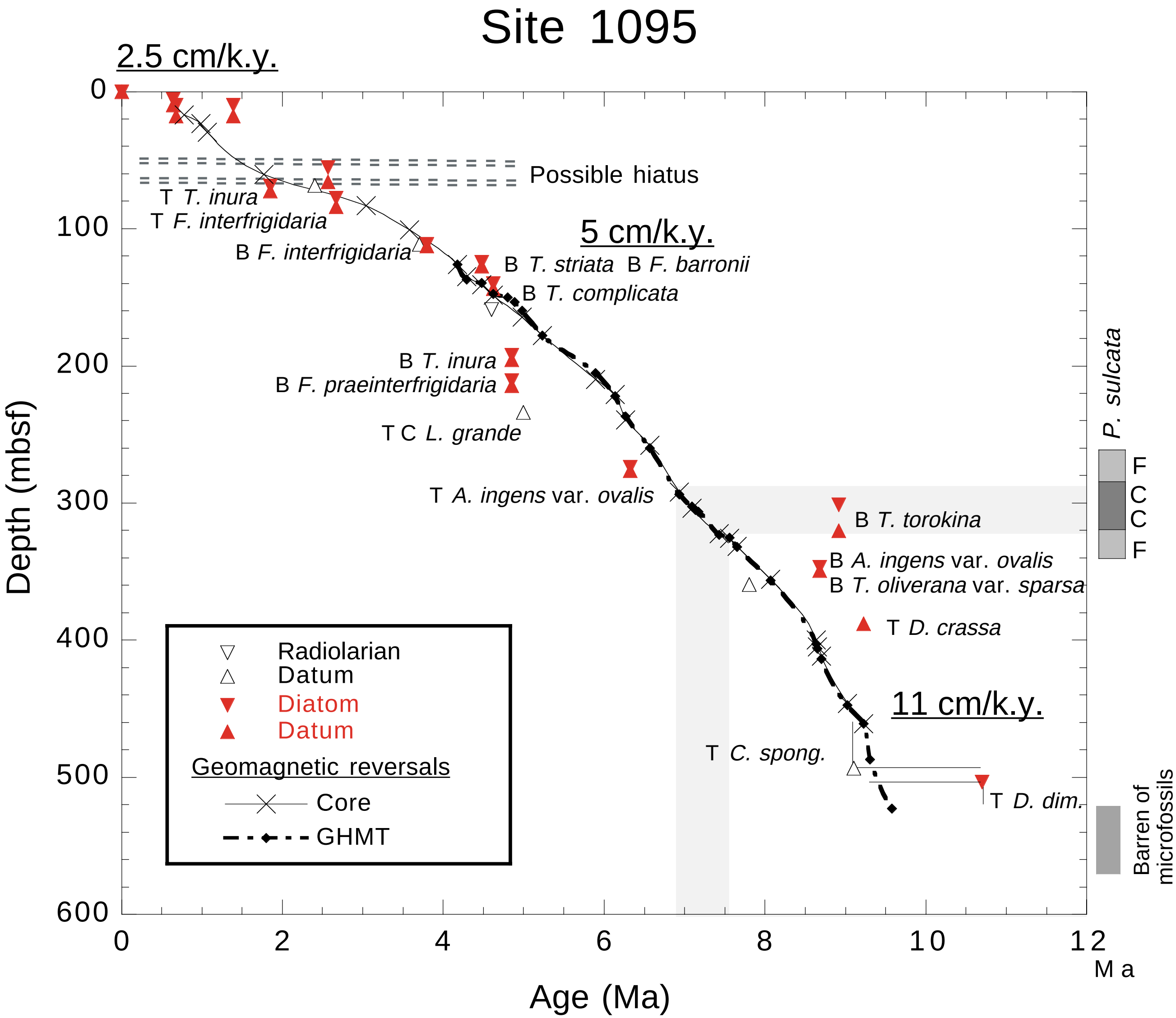
Site 1095
2.5 cm/k.y.
5 cm/k.y.
11 cm/k.y.
Possible hiatus
T T. inura
T F. interfrigidaria
B F. interfrigidaria
B T. striata B F. barronii
B T. complicata
B T. inura
B F. praeinterfrigidaria
T C L. grande
T A. ingens var. ovalis
B T. torokina
B A. ingens var. ovalis
B T. oliverana var. sparsa
T D. crassa
T C. spong.
T D. dim.
P. sulcata
F
C
C
F
Barren of microfossils
Radiolarian Datum
Diatom Datum
Geomagnetic reversals
Core
GHMT
Depth (mbsf)
Age (Ma)
Ma
0
100
200
300
400
500
600
0
2
4
6
8
10
12

Figure 9.

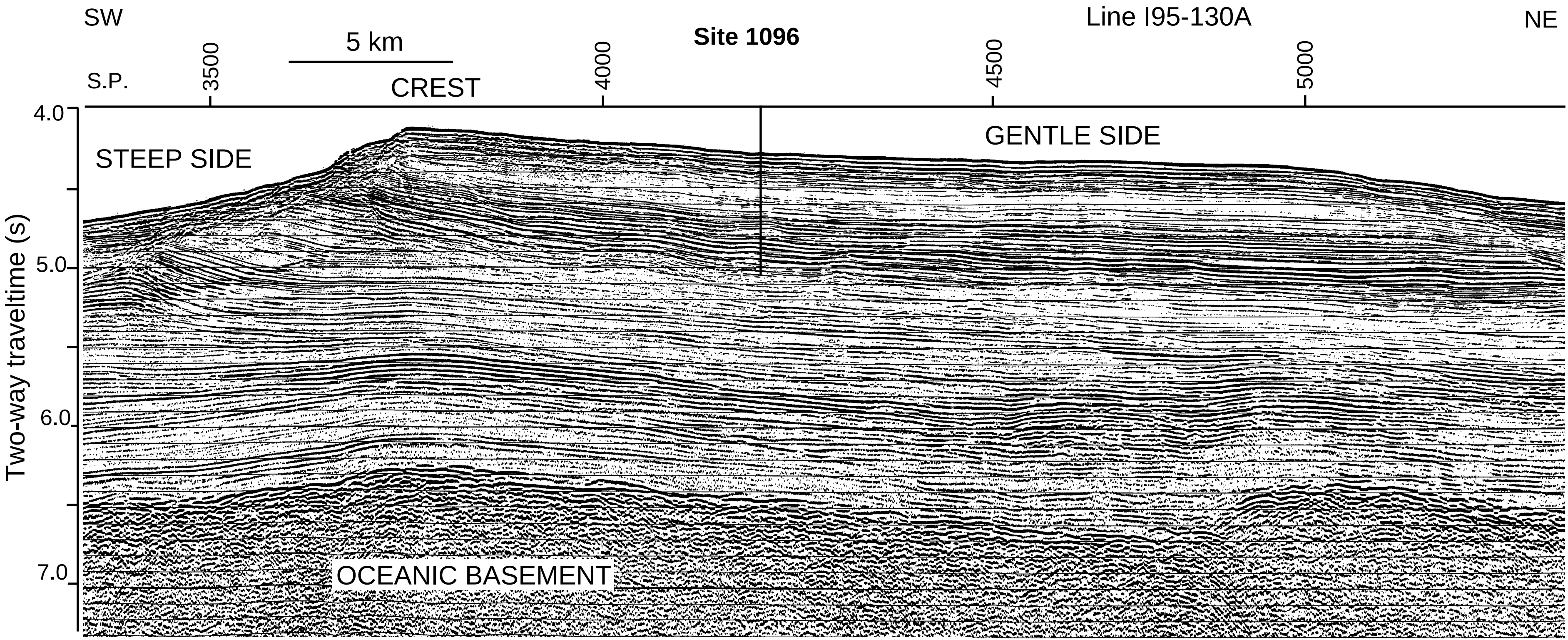
SW
Line I95-130A
NE
Site 1096
5 km
S.P.
3500
4000
4500
5000
CREST
STEEP SIDE
GENTLE SIDE
OCEANIC BASEMENT
Two-way traveltime (s)
4.0
5.0
6.0
7.0

Figure 10.

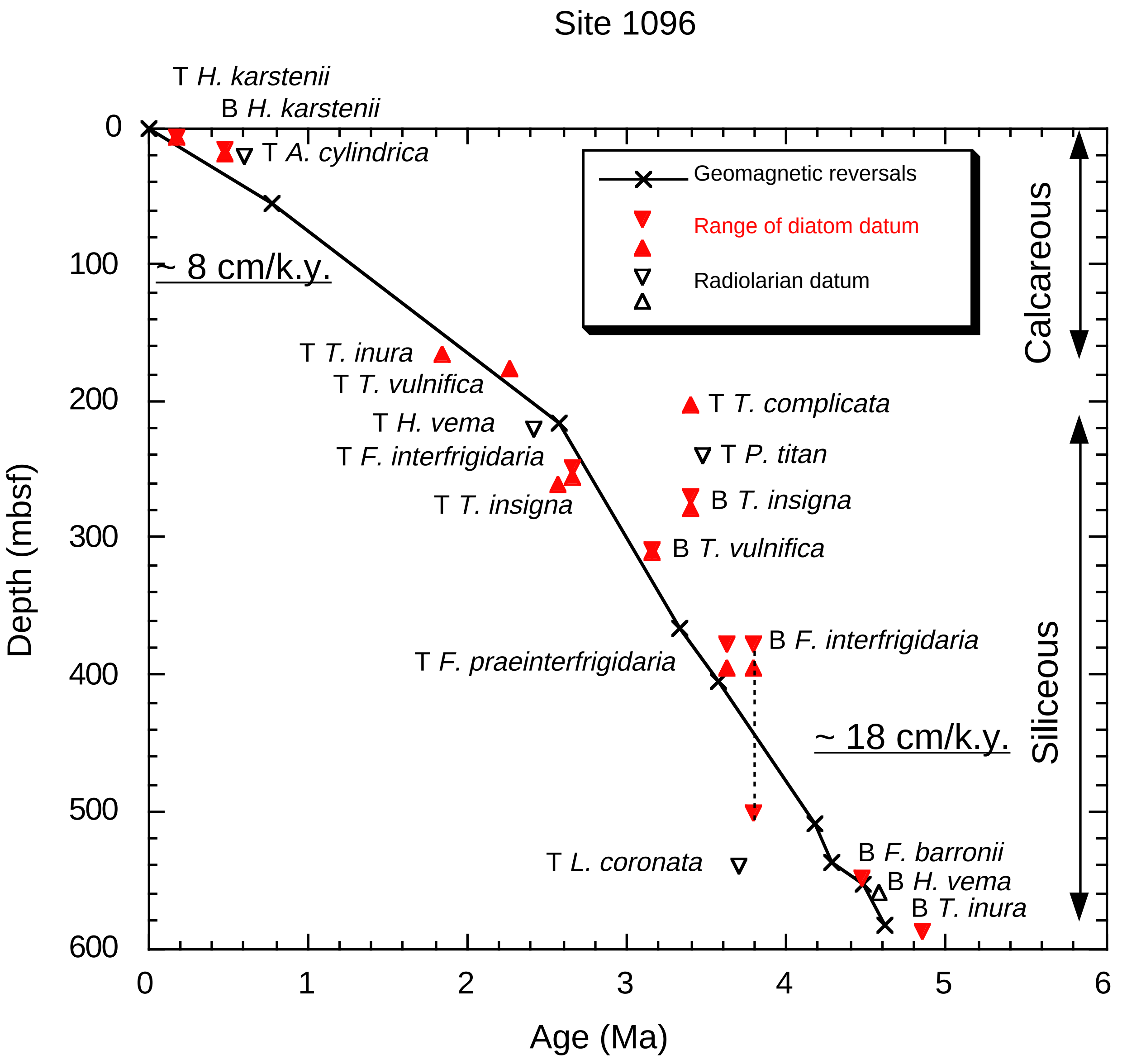
Site 1096
T H. karstenii
B H. karstenii
T A. cylindrica
Geomagnetic reversals
Range of diatom datum
Radiolarian datum
~ 8 cm/k.y.
T T. inura
T T. vulnifica
T H. vema
T F. interfrigidaria
T T. insigna
T T. complicata
T P. titan
B T. insigna
B T. vulnifica
B F. interfrigidaria
T F. praeinterfrigidaria
~ 18 cm/k.y.
T L. coronata
B F. barronii
B H. vema
B T. inura
Calcareous
Siliceous
Depth (mbsf)
0
100
200
300
400
500
600
0
1
2
3
4
5
6
Age (Ma)

Figure 11.

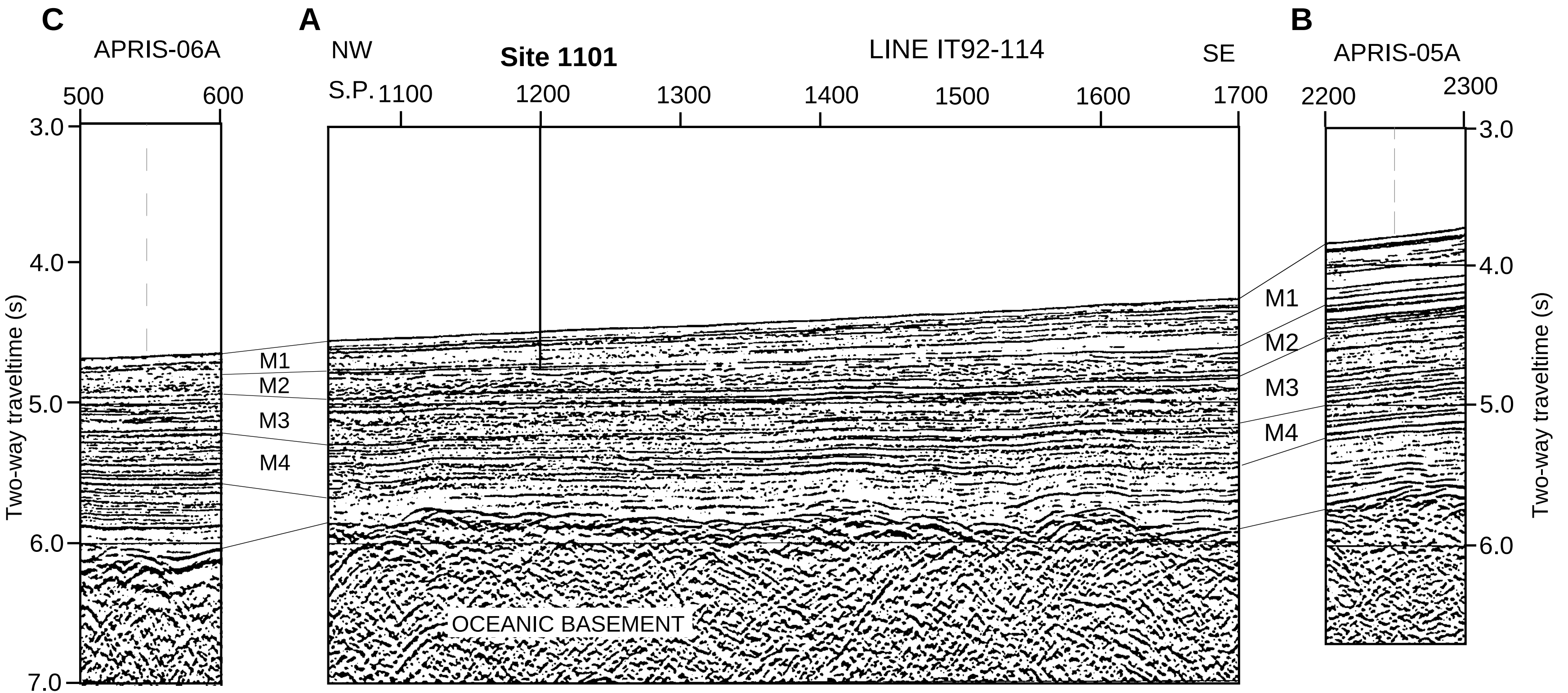
C
APRIS-06A
500
600
A
NW
Site 1101
LINE IT92-114
SE
S.P.
1100
1200
1300
1400
1500
1600
1700
B
APRIS-05A
2200
2300
3.0
4.0
5.0
6.0
7.0
Two-way traveltime (s)
M1
M2
M3
M4
OCEANIC BASEMENT

Figure 12.

Site 1101

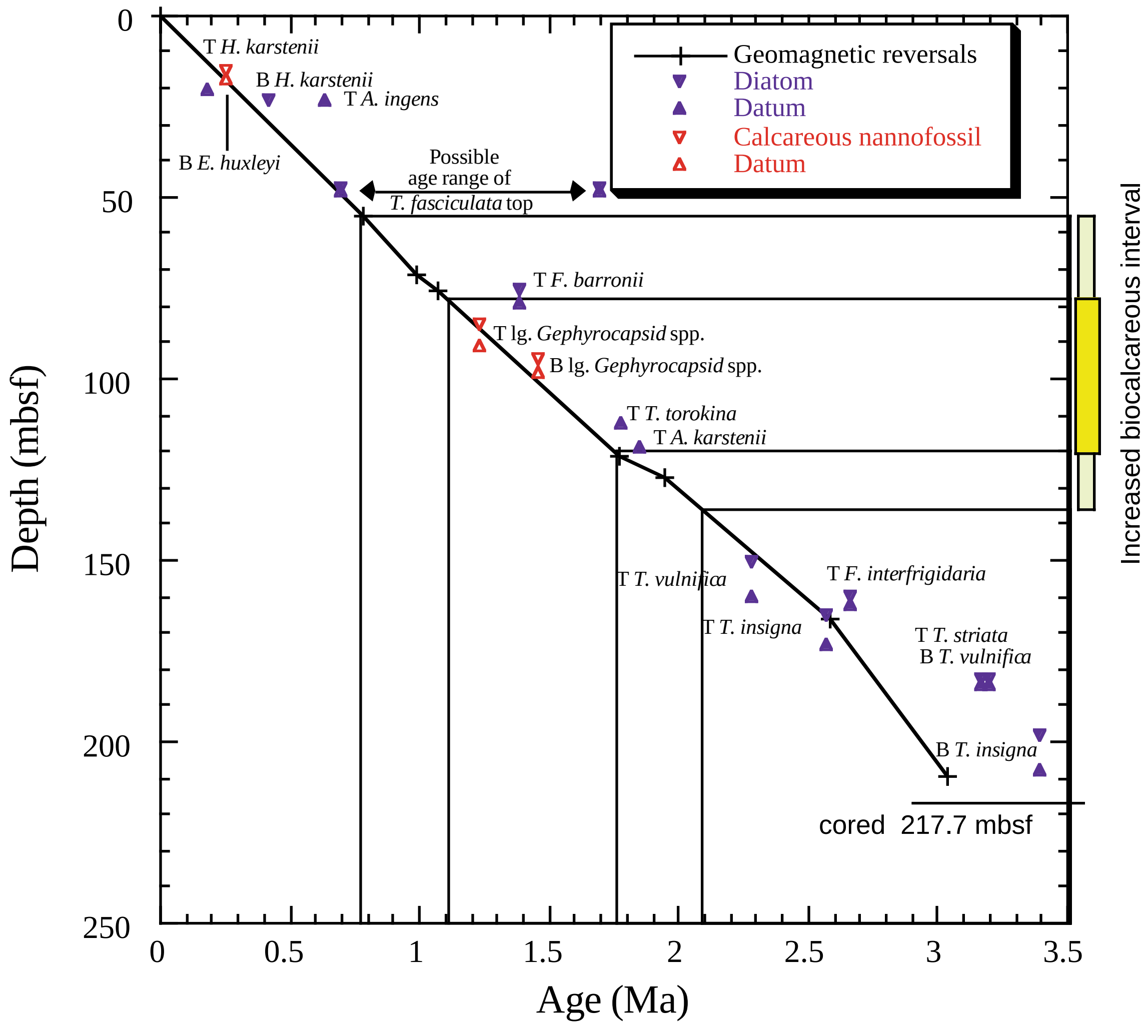

Figure 13.

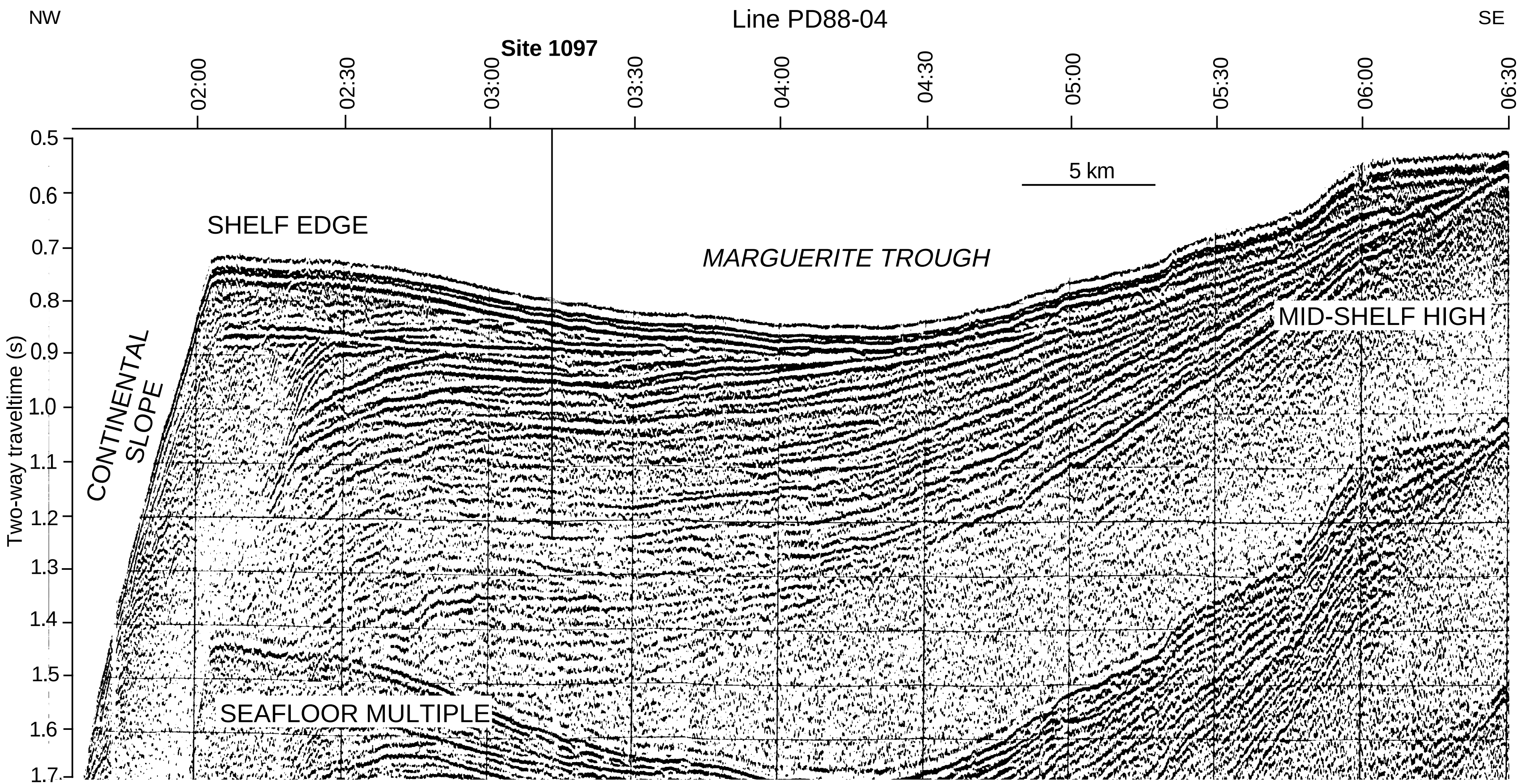
NW
Line PD88-04
SE
Site 1097
02:00
02:30
03:00
03:30
04:00
04:30
05:00
05:30
06:00
06:30
0.5
0.6
0.7
0.8
0.9
1.0
1.1
1.2
1.3
1.4
1.5
1.6
1.7
Two-way traveltime (s)
5 km
SHELF EDGE
MARGUERITE TROUGH
MID-SHELF HIGH
CONTINENTAL SLOPE
SEAFLOOR MULTIPLE

Figure 14.

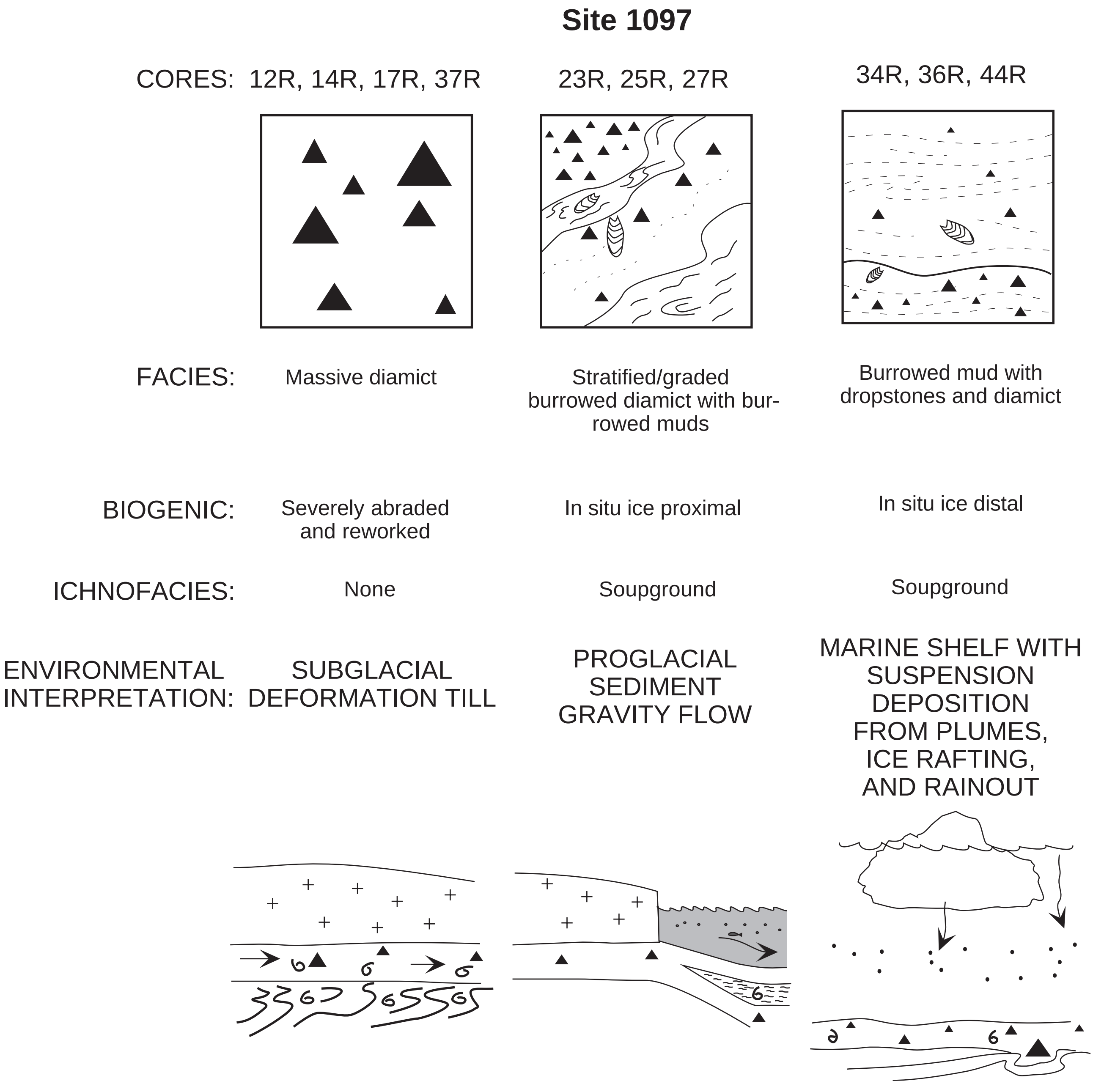

Site 1097
CORES: 12R, 14R, 17R, 37R
23R, 25R, 27R
34R, 36R, 44R
FACIES:
Massive diamict
Stratified/graded burrowed diamict with burrowed muds
Burrowed mud with dropstones and diamict
BIOGENIC:
Severely abraded and reworked
In situ ice proximal
In situ ice distal
ICHNOFACIES:
None
Soupground
Soupground
ENVIRONMENTAL INTERPRETATION:
SUBGLACIAL DEFORMATION TILL
PROGLACIAL SEDIMENT GRAVITY FLOW
MARINE SHELF WITH SUSPENSION DEPOSITION FROM PLUMES, ICE RAFTING, AND RAINOUT

Figure 15.

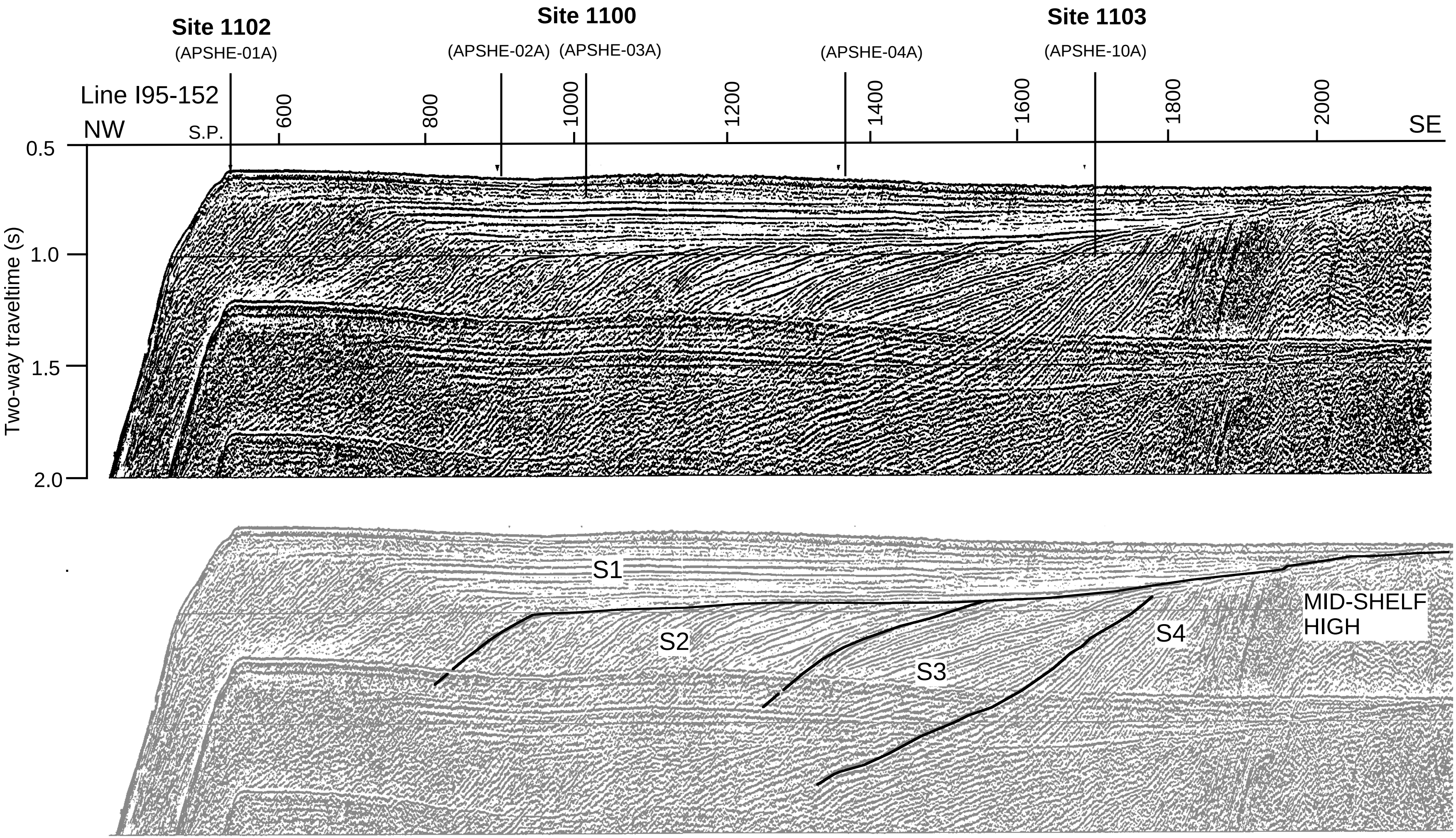
Site 1102
(APSHE-01A)
Site 1100
(APSHE-02A)
(APSHE-03A)
(APSHE-04A)
Site 1103
(APSHE-10A)
Line I95-152
NW
S.P.
600
800
1000
1200
1400
1600
1800
2000
SE
0.5
1.0
1.5
2.0
Two-way traveltime (s)
S1
S2
S3
S4
MID-SHELF
HIGH

Figure 16.

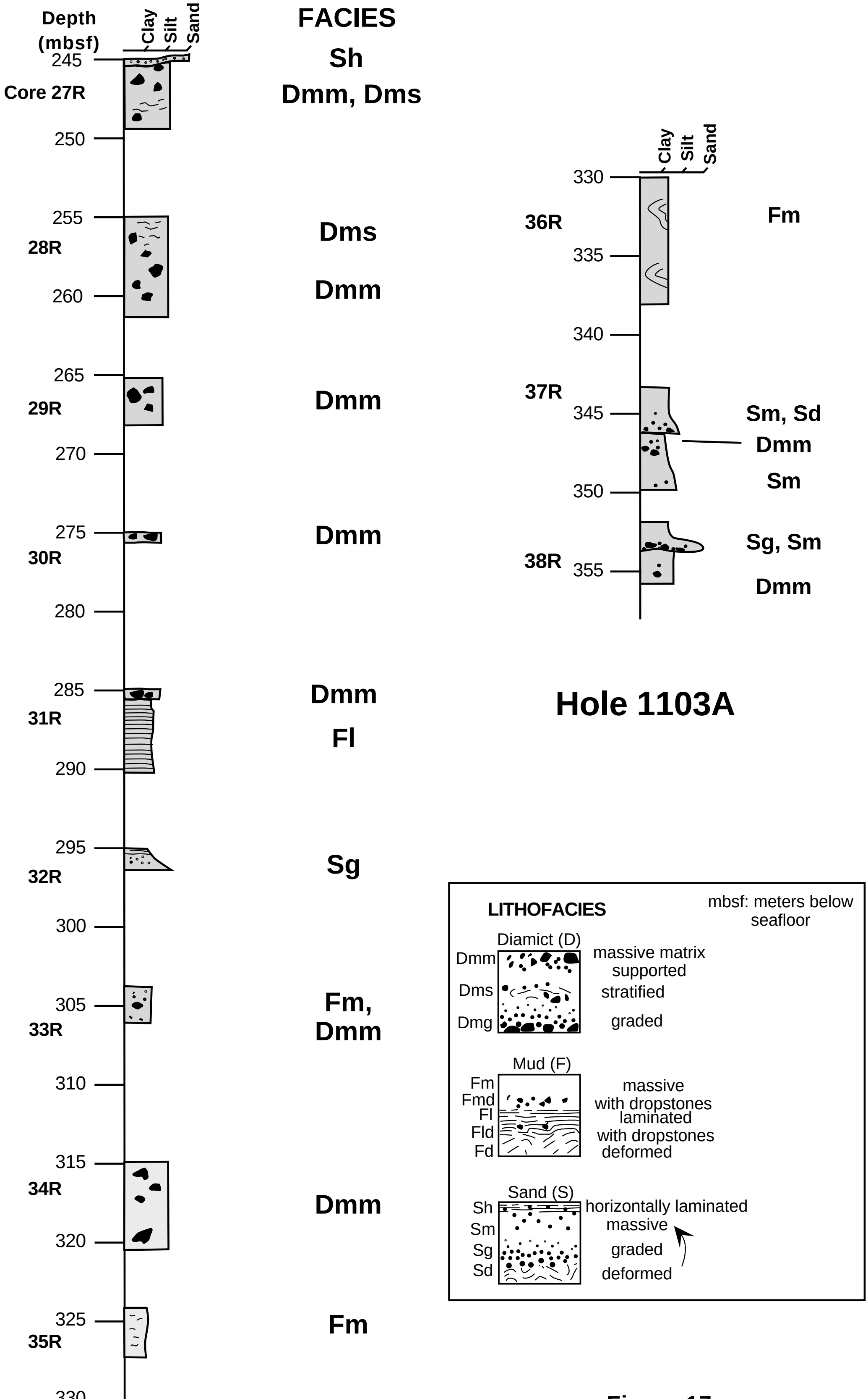
Depth (mbsf)
Clay
Silt
Sand
FACIES
Core 27R
28R
29R
30R
31R
32R
33R
34R
35R
245
250
255
260
265
270
275
280
285
290
295
300
305
310
315
320
325
330
Sh
Dmm, Dms
Dms
Dmm
Dmm
Dmm
Dmm
Fl
Sg
Fm,
Dmm
Dmm
Fm
36R
37R
38R
330
335
340
345
350
355
Fm
Sm, Sd
Dmm
Sm
Sg, Sm
Dmm
Hole 1103A
LITHOFACIES
mbsf: meters below seafloor
Diamict (D)
Dmm
Dms
Dmg
massive matrix supported
stratified
graded
Mud (F)
Fm
Fmd
Fl
Fld
Fd
massive
with dropstones
laminated
with dropstones
deformed
Sand (S)
Sh
Sm
Sg
Sd
horizontally laminated
massive
graded
deformed

Figure 17.

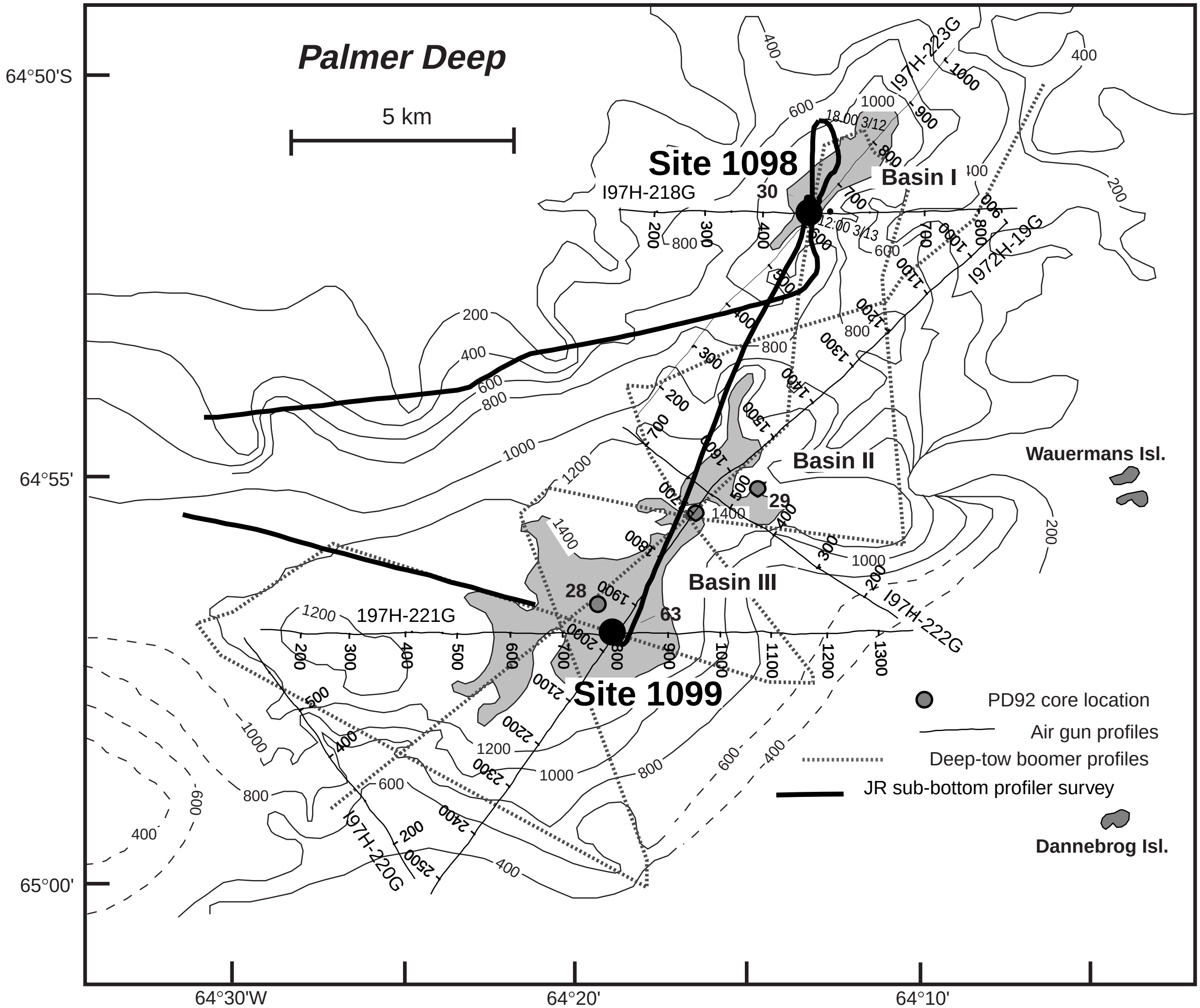
Palmer Deep
5 km
64°50'S
64°55'
65°00'
64°30'W
64°20'
64°10'
Site 1098
Site 1099
Basin I
Basin II
Basin III
Wauermans Isl.
Dannebrog Isl.
I97H-218G
I97H-223G
I972H-19G
197H-221G
I97H-222G
I97H-220G
30
29
28
63
PD92 core location
Air gun profiles
Deep-tow boomer profiles
JR sub-bottom profiler survey

Figure 18.

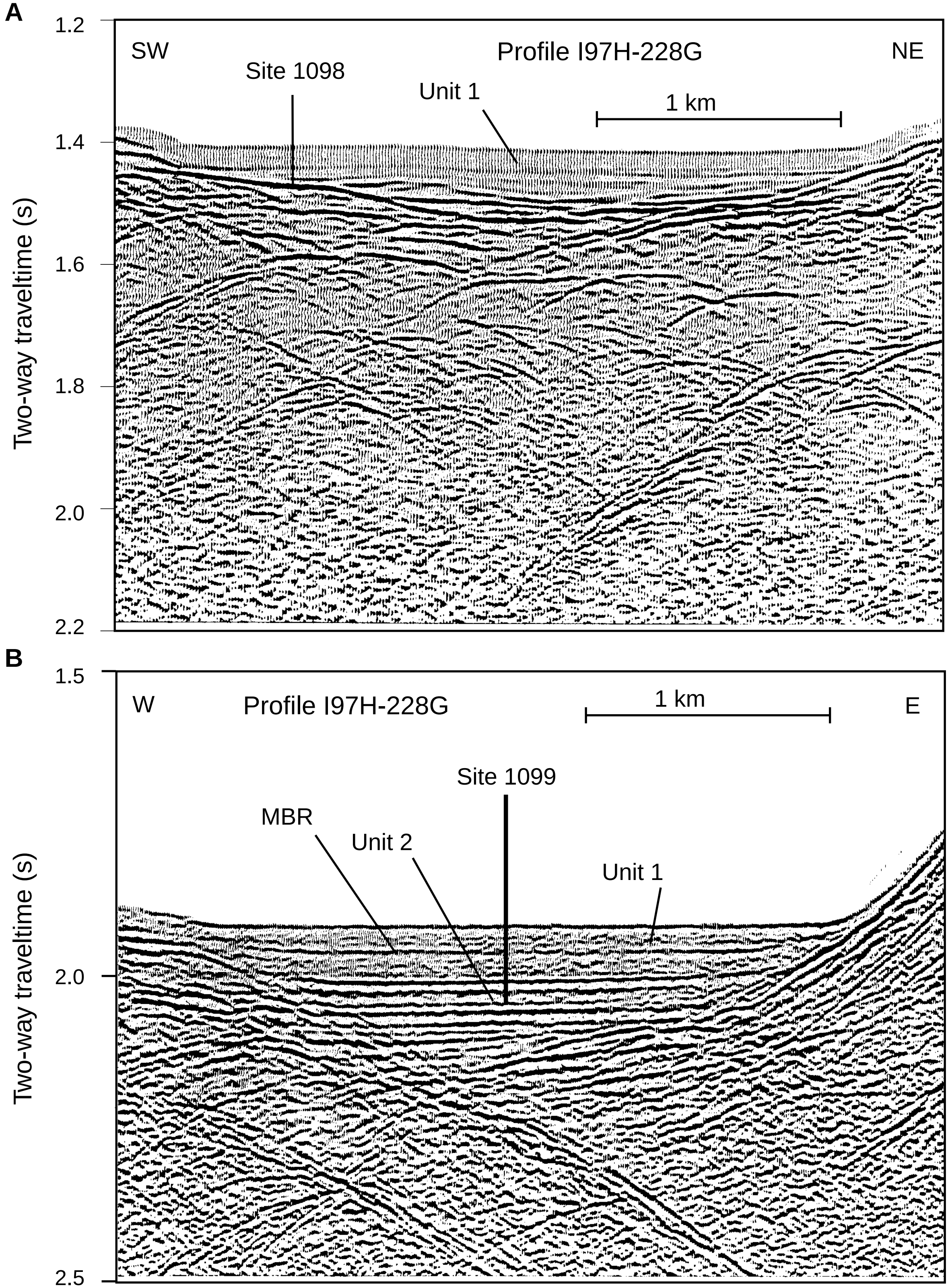
A
1.2
1.4
1.6
1.8
2.0
2.2
Two-way traveltime (s)
SW
Profile I97H-228G
NE
Site 1098
Unit 1
1 km
B
1.5
2.0
2.5
Two-way traveltime (s)
W
Profile I97H-228G
1 km
E
Site 1099
MBR
Unit 2
Unit 1

Figure 19A/B.

Site 1098

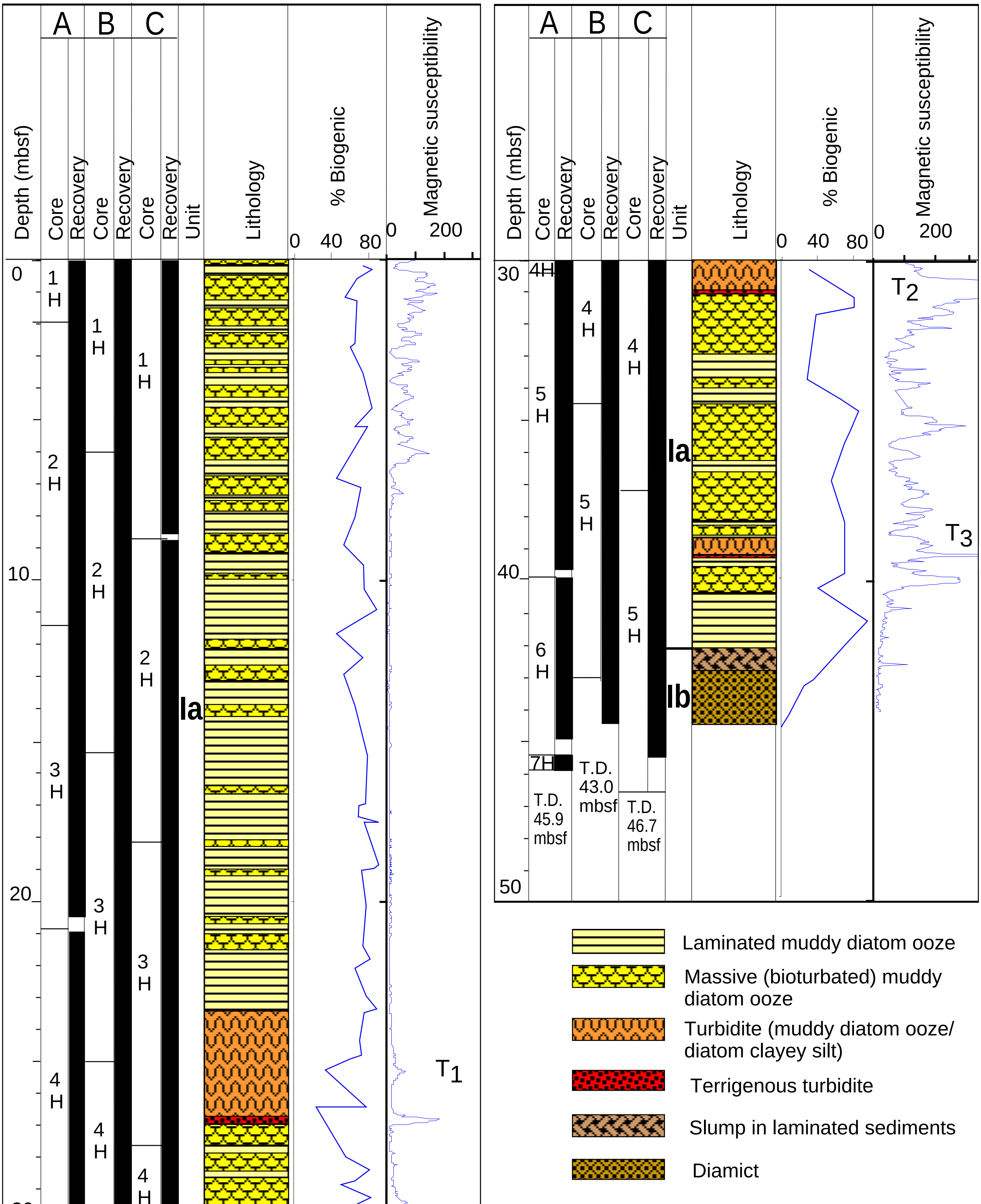

Figure 20A.

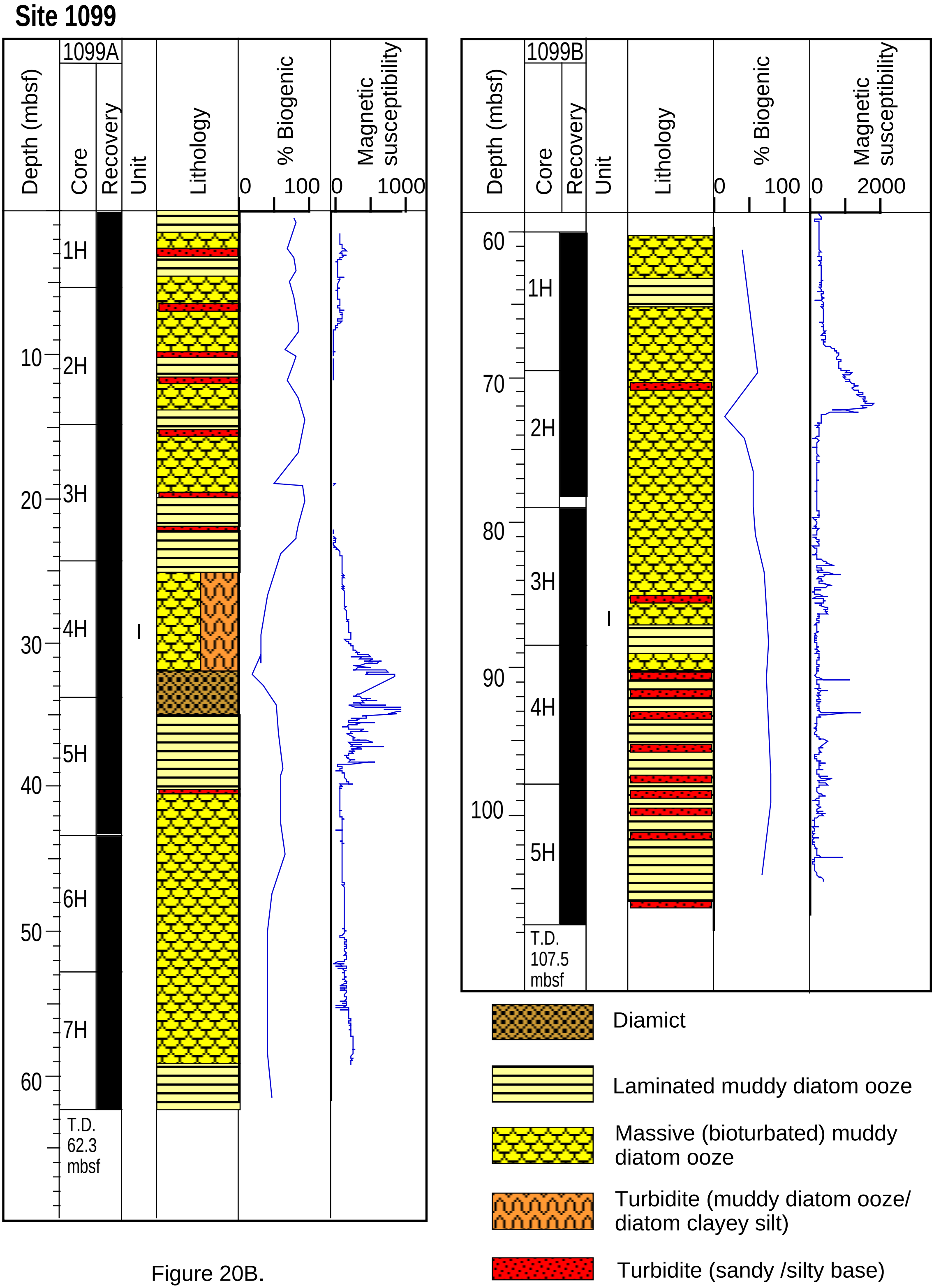
Site 1099
1099A
Depth (mbsf)
Core
Recovery
Unit
Lithology
% Biogenic
0
100
Magnetic susceptibility
0
1000
10
20
30
40
50
60
1H
2H
3H
4H
5H
6H
7H
I
T.D. 62.3 mbsf
1099B
Depth (mbsf)
Core
Recovery
Unit
Lithology
% Biogenic
0
100
Magnetic susceptibility
0
2000
60
70
80
90
100
1H
2H
3H
4H
5H
I
T.D. 107.5 mbsf
Diamict
Laminated muddy diatom ooze
Massive (bioturbated) muddy diatom ooze
Turbidite (muddy diatom ooze/ diatom clayey silt)
Turbidite (sandy /silty base)

Figure 20B.

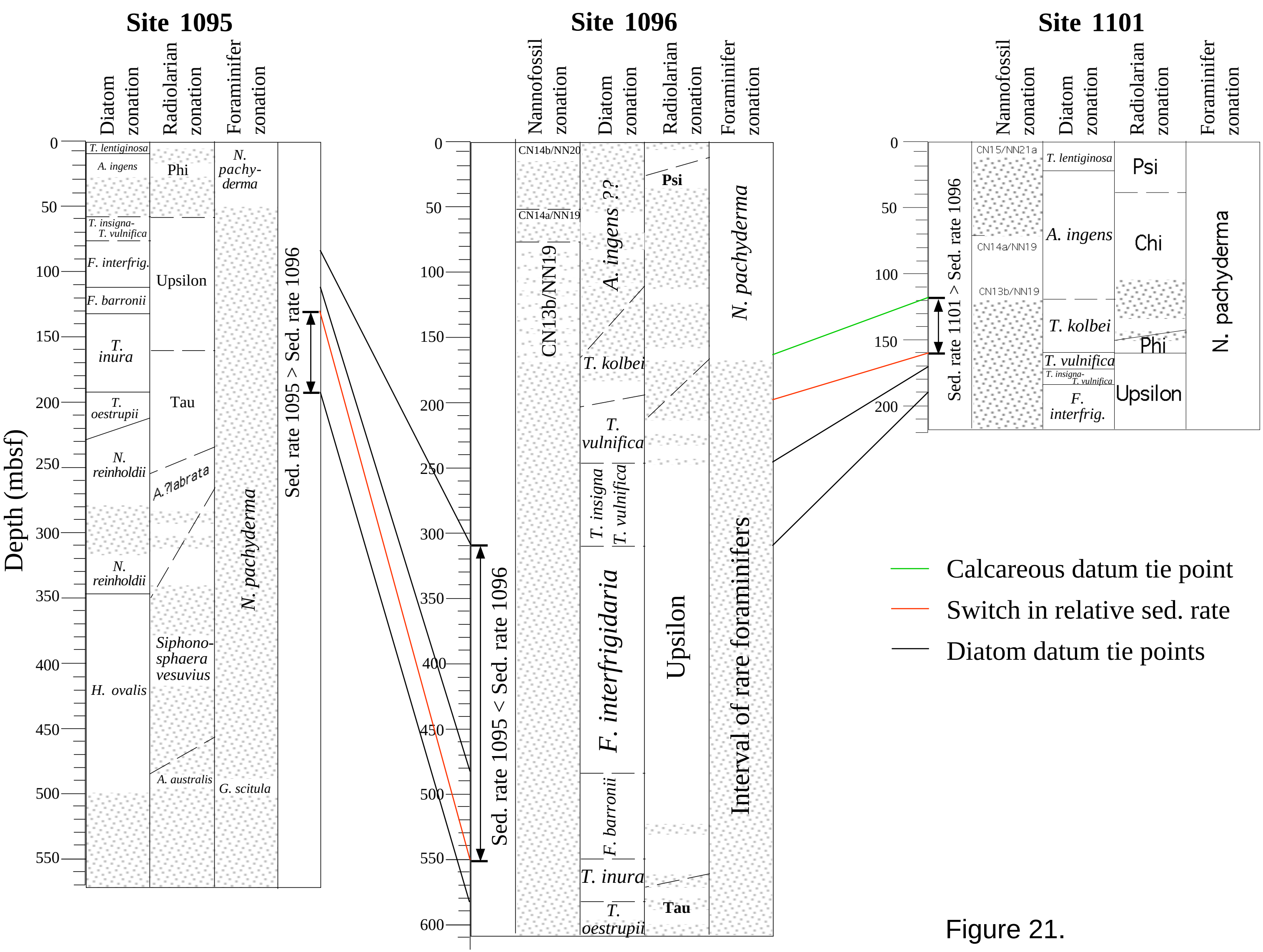
Site 1095
Site 1096
Site 1101
Depth (mbsf)
Diatom zonation
Radiolarian zonation
Foraminifer zonation
Nannofossil zonation
T. lentiginosa
A. ingens
T. insigna-T. vulnifica
F. interfrig.
F. barronii
T. inura
T. oestrupii
N. reinholdii
H. ovalis
Phi
Upsilon
Tau
A. ?labrata
Siphonosphaera vesuvius
A. australis
N. pachyderma
G. scitula
Sed. rate 1095 > Sed. rate 1096
Sed. rate 1095 < Sed. rate 1096
CN14b/NN20
CN14a/NN19
CN13b/NN19
A. ingens ??
T. kolbei
T. vulnifica
T. insigna
F. interfrigidaria
T. inura
Psi
Interval of rare foraminifers
CN15/NN21a
Chi
Sed. rate 1101 > Sed. rate 1096
Calcareous datum tie point
Switch in relative sed. rate
Diatom datum tie points

Figure 21.

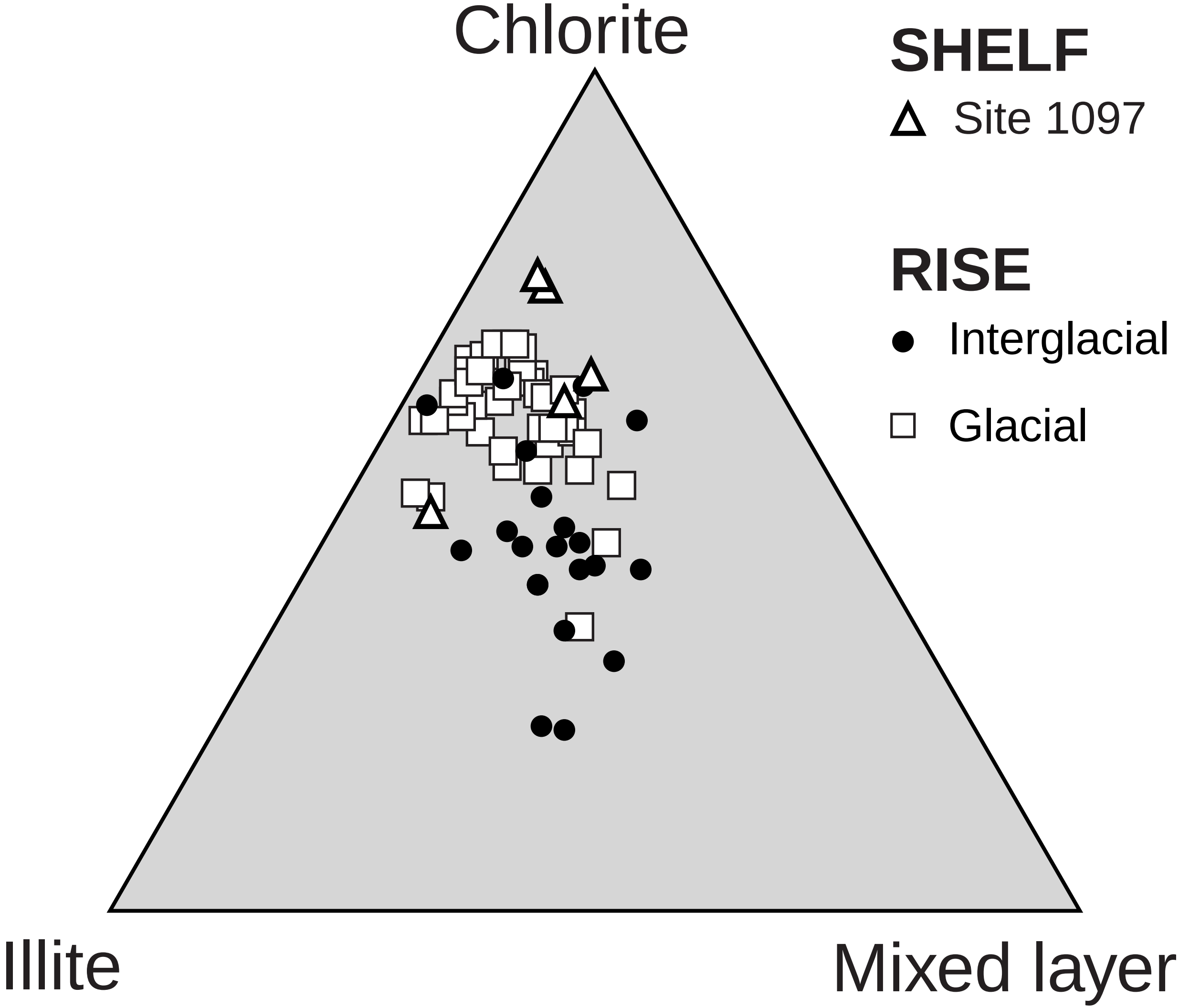
Chlorite
SHELF
Site 1097
RISE
Interglacial
Glacial
Illite
Mixed layer

Figure 22.

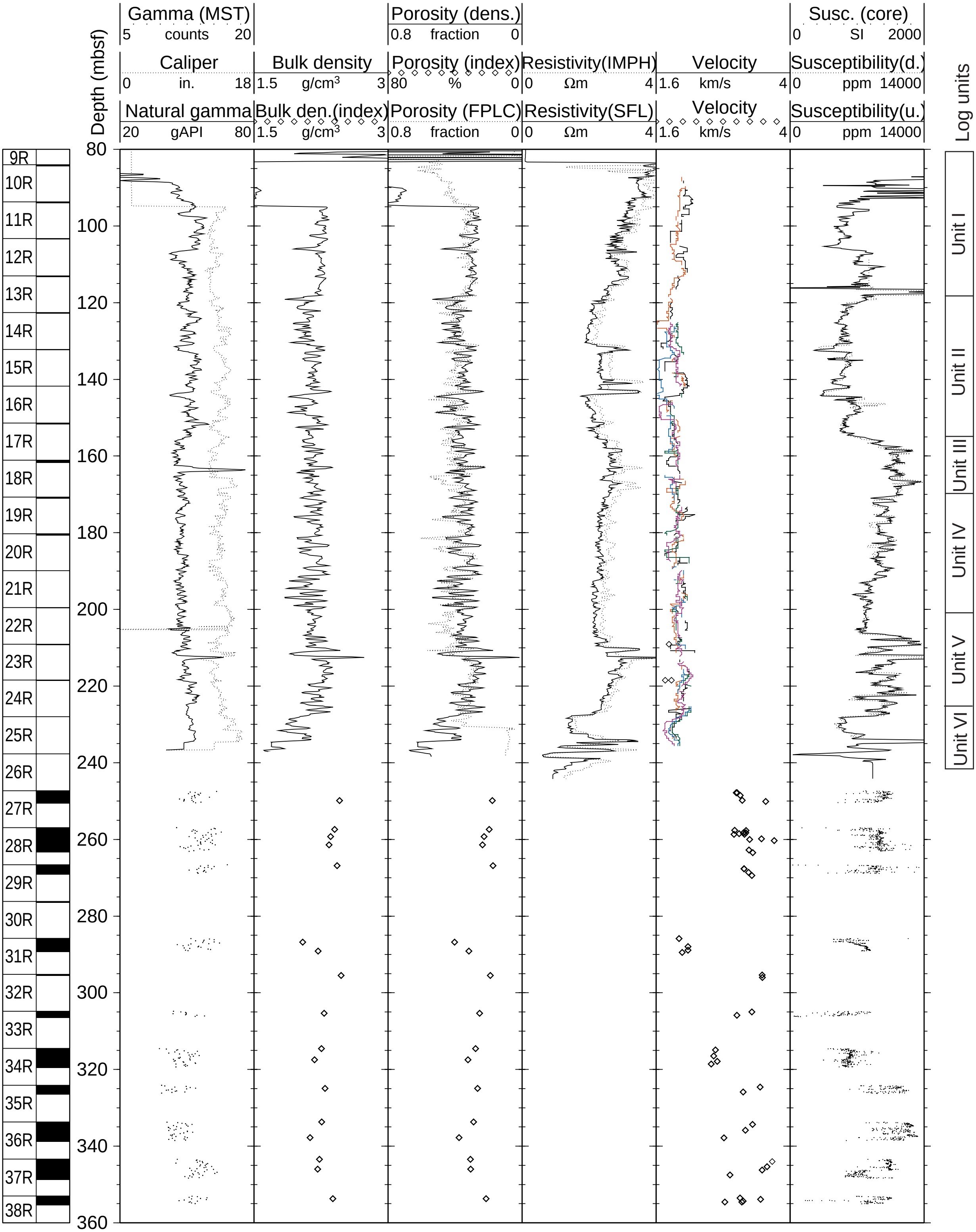
Gamma (MST)
5 counts 20
Caliper
0 in. 18
Natural gamma
20 gAPI 80
Bulk density
1.5 g/cm3 3
Bulk den.(index)
1.5 g/cm3 3
Porosity (dens.)
0.8 fraction 0
Porosity (index)
80 % 0
Porosity (FPLC)
0.8 fraction 0
Resistivity(IMPH)
0 Ωm 4
Resistivity(SFL)
0 Ωm 4
Velocity
1.6 km/s 4
Velocity
1.6 km/s 4
Susc. (core)
0 SI 2000
Susceptibility(d.)
0 ppm 14000
Susceptibility(u.)
0 ppm 14000
Log units
Depth (mbsf)
80
100
120
140
160
180
200
220
240
260
280
300
320
340
360
9R
10R
11R
12R
13R
14R
15R
16R
17R
18R
19R
20R
21R
22R
23R
24R
25R
26R
27R
28R
29R
30R
31R
32R
33R
34R
35R
36R
37R
38R
Unit I
Unit II
Unit III
Unit IV
Unit V
Unit VI

Figure 23.

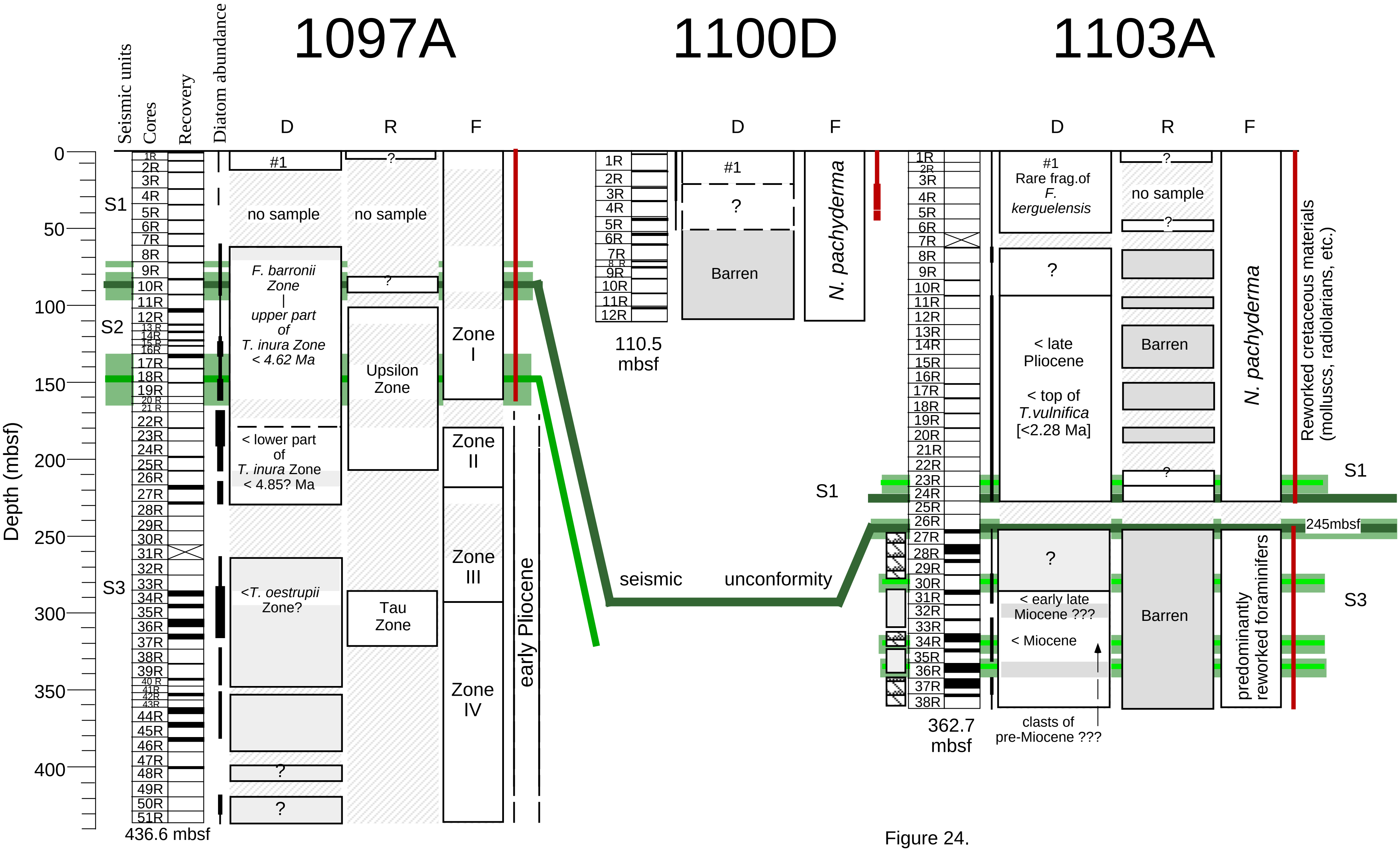
1097A
1100D
1103A
Seismic units
Cores
Recovery
Diatom abundance
D
R
F
Depth (mbsf)
S1
S2
S3
no sample
F. barronii Zone
upper part of T. inura Zone
< 4.62 Ma
< lower part of T. inura Zone
< 4.85? Ma
<T. oestrupii Zone?
Upsilon Zone
Tau Zone
Zone I
Zone II
Zone III
Zone IV
early Pliocene
436.6 mbsf
#1
Barren
N. pachyderma
110.5 mbsf
seismic
unconformity
Rare frag.of F. kerguelensis
< late Pliocene
< top of T.vulnifica [<2.28 Ma]
< early late Miocene ???
< Miocene
clasts of pre-Miocene ???
362.7 mbsf
245mbsf
predominantly reworked foraminifers
Reworked cretaceous materials (molluscs, radiolarians, etc.)

Figure 24.

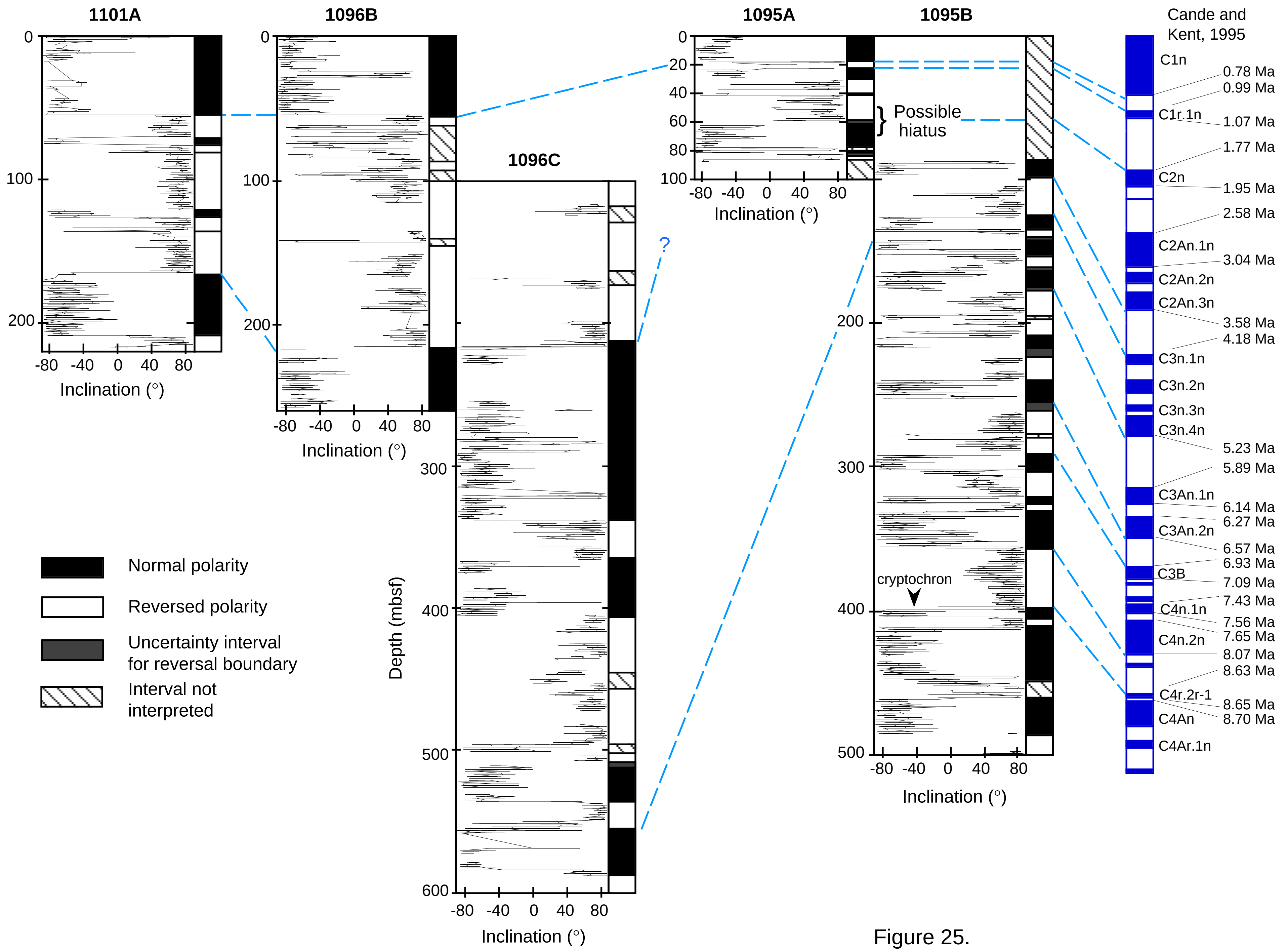
1101A
1096B
1096C
1095A
1095B
Cande and Kent, 1995
Inclination (°)
Depth (mbsf)
Possible hiatus
cryptochron
Normal polarity
Reversed polarity
Uncertainty interval for reversal boundary
Interval not interpreted
C1n
0.78 Ma
0.99 Ma
C1r.1n
1.07 Ma
1.77 Ma
C2n
1.95 Ma
2.58 Ma
C2An.1n
3.04 Ma
C2An.2n
C2An.3n
3.58 Ma
4.18 Ma
C3n.1n
C3n.2n
C3n.3n
C3n.4n
5.23 Ma
5.89 Ma
C3An.1n
6.14 Ma
6.27 Ma
C3An.2n
6.57 Ma
6.93 Ma
C3B
7.09 Ma
7.43 Ma
C4n.1n
7.56 Ma
7.65 Ma
C4n.2n
8.07 Ma
8.63 Ma
C4r.2r-1
8.65 Ma
C4An
8.70 Ma
C4Ar.1n

Figure 25.

OPERATIONS SYNOPSIS

The ODP Operations and Engineering personnel aboard the *JOIDES Resolution* for Leg 178 were

Operations Manager: Ron Grout

Development Engineer: Mark Robinson

Schlumberger Engineer: Robert Laronga

SITE 1095

Port Call Activities and Transit to Site 1095

Leg 178 began at 2100 hr (equals Universal Time Coordinated [UTC] minus 3 hr; all times are given in local time except where UTC is indicated) on 5 February 1998 upon the arrival of the *JOIDES Resolution* at Punta Arenas, Chile, nearly 3.5 days ahead of schedule. The early arrival resulted from a faster-than-expected transit and an earlier-than-planned departure from the last site of Leg 177, owing to the failure of the lower part of the port section of the lower guide horn (LGH).

While the vessel was at anchor, the drilling crew removed the upper guide horn (UGH) and then built a scaffolding in the moonpool area to help remove the starboard section of the LGH. At 0830 hr on 6 February, the ship moved to Muelle Arturo Prat. The starboard section of the LGH was removed, and the broken edge of the port section was beveled. The entire section was then sandblasted, painted, and returned to the vessel, where it was stored on the main deck for reinstallation in Cape Town, South Africa.

Concurrently, divers examined the moonpool area and rudder; their inspection indicated that no damage had occurred as a result of unrestrained LGH movement. In addition, two new motor generators, which were installed in the “Koomey Room” in Cape Town at the beginning of Leg 177, were connected to the 480-V switchboard and brought on-line.

A six-man Tuboscope inspection team attended the port call to inspect the drill pipe that was in the string during the drill-pipe failure at Hole 735B on Leg 176. The pipe was removed from the casing hold of the vessel and placed in a covered customs warehouse at the end of the pier. The team inspected 73 joints of 5-in drill pipe and downgraded one joint because of corrosion. An additional 54 joints of 5.5-in drill pipe were inspected, with three joints failing to pass inspection because of wall loss. Also during this port call, John Boyd of Patterson Coating examined 15 joints of specially treated and marked 5-in drill pipe to assess the effectiveness of different pipe-coating materials.

Because Leg 178 was in high latitudes, an ice observer (Andy Caldwell, a consultant contracted by Sedco) was added to the Overseas Drilling Limited (ODL) deck crew. In addition, the *Polar Duke* was chartered to provide ice detection services and emergency towing capabilities. Through competitive bidding, the *Polar Duke* was contracted from Rieber Shipping to carry out ice picket boat duties during Leg 178. This vessel was officially accepted on contract in Punta Arenas as of 0000 hr on 9 February. Roberto Laterza, an Italian technician, joined the crew of the *Polar Duke* to recover a mooring containing two current meters as part of a study conducted by the Osservatorio Geofisico Sperimentale, Trieste.

At 0806 hr on 12 February, the *Resolution* departed Punta Arenas. The 95-nmi transit through the eastern Straits of Magellan concluded when the pilot left the vessel at 1718 hr on 12 February. The vessel then headed south toward the first site of the leg, Site 1095 (scientific prospectus site APRIS-02A). Initially seas were calm, and it was sunny and surprisingly mild. At noon the next day (Friday the 13th), the weather began to deteriorate as the vessel approached the narrow channel between Isla de los Estados and Tierra del Fuego. As the ship entered Drake Passage, a full gale with wind gusting to 50 kt was in progress. The weather moderated, and we crossed the Antarctic Circle (66°37’S) at noon on 17 February.

Hole 1095A

As the *JOIDES Resolution* approached Site 1095, a short 3.5-kHz precision depth recorder (PDR) profile was acquired to refine the site selection. The positioning beacon was launched at 1615 hr on 17 February, beginning drilling operations for the leg. Before spudding, a drill pipe swab (pig) was pumped down to clear any rust that might have accumulated inside the drill pipe.

Hole 1095A was spudded with the first advanced hydraulic piston corer (APC) core at 0530 hr on 17 February, with the seafloor depth estimated from recovery as 3841.6 m (3852.6 meters below rig floor [mbrf]). APC coring advanced to 87.3 meters below seafloor (mbsf) with core recovery of 99.1% when operations had to be stopped because an iceberg (one of only two on the 24-mi radar screen) closed within 1.6 nmi. It had a computed closest point of approach (CPA) to the drill site of less than 0.5 nmi. The drill string was pulled above the seafloor and the vessel offset in dynamic position mode 330 m north of the location, while the iceberg passed directly over the drilling site. As the ice cleared the site, the vessel was repositioned 20 m west of Hole 1095A.

Hole 1095B

After three hours spent waiting on ice, Hole 1095B was spudded at 2145 hr on 18 February. The bit was washed down to 83.0 mbsf, where APC coring was resumed. The coring advanced from 83.0 to 205.0 mbsf and ceased when overpulls of 100 kilopounds (kips) could not dislodge the core barrel (Core 178-1095B-13H) from the formation. The stuck core barrel was drilled over to release it from the sediment. Coring continued in Hole 1095B with the extended core barrel (XCB) advancing to 483.3 mbsf (Core 43X) with 89.0% recovery. Below this, core recovery was only 18.1%. This factor, together with increasing vessel heave, influenced the decision to terminate drilling at 570 mbsf. Pump pressure was abnormally high below 483.3 mbsf, and on recovery, three of the four bit nozzles were found to be clogged with glacial debris.

In preparation for logging Hole 1095B, a wiper trip was conducted up to 89 mbsf with no drag. While running pipe back to bottom, the region from 541 to 570 mbsf was washed and reamed. The bit contacted 2 m of hard fill on the bottom, which was cleaned from the hole by circulating a 30-bbl high-viscosity mud pill. The drill string was pulled back to 95 mbsf with no drag experienced.

The Schlumberger logging equipment was rigged by 1615 hr on 22 February, and three downhole logging runs were completed in Hole 1095B: a triple combination (TC; caliper, lithodensity, porosity, resistivity, and natural gamma ray) log, a geologic high-sensitivity magnetic tool (GHMT) log, and a well seismic tool (WST) experiment. For the TC log, the vessel heave exceeded the maximum stroke of the wireline heave compensator, which was therefore turned off. At the start of the repeat TC run, the hostile environment lithodensity sonde (HLDS) caliper arm became detached, probably when the tool moved downward during a large heave. Because of concerns about tool safety, heave, and the large diameter of much of the hole (16–19 in), the Formation MicroScanner (FMS)–sonic tool string was not run. Seas were lower for the GHMT run, and the wireline heave compensator could be activated. The heave was still large enough to require slow (1000 m/hr) tool speeds through the pipe.

Holes 1095C and 1095D

Hole 1095C was spudded with the APC at 0215 hr on 24 February, 20 m west of Hole 1095B. After one mudline core, the driller repositioned the bit 5 m lower and spudded Hole

1095D at 0400 hr. APC coring advanced to the depth objective of 84.6 mbsf (Core 9H) with 93.3% recovery. The drill string was recovered, the positioning beacon released and retrieved, and the vessel departed for Site 1096 at 1930 hr on 24 February.

SITE 1096

On leaving Site 1095, we deployed the proton precession magnetometer before crossing over the site. A continuous total field magnetic and 3.5-kHz profile was obtained that extended over and just to the southeast of Site 1096. We averaged 8.1 kt during the 58 nmi transit to Site 1096.

Hole 1096A

Hole 1096A was spudded at 1130 hr on 25 February with the APC at a seafloor depth estimated from recovery to be 3152.0 m (3163.2 mbrf). APC coring advanced to refusal at a depth of 140.7 mbsf (Core 15H) with 84.2% recovery. The bit cleared the seafloor at 0145 hr on 26 February, and the *JOIDES Resolution* was offset 20 m west of Hole 1096A.

Hole 1096B

Before spudding Hole 1096B, a water-sampling temperature probe (WSTP) sample of bottom water was obtained. Hole 1096B was spudded with the APC at 0700 hr on 26 February at a seafloor depth of 3152.5 m (3163.7 mbrf). Piston coring advanced to 108.3 mbsf (Core 12H) without incident but on Core 13H encountered a change in the formation and only advanced 7.6 m. We switched to XCB for the next two cores (115.9 to 135.2 mbsf) but got virtually no recovery. The hole was then deepened with the APC to refusal at 166.9 mbsf. The interval from about 110 to 170 mbsf, besides causing some coring difficulties, marks a zone where physical properties change and where a lithologic boundary occurs. Adara temperature tool measurements were obtained at the mudline, 32.2 mbsf (Core 4H), 60.8 mbsf (Core 7H), and 89.3 mbsf (Core 10H). Orientation data were obtained for Cores 4H, 5H, and 6H.

Coring continued in Hole 1096B with the XCB, advancing steadily to 212.5 mbsf, where a Davis-Villinger Temperature Probe (DVTP) was deployed on the wireline to measure formation temperature. Thereafter, circulation was poor and recovery reduced. At 260.6 mbsf, after a second DVTP deployment, the drill string was tripped, and three of the four bit nozzles were found to be plugged with clay and glacial dropstones. The nozzles were cleared and the bit seal replaced. From DVTP data and other data collected during APC coring, an initial temperature gradient of about 80°C/km was estimated.

Hole 1096C

Hole 1096C was started 20 m west of Hole 1096B by first drilling to 114.0 mbsf. We then alternated between coring and drilling in the interval from 114.0 to 231.4 mbsf, taking two APC and four XCB cores to fill gaps in recovery from the first two holes.

Continuous XCB coring began at 255 mbsf and advanced to 588.6 mbsf (Core 41X) without incident and with generally good recovery (82.7%). While cutting Core 42X (588.6 to 598.1 mbsf), the hard formation cutting shoe failed downhole. Because of the need to ensure that sediments producing a prominent seismic reflector had been sampled, an additional core (43X) was obtained (598.1 to 607.7 mbsf), in which a small piece of ground-up cutting shoe was recovered.

In preparation for logging, a 20-bbl high-viscosity mud sweep was circulated and the pipe pulled back to 97.3 mbsf. The TC tool string was deployed at 0115 hr on 4 March but was retrieved without logging because of an electronic problem. The lithodensity, porosity, and natural gamma ray (IPLT) tool was then run into the pipe at 0600 hr and encountered an obstruction at 353 mbsf. The hole was logged up from this depth to the bit, with a short repeat section. During logging, additional tight spots were observed at 170 and 240 mbsf. In many parts of the hole, the diameter exceeded 18 in.

At noon the tool was recovered, and a wiper trip was conducted from 97 to 578 mbsf. The region from 578 to 607 mbsf was washed and reamed. After a 20-bbl mud flush was circulated, the bit was pulled back to 356 mbsf. The IPLT was deployed again and was able to advance from 356 to 556 mbsf, where an obstruction prevented further penetration. The hole was logged up from 556 mbsf to the bit.

At midnight on 4 March, the first tool string was recovered and the second tool (GHMT) deployed. The GHMT logged the hole up from 510 to 356 mbsf and was recovered and rigged down by 0930 hr on 5 March. The drill string was recovered, but the positioning beacon failed to release and was therefore not retrieved. The vessel departed for Site 1097 at 1530 hr on 5 March.

SITE 1097

With a following wind and calm seas, we made good time traveling at an average speed of 11.2 kt on the 163 nmi transit from Site 1096 to Site 1097 (scientific prospectus site APSHE-05A). During the transit north, 15 icebergs were spotted on radar, and the vessel was required to alter course to avoid one large iceberg. The *Polar Duke*, which had left Site 1096 before us to scout ahead, reported that there were six icebergs within 15 nmi of site location. The *JOIDES Resolution* proceeded directly to the Global Positioning System (GPS) coordinates for site APSHE-05A and dropped a positioning beacon at 0615 hr on 6 March.

Hole 1097A

Because this site did not have sediments suitable for coring with the APC or XCB, a rotary core barrel (RCB) bottom-hole assembly (BHA) was made up with a new Rock Bit International (RBI) C-3 bit and a mechanical bit release (MBR). Hole 1097A was spudded at 1045 hr on 6 March at an estimated seafloor depth of 551.7 m (563.0 mbrf), 1 m less than the computed PDR reading. For the next 13 hr, coring at Site 1097 proceeded slower than expected, and core recovery was very low (3.7% for the first 10 cores) as we attempted to penetrate glacial till through an abundance of cobbles and boulders.

Meanwhile, six icebergs were being monitored within 6 nmi of the rig. A free-fall funnel was deployed late on 7 March to allow us to re-enter the hole, given the likelihood that an iceberg would eventually force us off site. RCB coring resumed and advanced slowly to 164 mbsf, where the drill string stuck in the unstable hole. After 45 min of working the pipe and flushing the hole with mud, the pipe was freed. RCB coring resumed and advanced to 246 mbsf (Core 29R), with improving recovery (but still poor at less than 10%) and faster rates of penetration. At 1600 hr on 8 March, we suspended coring operations and pulled the bit to the top of the hole as an iceberg approached. Just after midnight the iceberg came within 1 nmi, so the drill string was pulled above the seafloor to allow the vessel to maneuver. Because the bit had accumulated 31 hr of rotating time in difficult conditions, we used the waiting time to change it.

At 0710 hr on 9 March, the hole was re-entered in less than 15 min via the free-fall funnel. From 0900 to 1230 hr, the bit was washed and reamed into the unstable formation to 246 mbsf, where circulation was lost after making a connection. The bit was pulled back to 236 mbsf, and attempts were made to clear the drill string and regain circulation. In a last-ditch effort to clear the bit and avoid another round trip of the drill string, a "swab cup" was run in on the wireline to 300 mbrf and then pulled back to the vessel with the drill string connection partially open at the rig floor. The swab cup essentially drained the water in the top 300 m of drill string (spraying the drill floor), which reduced the hydrostatic pressure at the bit. This differential pressure forced formation fluid back up through the bit nozzles, which cleared the blockage. The mud pumps were immediately turned on and the pipe flushed clean. As a precautionary move, a bit deplugger was deployed to clear any obstruction that might be in the throat of the bit.

Coring advanced from 246 to 294 mbsf but then was halted because of excessive vessel heave caused by complex large swells coming from two directions. After sea conditions improved, RCB coring advanced from 294 to 351 mbsf with better recovery (24%) and faster penetration (up to 15 m/hr). This was followed by another 4.3 hr of standby time as ship heave again exceeded 2 m as well as another 5.5 hr of washing and reaming to return to the bottom of the hole.

RCB coring had advanced to 436.6 mbsf by 0545 hr on 11 March with 13.6% core recovery when operations were again interrupted by the approach of an iceberg. The bit was raised to 400 mbsf while the iceberg remained within range. After the iceberg had passed out of range, the drillers encountered several difficulties attempting to reach the bottom of the hole, including having the pipe stuck. At the bottom of the hole, the drillers could not make a connection to retrieve the wash barrel. Because hole conditions were deteriorating, the coring program was terminated.

After the hole was displaced with 85 bbl of 10.5-gallon mud, the drill string was recovered. The bit cleared the seafloor at 1700 hr, and the BHA was at the rotary table at 1800 hr. The drill collar connections were then inspected for any damage incurred as a result of the rough drilling and unusual environmental conditions. The beacon was recovered, and the drilling equipment was secured for transit to Site 1098 by 2100 hr on 11 March.

PALMER DEEP (SITES 1098 AND 1099)

The 192-nmi transit to Site 1098 (scientific prospectus site APSHE-13A) was accomplished at an average speed of 10.5 kt. During the voyage, 52 icebergs were seen on the 24-nmi range of the radar, and the vessel was required to alter course to avoid one large berg. Once in the Palmer Deep area, we ran a short 3.5-kHz PDR survey from south to north over the site. Drilling operations began at 1530 hr on 12 March with the deployment of a beacon.

During operations at this site, Eugene Domack joined the vessel for less than a day from the *Laurence M. Gould* (*LMG*) to observe procedures. Domack was the lead proponent on the proposal for drilling the Palmer Deep sites. Shortly before the *LMG* arrived, the *Polar Duke* came alongside Crane 3 to offload a logging tool and acetone, which had been shipped to Punta Arenas but had failed to arrive at the port call in time. These supplies had been delivered to the American base at Palmer Station a few miles away by the *LMG* for pickup by the *Polar Duke*.

Site 1098

The initial core of Hole 1098A recovered 1.9 m, establishing seafloor depth at 1012 m (1022.6 mbrf). APC coring then continued through Core 7H, where contact with glacial till or hard basement concluded the hole exploration at 45.9 mbsf. Calm conditions permitted very good core recovery. The drill string was raised above the seafloor to begin Hole 1098B, and the ship was offset 10 m north.

To achieve stratigraphic overlap, Hole 1098B was spudded with the pipe 3.5 m lower than for the first core of Hole 1098A. Core recovery indicated a seafloor depth about 1.4 m shallower than at Hole 1098A. APC coring advanced to 43.0 mbsf (Core 5H). Adara tool heat-flow measurements were obtained with Cores 4H (34.5 mbsf) and 5H (43.0 mbsf). The drill string was raised above the seafloor at 0355 hr to begin Hole 1098C, and the vessel was offset 10 m north.

The pipe was set 3 m lower than at Hole 1098B for the first APC core at Hole 1098C. Coring began at 0430 hr 13 March with an Adara tool deployment just above the bottom before spudding on the first core. Five APC cores were collected, and coring operations ended at 0630 hr. Core recovery for the site averaged 101.6%. The drill string was recovered, the beacon successfully retrieved, and the vessel was under way at 0930 hr 13 March for a 6-nmi transit to Site 1099.

Site 1099

Site 1099 (scientific prospectus site APSHE-15A) was located using GPS coordinates, and a beacon was launched at 1030 hr 13 March. APC coring at Hole 1099A began at 1445 hr on 13 March with a 5.3-m core that established the seafloor depth at 1399.9 m (1411.2 mbrf). Continuous cores were taken to 62.3 mbsf (102% recovery) with Adara tool heat-flow measurements at Cores 5H (43.3 mbsf) and 7H (62.3 mbsf). An additional Adara tool was deployed with the initial core barrel before spudding the hole to measure the near-bottom-water temperature. A change of wind then moved several icebergs toward the vessel. The bit was pulled above the seafloor at 1900 hr, and the vessel was offset away from the icebergs.

At 2145 hr, after the icebergs had moved past, Hole 1099B was spudded and the bit washed down to 60 mbsf where APC coring resumed. Core recovery averaged 102% while advancing to 107.5 mbsf, which was considered the depth objective for the hole. The drill string was retrieved and the beacon recovered before the vessel's departure at 0445 hr on 14 March.

SITE 1101

Site 1101 (located between scientific prospectus sites APRIS-5A and 6A) was selected as an additional site, where several leg objectives could be accomplished while waiting for the heave to subside on the continental shelf. Hence, the order of events included leaving Hole 1100D at 2030 hr on 17 March, arriving at Site 1101 at 1030 hr on 18 March, conducting coring operations, and then returning to Hole 1100D (see "Shelf Transect" section below). The 122-nmi transit to Site 1101 was accomplished at an average speed of 8.8 kt, slower than normal because the ship traveled through a 5-m swell combined with a 2.3-m sea.

Hole 1101A

Hole 1101A was spudded at 1805 hr on 18 March with a standard APC/XCB BHA and C-3 bit. Water depth was estimated from recovery of the mudline in Core 1H as 3291.2 m. APC coring advanced to 142.7 mbsf (Core 16H); XCB coring continued to 217.7 mbsf (Core 24X), with 99.1% core recovery for the hole. Adara temperature tool estimates were made with Cores 1H, 2H, 4H, 7H, and 10H, with the first two deployments also measuring near-bottom-water temperature. The ship then returned to Hole 1100D for what appeared to be favorable weather over the continental shelf sites. The beacon was recovered and the drilling equipment secured for transit back to Site 1100 by 0145 hr on 20 March.

SHELF TRANSECT (SITES 1100, 1102, and 1103)

Operations for the continental shelf transect (Sites 1100, 1102, and 1103) were interrupted by a brief detour to the nearby continental rise (Site 1101), which was cored while waiting for the environmental conditions to improve on the shelf. The chronological order of events included drilling Holes 1100A through 1100D, proceeding to and completing operations at Site 1101, returning to Hole 1100D, and finally conducting operations at Sites 1102 and 1103.

Site 1100

The 77-nmi distance between Site 1099 in the Palmer Deep and Site 1100 on the outer continental shelf was traversed in 9.6 hr. The average speed, 8.8 kt, was slower than normal because of a combination of 7-m swells and 3-m seas, both nearly at right angles to the ship's track.

The beacon was dropped at Site 1100 at 1445 hr on 14 March, and an RCB BHA with a new C-4 coring bit was deployed. Because of the restriction of 2 m maximum heave in 300–650 m water depth, the vessel stood by from 1730 to 2000 hr to allow a large swell to ease.

Hole 1100A was spudded at 2030 hr, and coring proceeded to 33.8 mbsf with no recovery before operations had to be stopped because of vessel heave. From 0115 to 0745 hr on 15 March, the vessel stood by while a large mixed swell from the west and north-northwest generated heave exceeding 3 m.

At 0930 hr on 15 March, Hole 1100B was spudded with the RCB and drilled ahead with a wash barrel to 34 mbsf. Once the wash barrel was retrieved, rotary coring began. It advanced only 2 m, however, before operations had to be stopped again because of heave. The BHA was tripped to the drill floor, and the throat of the bit was found to contain cobbles and gravel. The bit was cleaned and the BHA reassembled with the core barrel in place.

After the heave had subsided to acceptable levels, Hole 1100C was spudded. Coring advanced only 5 m, however, before heave again exceeded the threshold. When attempts to retrieve the core barrel with the wireline failed, the drill string was tripped to the surface for the second time. The BHA was partially disassembled in an attempt to discover why the core barrel could not be recovered with the wireline. The core barrel was found to contain more than 4 m of olive gray diamict (81% recovery). Investigation of the BHA revealed that a seal-bore drill collar, which is a standard fixture for the APC/XCB BHA, had been mistakenly added to the RCB BHA. This collar has a narrower inside diameter (3.8 in) than the standard controlled-length drill collar (4.3 in) used with the RCB BHA. The RCB core barrel could not pass through the narrower collar, either down (in Holes 1100A and 1100B) or up (in Hole 1100C), hence the difficulty in recovering core from the first three holes.

Hole 1100D was spudded at 1030 hr on 16 March. RCB coring advanced with poor recovery to 62.5 mbsf and was then stopped while a free-fall funnel (FFF) was deployed. Coring resumed to 76.8 mbsf when operations had to be stopped for a fourth time because of excessive heave. The FFF was re-entered at 0330 hr on 17 March. After washing and reaming to bottom, coring resumed and advanced to 100.9 mbsf. At 1000 hr on 17 March, and for the fifth time on site, coring was interrupted by heave exceeding 2 m. The bit was pulled above the seafloor at 1030 hr.

After deliberating whether to remain on site in difficult heave conditions, the decision was made to move to a new, alternate site in deep water (i.e., beyond the heave restriction) 120 nmi southwest. We hoped that after coring at the new site was concluded, the swell would have abated and would allow another attempt at deepening Hole 1100D. Of the 77.8 hr spent on site, only 20.5 were spent coring; 24.8 were inactive, waiting for the swell to abate, and the remaining time was occupied by reentry, tripping pipe, and so forth, as consequences of the primary disruption. At 2030 hr the drill string was recovered and the beacon commanded into standby. The vessel was under way to Site 1101 at 2030 hr on 17 March.

On completion of operations at Site 1101, we traveled 127 nmi back to Hole 1100D in 11.2 hr at 11.3 kt. The FFF was re-entered at 1700 hr on 20 March. We reached the bottom of the hole and cored from 100.9 to 110.5 mbsf (Core 12R) with 0.54 m of recovery before being forced to stop by the 2-m heave limitation. After waiting about 6 hr, and because hole conditions were not promising, we decided to move to a new site.

Site 1102

After the hydrophones were retracted, the vessel moved 6 nmi to Site 1102 (prospectus site APSHE-01A) using the thrusters. Operations were difficult given the heave, which often exceeded 2 m, and the rocky surface layer, which extended to an unknown depth. We managed to spud four holes, but with little recovery and no real opportunity to deepen them.

At 0645 hr on 21 March a beacon was deployed, and Hole 1102A was spudded at 1015 hr on 21 March. Coring advanced only 7.9 m (Core 1R) when excessive heave forced a halt. At 1425 hr on 21 March, Hole 1102B was spudded; it advanced only 7.5 m, however, when coring was again suspended for excessive heave. While waiting for the swell to flatten, a television survey of the seabed within a 50-m radius of the site was conducted for 2 hr, allowing the choice of a boulder-free alternative hole position. The heave subsided at 0130 hr on 22 March, but only long enough for Hole 1102C to be cored to 6.5 mbsf. Finally, Hole 1102D was spudded at 0945 hr. Unfortunately, hole conditions were poor. After coring to 14 mbsf in 3.25 hr, half the advance was lost when the driller picked up to 7 mbsf to retrieve the core. For the next 1.5 hr, the hole was washed and reamed with high, erratic torque. Three meters was drilled but were again lost when the driller pulled back. It was clear that this site was populated with boulders, rocks, and gravel, to a much greater depth than was visible at the seabed, and was virtually undrillable. Of the 34.8 hr spent at Site 1102, 15.3 were passed waiting on weather related to excessive heave and only 8.5 in actual coring. The remaining time was used for tripping, washing and reaming, and the small television survey.

Site 1103

At 1730 hr, the vessel began the 16-nmi transit to Site 1103 (prospectus site APSHE-10A), arriving at 2000 hr on 22 March. Hole 1103A was spudded at 0130 hr on 22 March, with low expectations stemming from our recent experience with excessive ship heave. This time, however, fortune smiled, and ship heave was not a problem for the remainder of the leg.

RCB coring advanced quickly to 180.3 mbsf with very low recovery (2.6% or 4.7 m), which was attributed to a soft till matrix and hard rocks becoming jammed in the core catcher. At 1900 hr on 23 March, the third FFF of the leg was deployed as insurance in case the weather deteriorated or an iceberg appeared. Coring resumed at 2015 hr and continued with improving recovery and slowing rates of penetration. Coring ended at 363.7 mbsf at 0730 hr on 25 March to allow time for logging. The average recovery for the hole improved to 12.3% with an average rate of penetration of 15 m/hr.

The hole was washed and reamed in preparation for logging. Releasing the bit was made difficult by gravel inside the pipe but, following release, the bottom of the drill pipe was pulled back to logging depth (74 mbsf). On the first logging run, the TC tool string was unable to pass a tight spot at 242 mbsf. The hole was logged up from this depth to the seafloor with no repeat run. It took 2 hr to work the tool back into the drill pipe, and the bow-spring of the porosity tool was missing, presumably left in the hole. The second log (GHMT) was also run from 241 mbsf to the seafloor. The FMS was run successfully (from 241 m to the seafloor) only after repairing an electronic problem.

The hole was filled with mud and the drill string retrieved, which took longer than usual because of the routine end-of-leg inspection of drill-collar connections in the BHA. The positioning beacon was recalled, and the vessel departed the site for Cape Town at 1130 hr on 26 March. At 1800 hr, *Polar Duk*e was released in accordance with the contract.

The 3660-nmi transit to Cape Town took 13.8 days at an average speed of 11.3 kt. Leg 178 ended when the *JOIDES Resolution* was docked in Cape Town at 0900 hr on 9 April 1998.

OCEAN DRILLING PROGRAM
OPERATIONS RESUME
LEG 178

Total Days (5 February 1998 to 09 April 1998)	62.16
Total Days in Port	6.46
Total Days Underway	22.15
Total Days on Site	33.72

	Days
Drilling	0.45
Other	0.52
Tripping Time	5.82
Stuck Pipe/Hole Trouble	0.92
Logging/Downhole Science	3.97
Mechanical Repair Time (Contractor)	0.03
Re-entry Time	0.35
W.O.W.	2.59
Coring	18.74

Total Distance Traveled (nautical miles)	0.0
Average Speed Transit (knots):	0.0
Number of Sites	9.0
Number of Holes	23.0
Number of Cores Attempted	327.0
Total Interval Cored (m)	2923.7
Total Core Recovery (m)	1806.9
% Core Recovery	61.80
Total Interval Drilled (m)	374.7
Total Penetration	3298.4
Maximum Penetration (m)	607.7
Minimum Penetration (m)	2.9
Maximum Water Depth (m from drilling datum)	3852.6
Minimum Water Depth (m from drilling datum)	442.0

OCEAN DRILLING PROGRAM
SITE SUMMARY
LEG 178

Hole	Latitude	Longitude	Water depth (mbrf)	Number of cores	Interval cored (m)	Core recovered (m)	Recovery (%)	Drilled (m)	Total penetration (m)	Time on hole (hr)	Time on site (days)
1095A	66° 59.1262' S	78° 29.2384' W	3852.6	10	87.30	86.48	99.1%	0.0	87.30	27.25	1.1
1095B	66° 59.1261' S	78° 29.2696' W	3852.6	52	487.20	385.75	79.2%	83.0	570.20	125.25	5.2
1095C	66° 59.1218' S	78° 29.2949' W	3852.6	1	2.90	2.87	99.0%	0.0	2.90	1.50	0.1
1095D	66° 59.1212' S	78° 29.2854' W	3851.9	9	84.60	78.96	93.3%	0.0	84.60	0.00	0.0
			1095 site totals:	**72**	**662.00**	**554.06**	**83.7%**	**83.0**	**745.00**	**154.00**	**6.4**
1096A	67° 34.0084' S	76° 57.7935' W	3163.2	15	140.70	118.52	84.2%	0.0	140.70	22.75	0.9
1096B	67° 34.0093' S	76° 57.8118' W	3163.7	32	260.60	209.77	80.5%	0.0	260.60	56.75	2.4
1096C	67° 34.0094' S	76° 57.8263' W	3163.7	43	409.90	344.98	84.2%	197.8	607.70	125.00	5.2
			1096 site totals:	**90**	**811.20**	**673.27**	**83.0%**	**197.8**	**1009.00**	**204.50**	**8.5**
1097A	66° 23.5678' S	70° 45.3840' W	563.0	51	436.60	59.30	13.6%	0.0	436.60	134.50	5.6
			1097 site totals:	**51**	**436.60**	**59.30**	**13.6%**	**0.0**	**436.60**	**134.50**	**5.6**
1098A	64° 51.7235' S	64° 12.4712' W	1022.6	7	45.90	45.78	99.7%	0.0	45.90	17.00	0.7
1098B	64° 51.7162' S	64° 12.4795' W	1022.0	5	43.00	44.66	103.9%	0.0	43.00	4.67	0.2
1098C	64° 51.7105' S	64° 12.4690' W	1021.8	5	46.70	46.30	99.1%	0.0	46.70	5.58	0.2
			1098 site totals:	**17**	**135.60**	**136.74**	**100.8%**	**0.0**	**135.60**	**27.25**	**1.1**
1099A	64° 56.7079' S	64° 18.9171' W	1411.2	7	62.30	63.74	102.3%	0.0	62.30	8.50	0.4
1099B	64° 56.7072' S	64° 18.9155' W	1411.2	5	47.50	48.34	101.8%	60.0	107.50	9.75	0.4
			1099 site totals:	**12**	**109.80**	**112.08**	**102.1%**	**60.0**	**169.80**	**18.25**	**0.8**
1100A	63° 53.0009' S	65° 42.3388' W	470.0	4	33.80	0.00	0.0%	0.0	33.80	10.50	0.4
1100B	63° 53.0098' S	65° 42.3487' W	470.0	1	2.00	0.15	7.5%	33.9	35.90	12.00	0.5
1100C	63° 52.9987' S	65° 42.3635' W	470.0	1	5.00	4.05	81.0%	0.0	5.00	18.75	0.8
1100D	63° 53.0053' S	65° 42.3519' W	470.0	12	110.50	5.28	4.8%	0.0	110.50	52.50	2.2
			1100 site totals:	**18**	**151.30**	**9.48**	**6.3%**	**33.9**	**185.20**	**93.75**	**3.9**
1101A	64° 22.3312' S	70° 15.6708' W	3291.2	24	217.70	215.75	99.1%	0.0	217.70	39.25	1.6
			1101 site totals:	**24**	**217.70**	**215.75**	**99.1%**	**0.0**	**217.70**	**39.25**	**1.6**
1102A	63° 48.1708' S	65° 51.4934' W	442.0	1	7.90	0.42	5.3%	0.0	7.90	4.75	0.2
1102B	63° 48.1675' S	65° 51.4728' W	442.0	1	7.50	0.39	5.2%	0.0	7.50	4.50	0.2
1102C	63° 48.1401' S	65° 51.4920' W	442.0	2	6.50	0.01	0.2%	0.0	6.50	11.25	0.5
1102D	63° 48.0713' S	65° 51.3867' W	442.0	1	14.90	0.85	5.7%	0.0	14.90	14.25	0.6
			1102 site totals:	**5**	**36.80**	**1.67**	**4.5%**	**0.0**	**36.80**	**34.75**	**1.4**
1103A	63° 59.9700' S	65° 27.9190' W	505.0	38	362.70	44.54	12.3%	0.0	362.70	87.50	3.6
			1103 site totals:	**38**	**362.70**	**44.54**	**12.3%**	**0.0**	**362.70**	**87.50**	**3.6**
			Leg 178 totals:	**327**	**2923.70**	**1806.89**	**61.8%**	**374.70**	**3298.40**	**793.75**	**33.1**

The technical and logistics personnel aboard the *JOIDES Resolution* for Leg 178 were

Tim Fulton	Marine Lab Specialist (Photography)
Edwin Garrett	Marine Lab Specialist (Paleomagnetics)
Dennis Graham	Marine Lab Specialist (Chemistry)
Gus Gustafson	Acting Lab Officer/Marine Lab Specialist (Downhole/Thin Sections)
Patricia Harrison	Marine Lab Specialist
Michiko Hitchcox	Marine Lab Specialist (Yeoperson)
Mike Hodges	Marine Computer Specialist
Dave Kotz	Marine Computer Specialist
Roberto Larza	Marine Lab Specialist (transferred from *Polar Duke*)
Melissa McEwen	Marine Lab Specialist (Physical Properties)
Meghan McCarthy	Marine Lab Specialist
Larry Obee	Marine Logistics Coordinator (Storekeeper)
Bob Olivas	Marine Lab Specialist (X-ray)
Chieh Peng	Marine Lab Specialist (Chemistry)
Patrick Riley	Marine Lab Specialist
Larry St. John	Marine Electronics Specialist
Johanna M. Suhonen	Marine Lab Specialist
Paula Weiss	Marine Lab Specialist (Curation)

GENERAL LEG INFORMATION

Leg 178 began when the *JOIDES Resolution* docked in Punta Arenas, Chile, on 6 February 1998, three days earlier than scheduled. The Leg 178 technical crew boarded the vessel on the morning of 9 February for crossover activities with the off-going crew. On 12 February we departed Punta Arenas with a ship's complement of 111: 66 Sedco and 45 Ocean Drilling Program (ODP) representatives. The technical staff consisted of 17 members, and one additional technician joined the cruise: Roberto Laterza transferred from the *Polar Duke* on 26 February after successfully recovering a current meter that had been deployed the previous year. He participated as a marine laboratory specialist for the remainder of the leg. Four of the 18 technicians sailed for their first time on the *JOIDES Resolution*. Leg 178 ended on 9 April after a 3660-nmi transit from Site 1103 to Cape Town, South Africa, that took 14 days.

PORT CALL ACTIVITIES OVERVIEW

In addition to routine logistics and crew change, port call activities in Punta Arenas included drill-pipe inspections, the removal and examination of the lower starboard guide horn, bunkering from tanker trucks, and a general ship power-down to install and connect a motor-generator set. Also, the combined technical crews attended a radiation safety lecture. Port call activities were concluded at 0800 hr on 12 February.

Logging tools, acetone, and part of the ODP beacon battery shipment did not make it to the ship before departure. It was necessary, therefore, to purchase acetone locally. The logging tools and acetone shipments were later delivered to our agent in Punta Arenas and put aboard the *Gould*. They were taken to Palmer Station, picked up by the *Polar Duke,* and delivered to us while on location in Palmer Deep.

LAB ACTIVITIES

For the most part, laboratory activities were normal. More than 1800 m of core was recovered at nine sites. Shattered liners and those that needed to be extruded from the core barrel were troublesome at times; however, these represented perhaps only 5% to 6% of the total recovery. Until the arrival of our missing acetone shipment, we conserved acetone by diluting it with an equal amount of isopropyl alcohol (propanol).

LAB SERVICES SUMMARY

Downhole Measurements Lab

The Adara temperature tool was used extensively at four site locations. The Davis-Villinger temperature tool was used twice at one of the locations after the formation became too hard to use the Adara tool. The water-sampling temperature probe (WSTP) tool was used to collect near-bottom seawater samples at one location before spudding the hole. An Adara temperature tool was used with the WSTP.

Core Lab

Leg 178 recovered 1806.89 m of sediment in 327 cores. Each core was processed through the Core Lab using the standard procedure. The low recovery of sediment ensured a smooth flow of core through the various lab stations with little backlog. Shattered core liners often made core processing on the catwalk slow and tedious and reduced core quality.

Curation

Various sediment types as well as expanding cores and some shattered liners tested curatorial skills. In the glacial tills (diamict) from the shelf sites, often only large cobbles were recovered. These were handled similarly to hard-rock cores: we cut individual rocks in half (archive- and working-half pieces) and placed plastic spacers between each rock. Core flow through the lab was routine with a higher number of requests than usual for close-up photos. Many of the cores were redescribed and sampled a second time.

The JANUS Curation Application was used throughout the cruise but needs several new features to fulfill the needs of the shipboard staff. In particular, the Core Log Tracking Report needs to have output fields for core comments, section comments, catwalk sample intervals, and volumes.

Paleomagnetics Lab

The leg progressed smoothly as far as the hardware was concerned. There were some problems with the software for the magnetometer and with the new Cryoedit program used to upload the data to JANUS. These problems have been reported. The thermal demagnetizer, the D-Tech alternating field demagnetizer, and the impulse magnetometer were used and functioned without problems. The Tensor tool was used once and failed. It is the same unit that had similar problems during Leg 177 and is being returned for repairs.

Chemistry Lab

In addition to routine interstitial water analysis, solid core samples were analyzed for inorganic and total carbon. Real-time monitoring of volatile hydrocarbons in the sediments was provided. A high-resolution interstitial water-sampling program was requested at one of the Palmer Deep sites (Site 1098).

The HPChemStation upgrade is still in progress. We verified Leg 177 findings that the spare oxygen supply for the carbon-nitrogen-sulfur (CNS) analyzer was contaminated with nitrogen. It was necessary to conserve the remaining good bottle of oxygen by keeping the valve closed when the instrument was not in use. An intermittent problem with the atomic absorption unit was fixed by replacing a control board. After 13 yr the unit is showing signs of wear, and replacement parts may be hard to find.

Physical Properties Lab

Core processing through this lab was fairly routine and equipment problems minor. The susceptibility, gamma-ray attenuation porosity evaluator (GRAPE), *P*-wave logger, and natural gamma ray (NGR) data were uploaded into JANUS without difficulty, with the exception of a user data entry error. A small percentage of GRAPE control files was not successfully uploaded. Pore-water sampler and moisture and density (MAD) data had to be transferred from the DATA1 drive to a local computer drive in the computer user room and uploaded from there. A new NGR/GRAPE standard was brought on board in Punta Arenas to be tested. These results, as well as the dimensions and calculated density values for the current GRAPE standard, were sent to shore.

X-ray Lab

The X-ray laboratory equipment operated without major problems. There were a total of 56 X-ray fluorescence samples taken from sediments and prepared for shipboard trace analysis including loss on ignition calculations. These will be run on Leg 179. X-ray diffraction (XRD) analyses were run on 333 samples and standards. The new version of MacDiff was used to interpret XRD data.

Paleontology Lab

Assistance with sample preparation was provided to the shipboard paleontologists for much of the leg. Maintenance included repairing the sink and dishwasher, restoring cabinets and bookcases, and fixing the broken backs of reference books.

Underway Geophysics and Fantail

Navigation data, as well as 3.5-kHz bathymetry data, were routinely collected during transits. In addition, the 12-kHz precision depth recorder on the bridge was used during the Palmer Deep survey. Magnetic data were also collected most of the time with some exceptions resulting from equipment problems, shallow-water maneuvering, or ice concerns. Both magnetometer levelwinds were troublesome and have suffered from moisture damage to circuit boards and components. Essential spares have been ordered. A new version of Winfrog was installed, and it was found to have several unacceptable “bugs.” There was no request for seismic work other than for vertical seismic profile logging, for which a Generator Injector (GI) air-gun, supplied by a third party, was used.

Thin Section Lab

There were 11 requests for thin sections. Maintenance included the replacement of a vacuum pump valve and the repair and calibration of a motor-speed controller.

Photography Lab and Microscope Services

The lab was busy with an average core recovery plus a large amount of close-up core photo work, all within a short 5-week period while on location. There was a lab stack water heater problem that resulted in steam flowing through cold-water lines in the lab. This caused a film processor flow meter to crack and several flexible hose lines and connections to either burst or leak. The only special project was to get some public relations photos; this was accomplished from aboard both the *Polar Duke* and *JOIDES Resolution*.

Microscopes required only cleaning and aligning. They are configured the same as the last leg. Only one roll of photomicrographs was taken.

Computer Services

Systems management for Leg 178 was mostly uneventful. The NetWare servers were fairly well behaved with no sudden crashes. They were shut down three times during the leg under controlled circumstances. JANUS also worked well, with most problems arising from human error. Scientists and technicians made extensive use of PC, Mac, and Unix workstations during this leg. Most support time was spent on routine Mac troubleshooting and maintenance. There was very little trouble with the PCs and almost none with the Suns, although these are used less than Mac computers.

Safety

Excess overstocked powdered chemicals have been identified for disposal. Marine emergency technical squad (METS) participation in weekly drills was limited. Three of the four METS team members were full-time staff; the other was temporary. Early in the cruise, we identified a need for additional small-size survival suits to properly fit the smaller women participants. They have been ordered.

Problems

Dirty drill water continues to plague those lab stack sinks that are not presently hooked up to potable water. The incinerator is showing signs of wear and tear after two legs of almost continuous usage and appears to perhaps be inadequate for the task.

LEG 178 LABORATORY STATISTICS

General Statistics

Sites:	9
Holes:	22
No. of cores:	327
Meters cored:	2923.7
Meters recovered:	1806.89
Number of general samples:	9040

Whole-Core Multisensor Track

GRAPE (sections):	1271
Natural gamma radiation (sections):	1270
Magnetic susceptibility (sections):	1271
P-wave:	637

Physical Properties Lab

PVS #1 velocity:	57
PVS #2 velocity:	57
PVS #3 velocity:	857
Moisture-density:	649
Thermal conductivity:	109
Vane shear:	46

X-ray Lab

X-ray fluorescence (samples prepared):	56
Major (no trace done):	
X-ray diffraction:	333

Thin Section Lab

Thin Sections:	11

Chemistry Lab

Carbon-nitrogen-hydrogen-sulfur:	160
Carbonate:	586
Interstitial water:	125
Head space:	170
Rock-Eval:	12

Underway Geophysics

Total transit (nmi):	5486
Bathymetry (nmi):	4900
Magnetic (nmi):	4300
Vertical seismic profile:	1

Paleomagnetics Lab

Cryogenic magnetometer (sections):	1350
Discrete:	450

Downhole Tools

WSTP:	1
Adara tool:	18
Davis-Villinger:	2

Note: X-ray fluorescence measurements were done on Leg 179.